AD-A184 437 GENERATION OF SPIRAL BEVEL GEARS WITH CONJUGATE TOOTH SURFACES AND TOOTH (U) ILLINOIS UNIV AT CHICAGO CIRCLE DEPT OF MECHANICAL ENGINEERIN F L LITVIN ET AL 1/2

UNCLASSIFIED AUG 87 NASA-CR-4088 NAG3-48 F/G 13/9 NL

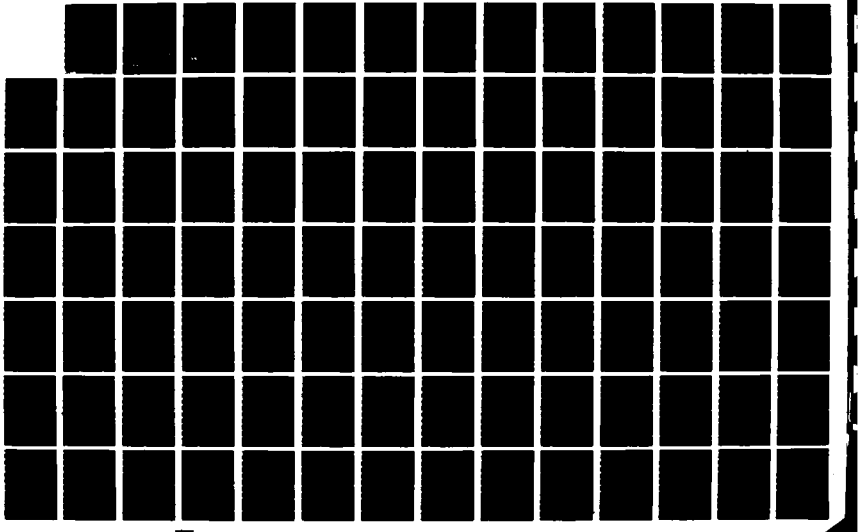

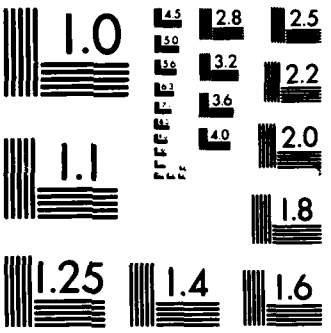

MICROCOPY RESOLUTION TEST CHART
NATIONAL BUREAU OF STANDARDS-1963-A

NASA
Contractor Report 4088

AVSCOM
Technical Report 87-C-22

Generation of Spiral Bevel Gears With Conjugate Tooth Surfaces and Tooth Contact Analysis

Faydor L. Litvin, Wei-Jiung Tsung,
and Hong-Tao Lee

GRANT NAG3-48
AUGUST 1987

NASA

US ARMY
AVIATION
SYSTEMS COMMAND
AVIATION R&T ACTIVITY

NASA
Contractor Report 4088

AVSCOM
Technical Report 87-C-22

Generation of Spiral Bevel Gears With Conjugate Tooth Surfaces and Tooth Contact Analysis

Faydor L. Litvin, Wei-Jiung Tsung,
and Hong-Tao Lee

The University of Illinois at Chicago
Chicago, Illinois

Prepared for
Propulsion Directorate
USAARTA-AVSCOM and
NASA Lewis Research Center
under Grant NAG3-48

National Aeronautics
and Space Administration

**Scientific and Technical
Information Office**

1987

TABLE OF CONTENTS

A-1

Nomenclature

$\underset{\sim}{a}$	vector of pitch line
a_p, b_p	major and minor axes of gear cradle ellipse
a_f, b_f	major and minor axes of pinion cradle ellipse
$d^{(P)}$	gear head cutter diameter
L	Mean pitch cone distance
m_{12}	gear ratio: $m_{12} = \omega^{(1)}/\omega^{(2)}$
m_{F1}	pinion cutting ratio
m_{p2}	gear cutting ratio
$\underset{\sim}{n}^{(F)}$, $\underset{\sim}{n}^{(P)}$	unit normal to pinion and gear tooth surface
q	direction angle of normal in coordinate system S_n
q_F, q_P	parameters of pinion and gear machine-tool setting
$r_c^{(P)}$, $r_c^{(F)}$	radius of generating surface measured in plane $X_m^{(i)} = 0$ (i = 1, 2)
u_F, u_P	generating cone surface coordinate
$\underset{\sim}{v}^{(F)}$, $\underset{\sim}{v}^{(P)}$	surface Σ_F, Σ_P contact point velocity
$\underset{\sim}{v}^{(1)}$, $\underset{\sim}{v}^{(2)}$	surface Σ_1, Σ_2 contact point velocity
$\underset{\sim}{v}_A$	velocity of intersection point at gear cutter axis in plane Π
$\underset{\sim}{v}_c$	velocity of intersection point at pinion cutter axis in plane Π
W	gear cutter width
β_p	mean spiral angle
γ_1, γ_2	pinion and gear pitch angle
γ_R	pinion root angle
δ_F, δ_P	orientation angle of pinion and gear cradle ellipses

ε	rotation angle of frame S_h relative to frame S_f about axis Z_1
η	rotation angle of frame S_f relative to frame S_n
Δ_1, Δ_2	pinion and gear dedendum angle
ΔE_1, ΔL_1	pinion machine-tool settings
θ_F, θ_P	generating pinion and gear cone surface coordinates
μ	motion parameter of cradle ellipse
μ_F, μ_P	motion parameter of pinion and gear ellipses
Π	plane of normals
Σ_1, Σ_2	pinion and gear tooth surfaces
Σ_F, Σ_p	generating surfaces of pinion and gear
ϕ_F, ϕ_p	generating surfaces rotation angle
$\psi_c^{(F)}$, $\psi_c^{(p)}$	pinion and gear blade angle
$\underset{\sim}{\omega}^{(1)}$, $\underset{\sim}{\omega}^{(2)}$	pinion and gear angular velocities
$\underset{\sim}{\omega}^{(F)}$, $\underset{\sim}{\omega}^{(p)}$	cradle angular velocities for cutting the pinion and gear

Cartesian Coordinate Frame

$S_s^{(j)}$	connected to tool cone, j = F, p
$S_c^{(j)}$	conntected to cradle
$S_m^{(i)}$	connected to machine frame, i = 1, 2
S_1, S_2	connected to pinion, gear
S_h	fixed to machine, used for mesh of Σ_F and Σ_1

S_f fixed to frame of gearbox, used for mesh of Σ_p and Σ_2

S_n connected to plane of normals

SUMMARY

Spiral bevel gears are used in many applications where mechanical power must be transmitted between intersecting axes of drive shafts. Namely, two such applications are the rear axle differential gearbox for land vehicles and the transmissions used in helicopters. For spiral bevel gears, there is a continuing need for ever stronger, lighter weight, longer-lived and quieter running gears. Above all, a rapid and economical manufacturing method is essential to the industries that use bevel gearing in their products.

For many years, the Gleason Works (Dudley, 1962; Anon. Gleason Works, 1964 and 1980) has provided the machinery for manufacture of spiral bevel gears. There are several important advantages to the Gleason methods of manufacture over hobbing methods. The machines are rigid and produce gears of high quality and consistency. The cutting methods may be used for both milling and grinding. Grinding is especially important for producing hardened high quality aircraft gears. Both milling and grinding are possible with Gleason's method. The velocity of the cutting wheel does not have to be related in any way with the machine's generating motion.

Generally speaking Gleason's method for generation of spiral bevel gears does not provide conjugate gear tooth surfaces. This means that the gear ratio is not constant during the tooth engagement cycle, and, therefore, there are kinematical errors in the transformation of rotation from the driving gear to the driven gear. The research that had been performed by the Gleason Works was directed at the minimization of gear kinematical errors and the improvement of gear bearing contact by using special machine-tool settings. The determination of such machine-tool setting is accomplished by a computer program. It is known that Oerlicon

(Switzerland) and Klingelnberg (West Germany) have developed methods for generation of spiral bevel gears that can provide conjugate gear tooth surfaces. The disadvantage of these methods is that the gear tooth surfaces cannot be ground and the tooth element proportions are unfavorable due to the constant height of the teeth.

The objective of the new method for generation of spiral bevel gears presented herein was to find a way to eliminate the kinematical errors for spiral bevel gears, obtain gears with higher contact ratio, and improve bearing contact and conditions of lubrication, while using the existing Gleason's equipment and retaining all the advantages of the Gleason system of manufacturing such gears. The proposed method for generation is based on the following:

(i) Four surfaces - two generating cone surfaces (Σ_p and Σ_F) and gear and pinion tooth surfaces (Σ_2 and Σ_1) are in continuous tangency at every instant. The ratio of angular velocities in motion of the above mentioned surfaces satisfies the requirement that the generated pinion and gear transform rotation with zero kinematical errors.

(ii) The cones have a common normal at the instantaneous point of contact but their surfaces interfere with each other in the neighborhood of contact point.

(iii) The point of contact of the above mentioned surfaces moves in a plane (Π) that is rigidly connected to the gear housing. The normal to the contacting surfaces lies in plane Π and performs a parallel motion in the process of meshing.

(iv) Due to the elasticity of gear tooth surfaces their contact is spread over an elliptical area. The proposed method for generation

provides that the instantaneous contact ellipse moves along but not across the gear tooth surface. This provides improved conditions for lubrication and a higher contact ratio will result.

(v) Until now, the reduction of kinematical errors of Gleason spiral bevel gears was a subject of the computer search for the optimal machine-tool settings. The computer program developed for this purpose is called the TCA (Tooth Contact Analysis) program. The proposed method is for direct determination of machine-tool settings that result in zero kinematical errors because the gear tooth surfaces are generated as conjugate gear tooth surfaces.

(vi) A new TCA program directed at the simulation of bearing contact and the influence of errors of assembly and manufacturing has been developed.

The contents of this report covers the new method for generation of spiral bevel gears, their geometry, the bearing contact and simulation of meshing. Special attention has been paid to the proposed principle of performance of parallel motion by two related ellipses that results in the desired parallel motion for the contact normal.

1. THE GLEASON MANUFACTURING METHOD

The gear cutter cuts a single space during a single index cycle. The gear cutter is mounted to the cradle of the cutting machine. The machine cradle with the cutter may be imagined as a crown gear that meshes with the gear being cut. The cradle with the mounted head cutter rotates slowly

about its axis, as does the gear which is being cut. The combined process generates the gear tooth surface. The cradle only rotates far enough so that one space is cut out and then it rapidly reverses while the workpiece is withdrawn from the cutter and indexed ahead in preparation for the cutting the next tooth. The desired cutter velocity is provided while the cutter spins about its axis which itself moves in a circular path.

We consider that two generating surfaces, Σ_F and Σ_p, are used for the generation of the pinion tooth surface, Σ_1, and the gear tooth surface, Σ_2, respectively. Both sides of the gear tooth are cut simultaneously (duplex method) but both sides of the pinion tooth are cut separately (single method). The basic machine-tool settings provide that four surfaces, Σ_F, Σ_p, Σ_1 and Σ_2, are in contact at the main contact point. In the process of meshing, surfaces Σ_F and Σ_1, and respectively surfaces Σ_p and Σ_2, contact each other at every instant at a line (contact line) which is a spatial curve. The shape of the contact line and its location on the contacting surfaces is changed in the process of meshing. The generated pinion and gear tooth surfaces are in contact at a point (contact point) at every instant.

A head-cutter used for the gear generation is shown in Fig. 1.1. The shapes of the blades of the head-cutter are straight lines which generate a cone while the head-cutter rotates about axis C-C. The angular velocity about axis C-C does not depend on the generation motion but only on the desired cutting velocity. Two head-cutters are used for the pinion generation; they are provided with one-sided blades and cut the respective tooth sides separately. The head cutter is mounted to the cradle of the machine. Fig. 1.2 shows schematically the positioning of the cradle of the gear machine, the head cutter and the gear to-be generated.

2. GENERATING SURFACES AND COORDINATE SYSTEMS

The generating surface is a cone surface (Fig. 2.1). This surface is generated in coordinate system $S_c^{(j)}$ while the blades of the head-cutter rotate about axis C-C (Fig. 1.1). The generation of gear tooth surfaces is based on application of two tool surfaces, Σ_F and Σ_P, which generate gears 1 and 2, respectively. The generating surfaces (generating cones) do not coincide: they have different cone angles $\psi_c^{(F)}$ and $\psi_c^{(P)}$, and different mean radii $r_c^{(F)}$ and $r_c^{(P)}$ (Fig. 2.1,a). Special machine-tool settings, ΔE_1 and ΔL_1 (Fig. 2.3,b), must be used for the generation of the pinion.

Considering the generation of gear 2 tooth surface we use the following coordinate systems: (i) $S_c^{(P)}$ which is rigidly connected to the generating surface Σ_p (Fig. 2.1,b); (ii) the fixed coordinate system $S_m^{(2)}$ which is rigidly connected to the frame of the cutting machine, and (iii) the coordinate system S_2 which is rigidly connected to gear 2 (Fig. 2.2). In the process of generation the generating surface rotates about the $X_m^{(2)}$ - axis with the angular velocity $\underset{\sim}{\omega}^{(P)}$ while the gear blank rotates about the Z_2 axis with the angular velocity $\underset{\sim}{\omega}^{(2)}$. Axes $X_m^{(2)}$ and Z_2 intersect each other and form the angle $90° + \gamma_2 - \Delta_2$, where Δ_2 is the dedendum angle for gear 2. Axis $X_m^{(2)}$ is perpendicular to the generatrix of the root cone of gear 2. The coordinate system S_f shown in Fig. 2.2 is rigidly connected to the housing of the gears and will be used for the analysis of conditions of meshing of the gears.

Considering the generation of the pinion we use the following coordinate systems: (i) $S_c^{(F)}$ which is rigidly connected to the generating surface Σ_F, (ii) $S_m^{(1)}$ which is rigidly connected to the frame of the cutting machine and (iii) S_1 which is rigidly connected to the pinion (gear (Fig. 2.3). Axes $X_m^{(1)}$ and Z_1 do not intersect but cross each other; ΔE_1

and ΔL_1 are the corrections of machine-tool settings which are used for the improvement of meshing of the gears. In the process of generation the generating surface rotates about the $X_m^{(1)}$ -axis with the angular velocity $\underset{\sim}{\omega}^{(F)}$ while the gear 1 blank rotates about the Z_1 -axis with the angular velocity $\underset{\sim}{\omega}^{(1)}$. Axes $X_m^{(1)}$ and Z_1 form the angle $90° - \gamma_1 + \Delta_1$, where Δ_1 is the dedendum angle of gear 1; axis $X_m^{(1)}$ is perpendicular to the generatrix of the root cone of gear 1.

3. GENERATING TOOL SURFACES

The tool surface is a cone and is represented in the coordinate system $S_s^{(j)}$ as follows (Fig. 2.1)

$$\begin{bmatrix} x_s^{(j)} \\ y_s^{(j)} \\ z_s^{(j)} \\ 1 \end{bmatrix} = \begin{bmatrix} r_c^{(j)}\cot\psi_c^{(j)} - u_j\cos\psi_c^{(j)} \\ u_j\sin\psi_c^{(j)}\sin\theta_j \\ u_j\sin\psi_c^{(j)}\cos\theta_j \\ 1 \end{bmatrix} \quad (j = F, P) \qquad (3.1)$$

where u_j and θ_j are the surface coordinates.

The coordinate system $S_c^{(j)}$ (j = F, P) is an auxiliary coordinate system which is also rigidly connected to the tool (Fig. 2.1,b). To represent the generating surfaces Σ_F and Σ_P in coordinate system $S_c^{(j)}$ we use the following matrix equation

$$\begin{bmatrix} x_c^{(j)} \\ y_c^{(j)} \\ z_c^{(j)} \\ 1 \end{bmatrix} = [M_{cs}^{(j)}] \begin{bmatrix} x_s^{(j)} \\ y_s^{(j)} \\ z_s^{(j)} \\ 1 \end{bmatrix}$$

$$= \begin{bmatrix} 1 & 0 & 0 & 0 \\ 0 & \cos q_j & \mp \sin q_j & \mp b_j \sin q_j \\ 0 & \pm \sin q_j & \cos q_j & b_j \cos q_j \\ 0 & 0 & 0 & 1 \end{bmatrix} \begin{bmatrix} x_s^{(j)} \\ y_s^{(j)} \\ z_s^{(j)} \\ 1 \end{bmatrix} \qquad (3.2)$$

Here: b_j and q_j are parameters which determine the location of the tool in the coordinate system $S_c^{(j)}$. Henceforth, the upper sign corresponds to the generation of a left-hand spiral bevel gear that is shown in Fig. 2.1 and lower sign for a right-hand spiral bevel gear.

Equations (3.1) and (3.2) yield

$$\begin{aligned} x_c^{(j)} &= r_c^{(j)} \cot\psi_c^{(j)} - u_j \cos\psi_c^{(j)} \\ y_c^{(j)} &= u_j \sin\psi_c^{(j)} \sin(\theta_j \mp q_j) \mp b_j \sin q_j \\ z_c^{(j)} &= u_j \sin\psi_c^{(j)} \cos(\theta_j \mp q_j) + b_j \cos q_j \end{aligned} \qquad (3.3)$$

where j = (F, P).

The unit normal to the generating surface Σ_j (j = F, P) is represented

by

$$\underset{\sim c}{n}_{c}^{(j)} = \frac{\underset{\sim c}{N}_{c}^{(j)}}{|\underset{\sim c}{N}_{c}^{(j)}|} \quad , \text{ where } \underset{\sim c}{N}_{c}^{(j)} = \frac{\partial \underset{\sim c}{r}_{c}^{(j)}}{\partial \theta_j} \times \frac{\partial \underset{\sim c}{r}_{c}^{(j)}}{\partial u_j} \tag{3.4}$$

Using Eqs. (3.3) and (3.4) (provided $u_j \sin\psi_c^{(j)} \neq 0$), we obtain

$$\underset{\sim c}{n}_{c}^{(j)} = \sin\psi_c^{(j)} \underset{\sim c}{i}^{(j)} + \cos\psi_c^{(j)} [\sin(\theta_j \mp q_j) \underset{\sim c}{j}^{(j)} + \cos(\theta_j - q_j) \underset{\sim c}{k}^{(j)}] \tag{3.5}$$

4. EQUATIONS OF MESHING BY CUTTING

Generation of Σ_1. We derive the equation of meshing of the generating surface Σ_F and the gear tooth surface Σ_1 using the following procedure:

Step 1: First, we derive the family of surfaces Σ_F that we represent in the coordinate system $S_m^{(1)}$. Such a family is generated while the coordinate system $S_c^{(F)}$ is rotated about the $X_m^{(1)}$ -axis (Fig. 2.3). We recall that the generating surface Σ_F is rigidly connected to $S_c^{(F)}$. The coordinate transformation in transition from $S_c^{(F)}$ to $S_m^{(1)}$ is represented by the following matrix equation

$$\begin{bmatrix} x_m^{(1)} \\ y_m^{(1)} \\ z_m^{(1)} \\ 1 \end{bmatrix} = [M_{m\,c}^{(1)(F)}] \begin{bmatrix} x_c^{(F)} \\ y_c^{(F)} \\ z_c^{(F)} \\ 1 \end{bmatrix} \tag{4.1}$$

Here (Fig. 2.3):

$$[M_{mc}^{(1)(F)}] = \begin{bmatrix} 1 & 0 & 0 & 0 \\ 0 & \cos\phi_F & \sin\phi_F & 0 \\ 0 & -\sin\phi_F & \cos\phi_F & 0 \\ 0 & 0 & 0 & 1 \end{bmatrix} \tag{4.2}$$

where ϕ_F is the angle of rotation about the $X_m^{(1)}$ -axis.

Using Eqs. (4.1), (4.2) and (3.3), we obtain

$$[r_m^{(1)}] = \begin{bmatrix} x_m^{(1)} \\ y_m^{(1)} \\ z_m^{(1)} \\ 1 \end{bmatrix} = \begin{bmatrix} r_c^{(F)}\cot\psi_c^{(F)} - u_F\cos\psi_c^{(F)} \\ u_F\sin\psi_c^{(F)}\sin\tau_F \mp b_F\sin(q_F \mp \phi_F) \\ u_F\sin\psi_c^{(F)}\cos\tau_F + b_F\cos(q_F \mp \phi_F) \\ 1 \end{bmatrix} \tag{4.3}$$

where

$$\tau_F = \theta_F \mp q_F + \phi_F$$

The upper sign corresponds to the right-hand spiral bevel pinion.

Equations (4.3), with parameter ϕ_F fixed, represent a <u>single</u> surface of the family of generating surfaces.

<u>Step 2</u>: The unit normal to the generating surface Σ_F may be represented in the coordinate systems $S_m^{(1)}$ as follows:

$$\underset{\sim}{n}_m^{(1)} = \frac{\underset{\sim}{N}_m^{(1)}}{|\underset{\sim}{N}_m^{(1)}|} \quad , \text{ where } \underset{\sim}{N}_m^{(1)} = \frac{\partial \underset{\sim}{r}_m^{(1)}}{\partial\theta_F} \times \frac{\partial \underset{\sim}{r}_m^{(1)}}{\partial u_F} \tag{4.4}$$

We may also use an alternative method for the derivation of the unit normal. This method is based on the matrix equation.

$$[n_m^{(1)}] = [L_{m\ c}^{(1)(F)}]\ [n_c^{(F)}] \tag{4.5}$$

Matrix $[L_{m\ c}^{(1)(F)}]$ may be determined by deleting the 4^{th} column and rows in matrix (4.2).

The column matrix $[n_c^{(F)}]$ is given by vector equation (3.5). After transformations, we obtain

$$[n_m^{(1)}] = \begin{bmatrix} \sin\psi_c^{(F)} \\ \cos\psi_c^{(F)} \sin\tau_F \\ \cos\psi_c^{(F)} \cos\tau_F \end{bmatrix} \tag{4.6}$$

Step 3: We derive the equations of the relative velocity, $\underset{\sim m}{v}^{(F1)}$, as follows:

$$\underset{\sim m}{v}^{(F1)} = \underset{\sim m}{v}^{(F)} - \underset{\sim m}{v}^{(1)} \tag{4.7}$$

where $\underset{\sim m}{v}^{(F)}$ is the velocity of a point N on surface Σ_F and $\underset{\sim m}{v}^{(1)}$ is the velocity of the same point N on surface Σ_1.

Vector $\underset{\sim m}{v}^{(F)}$ is represented by the equation

$$\underset{\sim m}{v}^{(F)} = \underset{\sim m}{\omega}^{(F)} \times \underset{\sim m}{r}^{(1)} \tag{4.8}$$

Here (Fig. 2.3):

$$[\omega_m^{(F)}] = \begin{bmatrix} -\omega^{(F)} \\ 0 \\ 0 \end{bmatrix} \tag{4.9}$$

Vector $\underset{\sim}{r}_m^{(1)}$ is represented by equation (4.3).

Equations (4.8) and (4.9) yield

$$[v_m^{(F)}] = \omega^{(F)} \begin{bmatrix} 0 \\ z_m^{(1)} \\ -y_m^{(1)} \end{bmatrix} \tag{4.10}$$

Gear 1 rotates about the Z_1 - axis with the angular velocity $\underset{\sim}{\omega}^{(1)}$ (Fig.2.3). Since $\underset{\sim}{\omega}^{(1)}$ does not pass through the origin $O_m^{(1)}$, of the coordinate system $S_m^{(1)}$, we substitute $\underset{\sim}{\omega}^{(1)}$ by an equal vector which passes through $O_m^{(1)}$ and the vector moment represented by

$$\overline{O_m^{(1)}O_h} \times \underset{\sim}{\omega}^{(1)}$$

Then, we represent $\underset{\sim m}{v}^{(1)}$ as follows

$$\underset{\sim m}{v}^{(1)} = \underset{\sim m}{\omega}^{(1)} \times \underset{\sim m}{r}^{(1)} + \overline{O_m^{(1)}O_h} \times \underset{\sim m}{\omega}^{(1)} \tag{4.11}$$

Here:

$$\overline{O_m^{(1)}O_h} = \begin{bmatrix} L\sin\Delta_1 \\ -\Delta E_1 \\ -\Delta L_1 \end{bmatrix}, \text{ and } [\omega_m^{(1)}] = -\omega^{(1)} \begin{bmatrix} \sin(\gamma_1 - \Delta_1) \\ 0 \\ \cos(\gamma_1 - \Delta_1) \end{bmatrix} \tag{4.12}$$

where $L = O_h M$.

Equations (4.11) - (4.12) yield

$$[v_m^{(1)}] = -\omega^{(1)} \begin{vmatrix} \underset{\sim}{i}_m^{(1)} & j_m^{(1)} & \underset{\sim}{k}_m^{(1)} \\ \sin(\gamma_1 - \Delta_1) & 0 & \cos(\gamma_1 - \Delta_1) \\ x_m^{(1)} & y_m^{(1)} & z_m^{(1)} \end{vmatrix} -$$

$$\omega^{(1)} \begin{vmatrix} \underset{\sim}{i}_m^{(1)} & j_m^{(1)} & \underset{\sim}{k}_m^{(1)} \\ L\sin\Delta_1 & -\Delta E_1 & -\Delta L_1 \\ \sin(\gamma_1 - \Delta_1) & 0 & \cos(\gamma_1 - \Delta_1) \end{vmatrix} =$$

$$-\omega^{(1)} \begin{bmatrix} -(y_m^{(1)} + \Delta E_1)\cos(\gamma_1 - \Delta_1) \\ (x_m^{(1)} - L\sin\Delta_1)\cos(\gamma_1 - \Delta_1) - (z_m^{(1)} + \Delta L_1)\sin(\gamma_1 - \Delta_1) \\ (y_m^{(1)} + \Delta E_1)\sin(\gamma_1 - \Delta_1) \end{bmatrix} \tag{4.13}$$

The final expression for $\underset{\sim}{v}_m^{(F1)}$ is

$$[v_m^{(F1)}] =$$

$$\begin{bmatrix} -\omega^{(1)}(y_m^{(1)} + \Delta E_1)\cos(\gamma_1 - \Delta_1) \\ \omega^{(F)}z_m^{(1)} + \omega^{(1)}\left\{(x_m^{(1)} - L\sin\Delta_1)\cos(\gamma_1 - \Delta_1) - (z_m^{(1)} + \Delta L_1)\sin(\gamma_1 - \Delta_1)\right\} \\ -\omega^{(F)}y_m^{(1)} + \omega^{(1)}(y_m^{(1)} + \Delta E_1)\sin(\gamma_1 - \Delta_1) \end{bmatrix}$$

(4.14)

Step 4: The equation of meshing by cutting is represented by

$$\underset{\sim}{n}_m^{(1)} \cdot \underset{\sim}{v}_m^{(F1)} = 0 \tag{4.15}$$

Using equations (4.15), (4.14), (4.6) and (4.3), we obtain

$$\left\{-u_F + [r_c^{(F)}\cot\psi_c^{(F)} - L\sin\Delta_1 - \Delta L_1 \tan(\gamma_1 - \Delta_1)]\cos\psi_c^{(F)}\right\} \sin\tau_F \pm$$

$$b_F\left[\sin\psi_c^{(F)}\sin(q_F \mp \phi_F) \pm \cos\psi_c^{(F)}\sin\theta_F \frac{m_{F1} - \sin(\gamma_1 - \Delta_1)}{\cos(\gamma_1 - \Delta_1)}\right] -$$

$$\Delta E_1[\sin\psi_c^{(F)} - \cos\psi_c^{(F)}\tan(\gamma_1 - \Delta_1)\cos\tau_F] =$$

$$f_1(u_F, \theta_F, \phi_F) = 0 \tag{4.16}$$

Here:

$$m_{F1} = \frac{\omega^{(F)}}{\omega^{(1)}}$$

This equation relates the generating surface coordinates (u_F, θ_F) with the angle of rotation (ϕ_F).

Generation of Σ_2. By using a similar procedure we may obtain the equation of meshing for surface Σ_p and surface Σ_2 as follows

Step 1: Equations of the family of generating surfaces Σ_p represented in the coordinate system $S_m^{(2)}$ are:

$$\begin{bmatrix} x_m^{(2)} \\ y_m^{(2)} \\ z_m^{(2)} \end{bmatrix} = \begin{bmatrix} r_c^{(p)}\cot\psi_c^{(p)} - u_p\cos\psi_c^{(p)} \\ u_p\sin\psi_c^{(p)}\sin\tau_p \mp b_p\sin(q_p \mp \phi_p) \\ u_p\sin\psi_c^{(p)}\cos\tau_p + b_p\cos(q_p \mp \phi_p) \end{bmatrix} \tag{4.17}$$

Step 2: The unit normal to Σ_p is represented in $S_m^{(2)}$ by the column matrix

$$[n_m^{(2)}] = \begin{bmatrix} \sin\psi_c^{(p)} \\ \cos\psi_c^{(p)} \quad \sin\tau_p \\ \cos\psi_c^{(p)} \quad \cos\tau_p \end{bmatrix} \tag{4.18}$$

where

$$\tau_p = \theta_p \mp q_p + \phi_p$$

The upper sign corresponds to the left-hand spiral bevel gear and the lower to the right-hand spiral bevel gear.

Step 3: The velocities $\underset{\sim}{v}_m^{(P)}$, $\underset{\sim}{v}_m^{(2)}$ and $\underset{\sim}{v}_m^{(P2)}$ are represented in $S_m^{(2)}$ as follows

$$[v_m^{(P)}] = \omega^{(P)} \begin{bmatrix} 0 \\ z_m^{(2)} \\ -y_m^{(2)} \end{bmatrix} \tag{4.19}$$

$$[v_m^{(2)}] = -\omega^{(2)} \begin{bmatrix} y_m^{(2)}\cos(\gamma_2 - \Delta_2) \\ -(x_m^{(2)} + L\sin\Delta_2)\cos(\gamma_2 - \Delta_2) - z_m^{(2)}\sin(\gamma_2 - \Delta_2) \\ y_m^{(2)}\sin(\gamma_2 - \Delta_2) \end{bmatrix} \tag{4.20}$$

$$[v_m^{(P2)}] = [v_m^{(P)}] - [v_m^{(2)}] \tag{4.21}$$

Step 4: The equation of meshing

$$\underset{\sim}{n}_m^{(2)} \cdot \underset{\sim}{v}_m^{(P2)} = 0$$

yields the following equation

$$f_2(u_P, \theta_P, \phi_P) =$$

$$[u_P - (r_c^{(P)}\cot\psi_c^{(P)} + L\sin\Delta_2)\cos\psi_c^{(P)}]\sin\tau_P \mp$$

$$b_P\sin(q_P \mp \phi_P)\sin\psi_c^{(P)} + b_P\cos\psi_c^{(P)}\sin\theta_P \frac{m_{P2} - \sin(\gamma_2 - \Delta_2)}{\cos(\gamma_2 - \Delta_2)} = 0 \tag{4.22}$$

Here:

$$m_{P2} = \frac{\omega^{(P)}}{\omega^{(2)}}$$

5. ORIENTATION OF THE PINION CRADLE

Henceforth, we will consider two auxiliary coordinate systems S_f and S_h, that are rigidly connected to the gear and pinion cutting machines, respectively (Fig. 5.1).

Figure 2.2 shows coordinate system S_f that is rigidly connected to the gear cutting machine and to coordinate system $S_m^{(2)}$. Coordinate system S_f is also rigidly connected to the housing of the gear train and the meshing of the generated pinion and gear will be also considered in coordinate system S_f. Axis Z_f is the instantaneous axis of rotation of the pinion and the gear - the pitch line (the line of tangency of the pinion and gear pitch cones). The origin O_f of coordinate system S_f coincides with the points of intersection of 3 axes: $X_m^{(2)}$, Z_2 (Fig. 2.2) and Z_1 (Fig. 2.3). Here: $X_m^{(2)}$ is the axis of rotation of the gear cradle; Z_2 is the axis of rotation of the gear being in mesh with the generating gear Σ_P and Z_1 is the axis of rotation of the pinion being in mesh with the generating gear Σ_F and the gear member.

Figure 2.3 shows coordinate system S_h that is rigidly connected to the pinion cutting machine and coordinate system $S_m^{(1)}$. The origin O_h of coordinate system S_h coincides with the origin O_f but the orientation of system S_h with respect to S_f represents a parameter of the machine-tool settings (proposed by Litvin, 1968). This parameter is designated by ε in Fig. 5.1.

The coordinate transformation in transition from S_h to S_f is based on the following considerations.

(i) Consider two auxiliary coordinate systems, S_a and S_b, that are rigidly connected to systems S_f and S_h, respectively (Fig. 5.1,a and Fig. 5.1,b), axes Z_a and Z_b coincide with the pinion axis. Initially coordinate system S_b coincides with S_a and system S_h with S_f.

(ii) Assume now that coordinate systems S_b and S_h are rotated about the Z_a-axis, the axis of the pinion, through the angle ε (Fig. 5.1,c). This angle determines the orientation of coordinate system S_h with respect to S_f, or the orientation of the pinion cutting machine with respect to the gear cutting machine. Matrix $[M_{fh}]$ represents the coordinate transformation in transition from S_h to S_f and is represented by the following equation

$$[M_{fh}] = [M_{fa}]\ [M_{ab}]\ [M_{bh}]$$

$$= \begin{bmatrix} \cos\varepsilon\cos^2\gamma_1 + \sin^2\gamma_1 & \sin\varepsilon\cos\gamma_1 & \cos\gamma_1\sin\gamma_1(1 - \cos\varepsilon) & 0 \\ -\sin\varepsilon\cos\gamma_1 & \cos\varepsilon & \sin\varepsilon\sin\gamma_1 & 0 \\ \cos\gamma_1\sin\gamma_1\ (1 - \cos\varepsilon) & -\sin\varepsilon\sin\gamma_1 & \cos\varepsilon\sin^2\gamma_1 + \cos^2\gamma_1 & 0 \\ 0 & 0 & 0 & 1 \end{bmatrix} \tag{5.1}$$

6. PLANE OF NORMALS

It will be proven below that the generating surfaces Σ_P and Σ_F contact each other at a point that moves in the same plane, Π. The generated pinion and gear surfaces, Σ_1 and Σ_2, also contact each other at every instant at a point that coincides with the point of tangency of surfaces Σ_f and Σ_P. However, we have to emphasize that surfaces Σ_F and Σ_1 (respectively, Σ_P and Σ_2) are in line contact and the instantaneous line of contact moves over the contacting surfaces. The special property of the method developed for generation of spiral bevel gears is that the contact point moves in a plane (plane Π) that is rigidly connected to the fixed

coordinate system S_f. Also, the common normal to the contacting surfaces lies in plane Π and, as it will be shown later, performs a parallel motion in the process of meshing. Plane Π is called the plane of normals and it is determined as the plane that passes through the instantaneous axis of rotation, Z_f, and the normal $\underset{\sim}{N}$ to the generating surface Σ_p (Fig. 6.1). The above normal passes through point N that is the main gear contact point.

Figure 6.2 shows the orientation of coordinate system S_n with respect to coordinate system S_f. Origin O_n coincides with origin O_f and axis Z_f coincides with the Z_n - axis. The coordinate transformation in transition from S_n to S_f is given by the matrix

$$[L_{fn}] = \begin{bmatrix} \cos\eta & -\sin\eta & 0 \\ \sin\eta & \cos\eta & 0 \\ 0 & 0 & 1 \end{bmatrix} \tag{6.1}$$

The determination of angle η is based on the following considerations: (1) unit vector $\underset{\sim}{i}_n$ can be represented in coordinate system S_f by the following matrix equation

$$[i_f^{(n)}] = [L_{fn}][i_n] = \begin{bmatrix} \cos\eta & -\sin\eta & 0 \\ \sin\eta & \cos\eta & 0 \\ 0 & 0 & 1 \end{bmatrix} \begin{bmatrix} 1 \\ 0 \\ 0 \end{bmatrix}$$

$$= \begin{bmatrix} \cos\eta \\ \sin\eta \\ 0 \end{bmatrix} \tag{6.2}$$

(2) The unit normal $\underset{\sim}{n}_f^{(P)}$ to the generating surface Σ_p is represented as follows

$$[n_f^{(P)}] = [L_{fm}^{(2)}][n_m^{(2)}] \tag{6.3}$$

Here (Fig. 2.2)

$$[L_{fm}^{(2)}] = \begin{bmatrix} \cos\Delta_2 & 0 & -\sin\Delta_2 \\ 0 & 1 & 0 \\ \sin\Delta_2 & 0 & \cos\Delta_2 \end{bmatrix} \tag{6.4}$$

Unit vector $\underset{\sim}{n}_m^{(2)}$ is given by column matrix (4.18). Equations (6.3), (6.4) and (4.18) yield

$$[n_f^{(P)}] = \begin{bmatrix} \sin\psi_c^{(P)}\cos\Delta_2 - \cos\psi_c^{(P)}\cos\tau_p\sin\Delta_2 \\ \cos\psi_c^{(P)}\sin\tau_p \\ \sin\psi_c^{(P)}\sin\Delta_2 + \cos\psi_c^{(P)}\cos\tau_p\cos\Delta_2 \end{bmatrix} \tag{6.5}$$

(3) Vectors $\underset{\sim}{i}_f^{(n)}$ and $\underset{\sim}{n}_f^{(P)}$ are mutual perpendicular, i.e., $\underset{\sim}{i}_f^{(n)} \cdot \underset{\sim}{n}_f^{(P)} = 0$. This yields that

$$\tan\eta = -\frac{\tan\psi_c^{(P)}\cos\Delta_2 - \cos\tau_p\sin\Delta_2}{\sin\tau_p} \tag{6.6}$$

Here:

$$\tau_p = \theta_p \mp q_p + \phi_p$$

with the upper sign for the left-hand gear,

$\psi_c^{(P)} = \alpha_p$ for the convex gear tooth side,

$\psi_c^{(P)} = 180° - \alpha_p$ for the concave gear tooth side

where α_p is the angle of the cutter blade.

Equation (6.6) determines the angle of orientation η of the plane of normals (Fig. 6.2).

7. PERFORMANCE OF PARALLEL MOTION OF A STRAIGHT LINE PROVIDED BY TWO RELATED ELLIPSES.

An important part of the proposed approach is a new technique directed at the performance of a parallel motion of a straight line provided by two related ellipses. By using this technique it becomes possible to provide a parallel motion for the common normal to the gear-pinion tooth surfaces. This motion is performed in a plane (the plane of normals) that is rigidly connected to the gear housing and has the prescribed orientation.

It is well known that a translational motion of a straight line may be performed by a parallelogram linkage (Fig. 7.1,a). Consider that a straight line slides by its points A and C along two circles of equal radii. Vectors $\underset{\sim}{v}_A$ and $\underset{\sim}{v}_C$ which represent the velocities of points A and C of the moving straight line are equal. The moving straight line AC being initially installed parallel to the center distance OD will keep its original direction in the process of motion.

The discussed principle of translational motion of a straight line may be extended for the case where the straight line slides along two mating ellipses (Fig. 7.1,b). These ellipses have the same dimensions and orientation and again the velocity vectors $\underset{\sim}{v}_A$ and $\underset{\sim}{v}_C$ are equal. Consider that the moving straight line is initially installed parallel to OD where O

and D are the foci of symmetry of the ellipses. Then, with $\underset{\sim}{v}_A = \underset{\sim}{v}_C$ the moving straight line will keep its original direction in the process of motion.

Figure 7.1(a) and Fig. 7.1(b) show a translational motion of a segment of a straight line (AC) with constant length. A more general case is represented in Fig. 7.1(c). The straight line slides over two ellipses whose dimensions and orientation are different. The length of segment AC which slides along the ellipses is changed in the process of motion. The problem is how to provide a parallel motion of the the moving straight line. We call this motion a parallel one because the straight line has to keep its initial parallel to line OD where O and D are the foci of symmetry of two mating ellipses. Unlike the cases which are shown in Fig. 7.1(a) and Fig. 7.1(b) the motion of straight line is not translation because the velocities $\underset{\sim}{v}_A$ and $\underset{\sim}{v}_C$ of the tracing points A and C are not equal. The distance between the sliding points A and C is changed in the process of motion. It will be proven that the required parallel motion of straight line may be performed with certain relations between the dimensions and orientation parameters of two guiding ellipses which are shown in Fig. 7.1(c).

Consider that an ellipse (Fig. 7.2) is represented in coordinate system S_a by the equations

$$x_a = 0, \quad y_a = a_p \cos\mu_p, \quad z_a = b_p \sin\mu_p \tag{7.1}$$

where a_p and b_p are the lengths of the semimajor and semiminor axes, respectively, D is the origin of coordinate S_a and the symmetry focus of the ellipse; parameter μ_p determines the location of a point on the ellipse.

Coordinate system S_n has the same origin as S_a and the orientation of S_n with respect to S_a is given by angle δ_P. To represent the ellipse in coordinate system S_n we use the following matrix equation.

$$[r_n^{(P)}] = [M_{na}][r_a^{(P)}] \tag{7.2}$$

where

$$[M_{na}] = \begin{bmatrix} 1 & 0 & 0 & 0 \\ 0 & \cos\delta_P & -\sin\delta_P & 0 \\ 0 & \sin\delta_P & \cos\delta_P & 0 \\ 0 & 0 & 0 & 1 \end{bmatrix} \tag{7.3}$$

Matrix equation (7.2) yields

$$x_n^{(P)} = 0,\ y_n^{(P)} = a_P\cos\delta_P\cos\mu_P - b_P\sin\delta_P\sin\mu_P$$

$$z_n^{(P)} = a_P\sin\delta_P\cos\mu_P + b_P\cos\delta_P\sin\mu_P \tag{7.4}$$

The symmetry focus of the mating ellipse is point 0 given by coordinates: $C_1 = 0$, $C_2 = y_n^{(0)}$, $C_3 = z_n^{(0)}$ (C_2 and C_3 are algebraic values). The orientation of the ellipse is given by angle δ_F (Fig. 7.2). Equations of the mating ellipse are represented in coordinate system S_n as follows

$$x_n^{(F)} = 0,\ y_n^{(F)} = a_F\cos\delta_F\cos\mu_F - b_F\sin\delta_F\sin\mu_F + C_2,$$

$$Z_n^{(F)} = a_F\sin\delta_F\cos\mu_F + b_F\cos\delta_F\sin\mu_F + C_3 \tag{7.5}$$

Consider point A of ellipse 1 is determined by parameter μ_{PO}. Point C of ellipse 2 is determined with parameter μ_{FO}. Henceforth we will consider such a motion where $\mu_P - \mu_{PO} = \mu_F - \mu_{FO} = \mu$. Line AC is drawn through points A and C. Our goal is to provide that line AC will be parallel to the center distance DO for any value of the motion parameter μ and perform a parallel motion. The above-mentioned goal can be achieved with certain relations between the ellipse parameters a_P, b_P, δ_P, a_F, b_F and δ_F. We start the derivation of these relations by considering the vector equation

$$\overline{DA}(\mu) + \overline{AC}(\mu) = \overline{DO}(\mu) + \overline{OC}(\mu) \tag{7.6}$$

Vector equation $\overline{AC}(\mu) = \lambda\overline{DO}$ is satisfied with any value of μ if the parallel motion of line AC is provided. (Where λ is the constant required to make the two vectors of equal magnitude.)
Equation (7.6) yields

$$\frac{(\overline{OC} - \overline{DA}) \cdot \underset{\sim}{j}_n}{(\overline{OC} - \overline{DA}) \cdot \underset{\sim}{k}_n} = \frac{(\lambda-1)(\overline{DO} \cdot \underset{\sim}{j}_n)}{(\lambda-1)(\overline{DO} \cdot \underset{\sim}{k}_n)} = \frac{\cos q}{\sin q} \tag{7.7}$$

Here: $\underset{\sim}{j}_n$ and $\underset{\sim}{k}_n$ are the unit vectors of axes Y_n and Z_n, q is the angle formed by axis Y_n and vector $\overline{DO}$ (Fig. 7.2). For the further transformation we will represent μ_P and μ_F as follows

$$\mu_P = \mu_{PO} + \mu, \quad \mu_F = \mu_{FO} + \mu \tag{7.8}$$

Equations (7.7), (7.4), (7.5) and (7.8) yield

$$(b_{11}\sin q - a_{11}\sin q - b_{21}\cos q + a_{21}\cos q)\cos\mu$$

$$+ (-b_{12}\sin q + b_{22}\cos q + a_{12}\sin q - a_{22}\cos q)\sin\mu = 0 \tag{7.9}$$

Here:

$$a_{11} = a_P \cos\delta_P \cos\mu_{P0} - b_P \sin\delta_P \sin\mu_{P0}$$

$$a_{12} = a_P \cos\delta_P \sin\mu_{P0} + b_P \sin\delta_P \cos\mu_{P0}$$

$$a_{21} = a_P \sin\delta_P \cos\mu_{P0} + b_P \cos\delta_P \sin\mu_{P0}$$

$$a_{22} = a_P \sin\delta_P \sin\mu_{P0} - b_P \cos\delta_P \cos\mu_{P0} \qquad (7.10)$$

Coefficients b_{11}, b_{12}, b_{21} and b_{22} have similar expressions.

Equations (7.9) must be satisfied for any value of the motion parameter μ. This means that equation (7.9) will be satisfied for any value of μ if the following two equations are satisfied simultaneously.

$$b_{11}\sin q - b_{21}\cos q - a_{11}\sin q + a_{21}\cos q = 0 \qquad (7.11)$$

$$b_{12}\sin q - b_{22}\cos q - a_{12}\sin q + a_{22}\cos q = 0 \qquad (7.12)$$

Equations (7.10), (7.11) and (7.12) yield a system of two pseudo-linear equations in two unknowns ($\cos\mu_{F0}$ and $\sin\mu_{F0}$):

$$a_F \sin(q-\delta_F)\cos\mu_{F0} - b_F \cos(q-\delta_F)\sin\mu_{F0} = d_1 \qquad (7.13)$$

$$b_F \cos(q-\delta_F)\cos\mu_{F0} + a_F \sin(q-\delta_F)\sin\mu_{F0} = d_2 \qquad (7.14)$$

Here:

$$d_1 = a_P \sin(q-\delta_P)\cos\mu_{P0} - b_P \cos(q-\delta_P)\sin\mu_{P0} \qquad (7.15)$$

$$d_2 = a_P \sin(q-\delta_P)\sin\mu_{P0} + b_P \cos(q-\delta_P)\cos\mu_{P0} \qquad (7.16)$$

The solution of equations (7.13) and (7.14) for $\cos\mu_{FO}$ and $\sin\mu_{FO}$ is as follows

$$\cos\mu_{FO} = \frac{a_F d_1 \sin(q-\delta_F) + b_F d_2 \cos(q-\delta_F)}{a_F^2 \sin^2(q-\delta_F) + b_F^2 \cos^2(q-\delta_F)} \tag{7.17}$$

$$\sin\mu_{FO} = \frac{a_F d_2 \sin(q-\delta_F) - b_F d_1 \cos(q-\delta_F)}{a_F^2 \sin^2(q-\delta_F) + b_F^2 \cos^2(q-\delta_F)} \tag{7.18}$$

Equations (7.13) and (7.14) yield

$$a_F^2 \sin^2(q-\delta_F) + b_F^2 \cos^2(q-\delta_F) = d_1^2 + d_2^2 \tag{7.19}$$

Equations (7.19) relates 3 parameters of the mating ellipse: a_F, b_F and δ_F. (Parameters a_p, b_p, δ_p of the first ellipse and q are considered as given). Thus Eq. (7.19) can be satisfied with various combinations of a_F, b_F and δ_F.

Example: $a_p = 2$, $b_p = 1.25$, $\delta_p = 20°$, $q = 270°$, $\frac{a_F}{b_F} = 3$, $\mu_{PO} = \mu_{FO} = 0$. Then we obtain: $a_F = 2.2753$, $\delta_F = 34.3113°$. These ellipses are shown in Fig. 7.2.

A linkage which may perform the described parallel motion of line AC is shown in Fig. 7.3. Link 1 is in contact with two perpendicular slots and $DN = a_p$, $DM = b_p$ where $2a_p$ and $2b_p$ are the lengths of the axes of ellipse which is traced out by point A. Similarly, link 1' is in contact with two other perpendicular slots, $ON' = a_F$ and $OM' = b_F$, point C traces out ellipse 2. The orientation of a pair of slots with respect to the other one is determined by the angle $(\delta_F - \delta_p)$ (see Fig. 7.2). Links 1 and 1' rotate with the same angular velocity $\omega = \frac{d\mu}{dt}$. Line AC will perform a parallel motion if the ellipse parameters satisfy equation (7.19).

8. GEAR MACHINE-TOOL SETTINGS

Input Data. The following data are considered as given to set up the gear machine-tool settings.

N_2, the teeth number of the gear

γ_2, the gear pitch angle (Fig. 2.2)

Δ_2, the gear dedendum angle (Fig. 2.2)

β_p, the mean spiral angle (Fig. 2.1)

L , $O_f M_o$, the mean distance of the pitch cone (Fig. 2.2)

W , the point width of the gear cutter (Fig. 8.1)

$\psi^{(p)}$, the blade angle of the gear cutter (Fig. 8.1)

Gear cutting ratio. The gear cutting ratio represents the ratio between the angular velocities of the cradle and the generated gear and is designated by

$$m_{p2} = \frac{\omega^{(p)}}{\omega^{(2)}} \tag{8.1}$$

Henceforth, we will consider the two coordinate systems, $S_m^{(2)}$ and S_f, shown in Figure 2.2. Axis Z_f is the pitch line of the mating spiral bevel gears. It is also the instantaneous axis of rotation of the pinion and the gear that transform rotation with constant angular velocity ratio. Assuming that the generating cone surface, Σ_p, the gear tooth surface, Σ_2, and the pinion tooth surface, Σ_1, are in continuous tangency at every instant, it is required that the instantaneous axis of rotation by the gear cutting must

coincide with the pitch line, axis Z_f. Thus

$$\underset{\sim}{\omega}^{(p2)} = \underset{\sim}{\omega}^{(p)} - \underset{\sim}{\omega}^{(2)} = \lambda \underset{\sim}{k}_f \tag{8.2}$$

This means that vectors $\underset{\sim}{\omega}^{(p2)}$ and $\underset{\sim}{k}_f$ are collinear.

Vectors $\underset{\sim}{\omega}^{(p)}$, $\underset{\sim}{\omega}^{(2)}$ and $\underset{\sim}{k}_f$ are represented in coordinate system $S_m^{(2)}$ as follows

$$\underset{\sim}{\omega}^{(p)} = \begin{bmatrix} -\omega^{(p)} \\ 0 \\ 0 \end{bmatrix} \qquad \underset{\sim}{\omega}^{(2)} = \omega^{(2)} \begin{bmatrix} -\sin(\gamma_2 - \Delta_2) \\ 0 \\ \cos(\gamma_2 - \Delta_2) \end{bmatrix}$$

$$\underset{\sim}{k}_f = \begin{bmatrix} \sin\Delta_2 \\ 0 \\ \cos\Delta_2 \end{bmatrix} \tag{8.3}$$

Equations (8.2) and (8.3) yield that

$$\frac{-\omega^{(p)} + \omega^{(2)}\sin(\gamma_2 - \Delta_2)}{-\omega^{(2)}\cos(\gamma_2 - \Delta_2)} = \tan\Delta_2 \tag{8.4}$$

Equation (8.4) results in that

$$m_{p2} = \frac{\omega^{(p)}}{\omega^{(2)}} = \frac{\sin\gamma_2}{\cos\Delta_2} \tag{8.5}$$

Main Gear Contact Point. The main gear contact point is the center of the bearing contact on the gear tooth surface. The location of this point can be represented by the surface coordinates of the tool cone θ_p and u_p. We can vary the value of u_p by keeping θ_p fixed and obtain the desired location of the main gear contact point.

We start with the case when M_o^* coincides with the pitch point M_o (Figure 8.2). In this case N^* on the cutter surface is the contact point of the pinion and gear tooth surfaces since the normal at this point intersects the instantaneous axis of rotation, Z_f. The basic relations for the left-hand gear for this case are as follows:

$$\theta_p^* = 90° - \beta_p + q_p = \tau_p + q_p \tag{8.6}$$

$$b_p = \frac{L\cos\Delta_2 \sin(\theta_p^* - q_p)}{\sin\theta_p^*} = \frac{L\cos\Delta_2\cos\beta_p}{\cos(\beta_p - q_p)} \tag{8.7}$$

$$\frac{d_p}{2} = \frac{L\cos\Delta_2 \sin q_p}{\sin\theta_p^*} = \frac{L\cos\Delta_2 \sin q_p}{\cos(\beta_p - q_p)} \tag{8.8}$$

$$a = \frac{\omega}{2} + L\sin\Delta_2 \tan\psi_c^{(p)} \tag{8.9}$$

$$r_c^{(p)} = \frac{d_p}{2} - a = \frac{L\cos\Delta_2 \sin q_p}{\sin\theta_p^*} - \frac{\omega}{2} - L\sin\Delta_2 \tan\psi_c^{(p)} \tag{8.10}$$

$$u_p^* = \frac{r_c^{(p)}}{\sin\psi_c^{(p)}} + a\sin\psi_c^{(p)} \tag{8.11}$$

For right-hand gear we need the following changes:

$$\theta_p^* = 270° + \beta_p - q_p = \tau_p - q_p \tag{8.6a}$$

$$b_p = \frac{L\cos\Delta_2 \cos\beta_p}{\sin(\theta_p^* - 180°)} = \frac{L\cos\Delta_2 \cos\beta_p}{\cos(\beta_p - q_p)} \tag{8.7a}$$

$$\frac{d_p}{2} = \frac{L\cos\Delta_2 \sin q_p}{\sin(\theta_p^* - 180°)} = \frac{L\cos\Delta_2 \sin q_p}{\cos(\beta_p - q_p)} \tag{8.8a}$$

Let us now consider point N whose surface coordinates of the tool cone are θ_p^* and

$$u_p = O^{(p)}N = O^{(P)}N^* + N^*N = u_p^* + \Delta u_p \tag{8.12}$$

Point N will become the point of contact if the normal vector of this point passes through M_o'. This requirement will be observed if the cradle is turned at a certain angle ϕ_p that is shown in Figure 8.3. We can determine angle ϕ_p using the equation of meshing of the generating gear and the generated gear, equation (4.22), together with equations (8.5), (8.6), (8.7), (8.8), (8.9), (8.10), (8.11), and (8.12). This yields

$$f_2(\Delta u_p, \phi_p) =$$

$$\Delta u_p \cos(\beta_p \mp \phi_p) \pm L\cos\Delta_2 \sin\psi_c^{(p)} \sin\phi_p + L\sin\Delta_2 \cos\psi_c^{(p)} [\cos\beta_p - \cos(\beta_p \mp \phi_p)] = 0 \tag{8.13}$$

The upper sign corresponds to the left-hand spiral bevel gear and the lower to the right-hand spiral bevel gear. Based on trigonometry transformations a closed form solution for ϕ_p is obtained. That is

$$\tan\frac{\phi_p}{2} = \frac{-A \pm \sqrt{A^2 + B^2 - C^2}}{C - B} \tag{8.14}$$

Here:

$$A = \cos\Delta_2\sin\psi_c^{(p)} - \sin\Delta_2\cos\psi_c^{(p)}\sin\beta_p + \frac{\Delta u_p}{L}\sin\beta_p$$

$$B = \frac{\Delta u_p}{L}\cos\beta_p - \sin\Delta_2\cos\psi_c^{(p)}\cos\beta_p$$

$$C = \sin\Delta_2\cos\psi_c^{(p)}\cos\beta_p$$

For gear concave side using the same equations except

$$a = \frac{W}{2} - L\sin\Delta_2\tan\psi_c^{(p)} \tag{8.15}$$

and

$$r_c^{(p)} = \frac{d_p}{2} + a = \frac{L\cos\Delta_2\sin q_p}{\sin\vartheta_p^*} + \frac{W}{2} - L\sin\Delta_2\tan\psi_c^{(p)} \tag{8.16}$$

we can get the same result.

Equation (8.14) determines the main gear contact points for both convex side and concave side. In general, $\Delta u_p > 0$ for gear convex side, and $\Delta u_p < 0$ for gear concave side. The absolute value of Δu_p for gear convex side is

greater than that of Δu_p for gear concave side.

Direction of the Contact Path. The direction of the contact path may be determined by the direction of the tangent to the contact path at the main contact point. This can be done by differentiating equation (4.22). In the process of motion the contact normal performs a parallel motion. Thus parameter τ_p is a constant and this yields that

$$d\tau_p = 0 \qquad d\theta_p = -d\phi_p \tag{8.17}$$

Taking into account equations (8.17) and (8.5), we obtain after the differentiation of equation (4.22) the following equation

$$\frac{du_p}{d\phi_p} \sin\tau_p + b_p\cos(q_p \mp \phi_p)\sin\psi_c^{(p)} - b_p\cos\psi_c^{(p)}\cos\theta_p\tan\Delta_2 = 0$$

The upper sign corresponds to the left-hand gear and the lower to the right-hand gear. At the main contact point we have that $\theta_p = \theta_p^*$, $\cos\theta_p^* = \sin(\beta_p - q_p)$, $b_p = \frac{L\cos\Delta_2\cos\beta_p}{\cos(\beta_p - q_p)}$. Then we obtain

$$\frac{du_p}{d\phi_p} \sin\tau_p + \frac{L\cos\beta_p}{\cos(\beta_p - q_p)} \left[\cos\Delta_2 \cos(q_p \mp \phi_p)\sin\psi_c^{(p)} - \right.$$

$$\left. \sin\Delta_2\sin(\beta_p - q_p)\cos\psi_c^{(p)}\right] = 0 \tag{8.18}$$

This yields

$$\tan q_p = -\frac{E}{D} \tag{8.19}$$

Here:

$$D = \frac{du_p}{d\phi_p} \sin\beta_p \sin\tau_p \pm L\cos\Delta_2 \sin\psi_c^{(p)} \cos\beta_p \sin\phi_p + L\sin\Delta_2 \cos\psi_c^{(p)} \cos^2\beta_p$$

$$E = \frac{du_p}{d\phi_p} \cos\beta_p \sin\tau_p + L\cos\Delta_2 \sin\psi_c^{(p)} \cos\beta_p \cos\phi_p - L\sin\Delta_2 \cos\psi_c^{(p)} \sin\beta_p \cos\beta_p$$

There is a particular case when the direction of the contact path is parallel to the root cone and thus $\frac{du_p}{d\phi_p} = 0$. For this case, however, $\frac{d_p}{2}$ becomes substantially larger than $L\cos\Delta_2$. More favorable ratio for $\frac{d_p}{2L\cos\Delta_2}$ can be obtained by decreasing the value of $\frac{du_p}{d\phi_p}$, but a more inclined path of contact will occur. A reasonable value of $\frac{du_p}{d\phi_p}$ is about -0.5 for the left-hand gear convex side, or -0.2 for the left-hand gear concave side. Because both sides of the gear are cut by duplex method, the values of $\frac{du_p}{d\phi_p}$ for both sides are not independent, and we have to choose the value of $\frac{du_p}{d\phi_p}$ for both sides by a compromise.

9. BASIC PRINCIPLES FOR GENERATION OF CONJUGATE GEAR TOOTH SURFACES

INTRODUCTION

The method for generation of conjugate spiral bevel gear tooth surfaces is based on the following principles:

(1) Four surfaces-two generating surfaces (Σ_P and Σ_F) and pinion and gear tooth surfaces (Σ_1 and Σ_2) are in tangency at every instant. The ratio of the angular velocities in motion of surfaces Σ_P, Σ_F, Σ_1 and Σ_2 must satisfy the following requirements: (i) the above-mentioned surfaces must be in continuous tangency and (ii) the generated pinion and gear must transform rotation with zero kinematical errors, and (iii) Point N of contact of both pairs of contacting surfaces - Σ_P Σ_F, Σ_1 Σ_2 - moves in plane Π (Fig. 9.1) in the process of meshing and the common normal to above-mentioned surfaces

performs parallel motion in plane Π.

Figure 9.1 shows the drawings that are represented in the plane of normals, Π. Point A is the point of intersection of the gear head-cutter axis with plane Π and A is the initial position of the normal to surfaces Σ_P and Σ_2. Point D is the point of intersection of the gear cradle axis with plane Π. Simultaneously point D is the point of intersection of pinion and gear axes. Axes of the gear cradle and gear head-cutter are parallel (the head-cutter axis is not tilted with respect to the axis of the cradle). The cradle axis, $X_m^{(2)}$, is perpendicular to the gear root cone but it is inclined with respect to the plane of normals, Π.

Point C (Fig. 9.1) is the point of intersection of the pinion tool cone axis with plane Π. Surface Σ_F of the pinion tool cone will be in contact with surface Σ_P (and Σ_2) if the common normal to surfaces Σ_P and Σ_2 passes through point C. Simultaneously, the pinion surface, Σ_1, will be in contact with Σ_F (and Σ_P and Σ_2) at point N if the equation of meshing for surfaces Σ_1 and Σ_F is satisfied at N.

Point O that is shown in Fig. 9.1 is the point of intersection of the pinion cradle axis with plane Π. Point O does not coincide with point D of the gear cradle axis. We recall that specific machine tool-settings for the pinion, ΔE_1 and ΔL_1, (Fig. 2.3) have to be used to provide conjugate pinion and gear tooth surfaces. This method for generation provides the collinearity of vectors $\overline{DO}$ and $\overline{NA}$. We recall that the pinion cradle axis, $X_m^{(1)}$, is perpendicular to the pinion root cone but it is inclined with respect to gear cradle axis, $X_m^{(2)}$, and plane Π. The orientation of axes $X_m^{(1)}$ and $X_m^{(2)}$ with respect to each other and plane Π depends on gear and pinion dedendum angles, Δ_1 and Δ_2. The pinion cradle axis and the pinion head-cutter axis are parallel (the pinion cutter is not tilted with respect

to the pinion cradle).

Figure 9.1 shows the instantaneous positions of the contact normal $\underset{\sim}{N}$ and points A and C. In the process of meshing the normal performs a parallel motion in plane Π while point A (and respectively C) traces out an ellipse with the ellipse symmetry center D (symmetry center O, respectively). The dimensions and orientation of the gear ellipse centered at D are known since the gear machine settings are given. The dimensions and orientation of the ellipse centered at O must be determined to provide the desired parallel motion of the contact normal. Then it becomes possible to determine the pinion machine-tool settings.

10. SATISFACTION OF THE EQUATIONS OF MESHING

Four surfaces - Σ_P, Σ_F, Σ_1 and Σ_2 - will be in contact within the neighborhood of the instantaneous contact point if they have a common normal and the following equations of meshing are satisfied at the point of contact.

(1) The equation of meshing for surfaces Σ_1 and Σ_2 is represented as follows (Fig. 9.1):

$$\underset{\sim}{v}^{(12)} \cdot \underset{\sim}{N} = (\underset{\sim}{\omega}^{(12)} \times \underset{\sim}{r}^{(N)}) \cdot \underset{\sim}{N} = [\underset{\sim}{\omega}^{(12)} \underset{\sim}{r}^{(N)} \underset{\sim}{N}] = 0 \qquad (10.1)$$

Here: $\underset{\sim}{\omega}^{(12)} = \underset{\sim}{\omega}^{(1)} - \underset{\sim}{\omega}^{(2)}$ where $\underset{\sim}{\omega}^{(1)}$ and $\underset{\sim}{\omega}^{(2)}$ are the angular velocities of the pinion and the gear, respectively. Vector $\underset{\sim}{\omega}^{(12)}$ represents the velocity in relative motion. Vector $\underset{\sim}{r}^{(N)}$ is the position vector of contact point N and $\underset{\sim}{N}$ is the contact normal. Vector $\underset{\sim}{\omega}^{(12)}$ must be directed along the pitch line to provide transformation of rotation with the prescribed angular velocity ratio.

(2) The equation of meshing of surfaces Σ_P and Σ_2 is represented by the equation

$$[\underset{\sim}{\omega}^{(P2)} \underset{\sim}{r}^{(N)} \underset{\sim}{N}] = 0 \tag{10.2}$$

Equation (10.2) is satisfied if $\underset{\sim}{\omega}^{(P2)} = \underset{\sim}{\omega}^{(P)} - \underset{\sim}{\omega}^{(2)}$ is collinear to the unit vector $\underset{\sim}{a}$ of the pitch line. This requirement is observed already since the gear cutting ratio is determined with equation (8.5).

(3) The equation of meshing of tool surfaces Σ_P and Σ_F is represented as follows:

$$\underset{\sim}{v}^{(PF)} \cdot \underset{\sim}{N} = (\underset{\sim}{v}^{(P)} - \underset{\sim}{v}^{(F)}) \cdot \underset{\sim}{N} = \Big\{(\underset{\sim}{\omega}^{(P)} \times \underset{\sim}{r}^{(N)}) - [(\underset{\sim}{\omega}^{(F)} \times \underset{\sim}{r}^{(N)}) + (\overline{DO} \times \underset{\sim}{\omega}^{(F)}]\Big\} \cdot \underset{\sim}{N} = 0 \tag{10.3}$$

Deriving equation (10.3) we substitute the sliding vector $\underset{\sim}{\omega}^{(F)}$ that passes through O (Fig. 9.1) by an equal vector that passes through D and the vector moment represented by

$$\underset{\sim}{m} = \overline{DO} \times \underset{\sim}{\omega}^{(F)}$$

In the process of motion the contact normal keeps its original direction that is parallel to DO. Thus equation (10.3) yields

$$[\underset{\sim}{\omega}^{(PF)} \underset{\sim}{r}^{(N)} \underset{\sim}{N}] = [(\underset{\sim}{\omega}^{(P)} - \underset{\sim}{\omega}^{(F)}) \underset{\sim}{r}^{(N)} \underset{\sim}{N}] = 0 \tag{10.4}$$

Equation (10.4) may be interpreted kinematically as a requirement that vectors $\underset{\sim}{\omega}^{(PF)}$, $\underset{\sim}{r}^{(N)}$ and $\underset{\sim}{N}$ must line in the same plane, the plane of normals Π. This means that

$$(\underset{\sim}{\omega}^{(P)} - \underset{\sim}{\omega}^{(F)}) \cdot \underset{\sim}{i}_n = 0 \tag{10.5}$$

where $\underset{\sim}{i}_n$ is the unit vector of the X_n -axis that is perpendicular to plan Π.

It was mentioned above that the proposed method for generation is based on the parallel motion of the contact normal that slides along two related ellipses. It was assumed that this motion is performed with the following conditions (see Section 7):

$$\mu = \mu_F - \mu_{F0} = \mu_P - \mu_{P0} \quad \text{and} \quad \frac{d\mu_F}{dt} = \frac{d\mu_P}{dt} = \frac{d\mu}{dt} \tag{10.6}$$

where μ_F and μ_P are the ellipse parameters.

Let us prove that the requirement $\frac{d\mu_F}{dt} = \frac{d\mu_P}{dt}$ can be observed if $|\underset{\sim}{\omega}^{(F)}| = |\underset{\sim}{\omega}^{(P)}|$ and equation (10.5) is satisfied.

Vectors $\underset{\sim}{\omega}^{(F)}$ and $\underset{\sim}{\omega}^{(P)}$ are directed along the $X_m^{(1)}$ - and $X_m^{(2)}$ axes and equation (10.5) may be represented as follows

$$\underset{\sim}{\omega}^{(F)} \cdot \underset{\sim}{i}_n = \underset{\sim}{\omega}^{(P)} \cdot \underset{\sim}{i}_n \tag{10.7}$$

Since $\omega^{(F)} = \omega^{(P)} = \omega$ we obtain that projections of vectors $\underset{\sim}{\omega}^{(F)}$ and $\underset{\sim}{\omega}^{(P)}$ on the normal to the plane are equal.

This yields that

$$\frac{d\underset{\sim}{\mu}_F}{dt} = \frac{d\underset{\sim}{\mu}_P}{dt} = \frac{d\mu}{dt} \cdot \underset{\sim}{i}_n$$

Here:

$$\frac{d\mu}{dt} = \omega(\underset{\sim}{i}_m^{(1)} \cdot \underset{\sim}{i}_n) = \omega(\underset{\sim}{i}_m^{(2)} \cdot \underset{\sim}{i}_n) \tag{10.8}$$

Vectors $\frac{d\underset{\sim}{\mu}_F}{dt}$ and $\frac{d\underset{\sim}{\mu}_P}{dt}$ represent the angular velocities of links 1 and 1′ (Fig. 7.3) in their rotational motions. Equations (10.8) also yields that

$$\underset{\sim}{i}_m^{(1)} \cdot \underset{\sim}{i}_n = \underset{\sim}{i}_m^{(2)} \cdot \underset{\sim}{i}_n \tag{10.9}$$

Requirement (10.9) can be satisfied with a specific orientation of the pinion cradle coordinate system, S_h, with respect to gear cradle coordinate system, S_f. This orientation may be achieved with a certain value of angle ε (Fig. 5.1,c) that may be determined by using equation (10.9). The matrix representation of equation (10.10) is given as follows:

$$[1\ 0\ 0][L_{nf}][L_{fm}{}^{(2)}]\begin{bmatrix}1\\0\\0\end{bmatrix} =$$

$$[1\ 0\ 0]\ [L_{nf}][L_{fh}][L_{hm}{}^{(1)}]\begin{bmatrix}1\\0\\0\end{bmatrix} \tag{10.10}$$

Here, matrix $[L_{fm}{}^{(2)}]$ is given by Eq. (6.4); matrix $[L_{nf}]$ is the transpose matrix of $[L_{fn}]$ given by equation (6.1); matrix $[L_{fh}]$ is the sub-matrix of $[M_{fh}]$ given by equation (5.1); matrix $[L_{hm}{}^{(1)}]$ is represented as follows (Fig. 2.3):

$$[L_{hm}{}^{(1)}] = \begin{bmatrix} \cos\Delta_1 & 0 & \sin\Delta_1 \\ 0 & 1 & 0 \\ -\sin\Delta_1 & 0 & \cos\Delta_1 \end{bmatrix} \tag{10.11}$$

Equation (10.10) yields

$$\cos\gamma_1\cos\varepsilon - \sin\varepsilon\tan\eta - \frac{\cos\Delta_2 - \sin\gamma_1\sin(\gamma_1 - \Delta_1)}{\cos(\gamma_1 - \Delta_1)} = 0 \qquad (10.12)$$

Equations (10.12) provides two solutions for angle ε and the smaller value of ε is to-be chosen.

11. EQUATIONS OF SURFACE TANGENCY AT THE MAIN CONTACT POINT

We consider that the coordinates of the main contact point N on surface Σ_P (Fig. 8.2) and the direction of the surface unit normal $\underset{\sim}{n}^{(P)}$ at point N are known. We have to provide that surfaces Σ_P, Σ_2, Σ_1 and Σ_F will be in tangency at the chosen point N. Surfaces Σ_P and Σ_2 are already in tangency at N since the equation of meshing of Σ_P and Σ_2 is satisifed at this point (see Section 8). Then we have to provide the tangency of surfaces Σ_P and Σ_F, Σ_F and Σ_1 and Σ_1 and Σ_2.

Equations of Tangency of Σ_P and Σ_F

The tangency of generating surfaces Σ_P and Σ_F at point N is provided if the following equations are satisfied at N:

$$\underset{\sim}{r}^{(F)}(u_F, \theta_F, \phi_F, \psi_c^{(F)}, q_F, r_c^{(F)}, \Delta E_1, \Delta L_1) = \underset{\sim}{r}^{(P)} \qquad (11.1)$$

$$\underset{\sim}{n}^{(F)}(\theta_F, \phi_F, \psi_c^{(F)}, q_F) = \underset{\sim}{n}^{(P)} \qquad (11.2)$$

Here $\underset{\sim}{r}^{(P)}$ and $\underset{\sim}{n}^{(P)}$ are the given position vector and surface Σ_P unit normal. Vector Eqs. (11.1) and (11.2) may be considered in any coordinate system, for instance, in system $S_m^{(1)}$. Vector Eq. (11.1) provides three independent scalar equations but Eq. (11.2) provides only two ones since $|\underset{\sim}{n}| = 1$. Parameters u_F and θ_F are the surface Σ_F coordinates for the point of tangency. Parameter ϕ_F, is the angle of cradle turn for the installment

of the generating surface Σ_F and it may be chosen of any value, including $\phi_F = 0$. Parameters q_F and b_F determine the location and orientation of the pinion head-cutter in coordinate system $S_m^{(1)}$ (Fig. 2.1); $\psi_c^{(F)}$ is the blade angle (Fig. 2.1); ΔE_1 and ΔL_1 are the machine-tool settings that have been shown in Fig. 2.3; $r_c^{(F)}$ is the radius of the head-cutter circle obtained by the intersection of the head-cutter surface with plane $X_m^{(1)} = 0$ (Fig. 2.1).

We may represent vector equations of tangency (11.1) and (11.2) as follows

$$[r_{m(1)}^{(F)}] = [M_m^{(1)}{}_m^{(2)}][r_{m(2)}^{(P)}] = [M_m^{(1)}{}_h][M_{hf}][M_{fm}^{(2)}][r_{m(2)}^{(P)}] \tag{11.3}$$

$$[n_{m(1)}^{(F)}] = [L_m^{(1)}{}_m^{(2)}][n_{m(2)}^{(P)}] = [L_m^{(1)}{}_h][L_{hf}][L_{fm}^{(2)}][n_{m(2)}^{(P)}] \tag{11.4}$$

Matrix $[M_{fm}^{(2)}]$ is represented by the following equation (Fig. 11.1)

$$[M_{fm}^{(2)}] = \begin{bmatrix} \cos\Delta_2 & 0 & -\sin\Delta_2 & L\sin\Delta_2\cos\Delta_2 \\ 0 & 1 & 0 & 0 \\ \sin\Delta_2 & 0 & \cos\Delta_2 & L\sin^2\Delta_2 \\ 0 & 0 & 0 & 1 \end{bmatrix} \tag{11.5}$$

Matrix $[M_{hf}]$ is the transpose matrix of matrix $[M_{fh}]$ that is represented by equation (5.1).

Matrix $[M_m^{(1)}{}_h]$ is represented as follows (Fig. 2.3)

$$[M_m^{(1)}{}_h] = \begin{bmatrix} \cos\Delta_1 & 0 & -\sin\Delta_1 & L\sin\Delta_1 \\ 0 & 1 & 0 & -\Delta E_1 \\ \sin\Delta_1 & 0 & \cos\Delta_1 & -\Delta L_1 \\ 0 & 0 & 0 & 1 \end{bmatrix} \tag{11.6}$$

The column matrix $[r_{m(2)}^{(P)}]$ and $[n_{m(2)}^{(P)}]$ are represented by equation (4.17) and (4.18). After matrix multiplications we obtain

$$[M_m^{(1)}{}_m^{(2)}] = \begin{bmatrix} b_{11} & b_{12} & b_{13} & b_{14} \\ b_{21} & b_{22} & b_{23} & b_{24} \\ b_{31} & b_{32} & b_{33} & b_{34} \\ 0 & 0 & 0 & 1 \end{bmatrix} \tag{11.7}$$

Here:

$$b_{11} = \cos\varepsilon\cos(\gamma_1 - \Delta_1)\cos(\gamma_1 + \Delta_2) + \sin(\gamma_1 - \Delta_1)\sin(\gamma_1 + \Delta_2)$$

$$b_{12} = -\sin\varepsilon\cos(\gamma_1 - \Delta_1)$$

$$b_{13} = -\cos\varepsilon\cos(\gamma_1 - \Delta_1)\sin(\gamma_1 + \Delta_2) + \sin(\gamma_1 - \Delta_1)\cos(\gamma_1 + \Delta_2)$$

$$b_{14} = L\sin\Delta_1 + L\sin\Delta_2\, b_{11}$$

$$b_{21} = \sin\varepsilon\cos(\gamma_1 + \Delta_2)$$

$$b_{22} = \cos\varepsilon$$

$$b_{23} = -\sin\varepsilon\sin(\gamma_1 + \Delta_2)$$

$$b_{24} = -\Delta E_1 + L\sin\Delta_2\, b_{21}$$

$$b_{31} = -\cos\varepsilon\sin(\gamma_1 - \Delta_1)\cos(\gamma_1 + \Delta_2) + \cos(\gamma_1 - \Delta_1)\sin(\gamma_1 + \Delta_2)$$

$$b_{32} = \sin\varepsilon\sin(\gamma_1 - \Delta_1)$$

$$b_{33} = \cos\varepsilon\sin(\gamma_1 - \Delta_1)\sin(\gamma_1 + \Delta_2) + \cos(\gamma_1 - \Delta_1)\cos(\gamma_1 + \Delta_2)$$

$$b_{34} = -\Delta L_1 + L\sin\Delta_2\, b_{31}$$

Equations (11.3) and (11.4) are used for the determination of pinion machine-tool settings.

12. PINION MACHINE-TOOL SETTINGS

The pinion machine-tool settings are represented by the following parameters: $r_c^{(F)}$ - the radius of the head-cutter circle measured in plane $X_m^{(1)} = 0$; b_F and q_F - parameters that determine the location of the head-cutter in plane $X_m^{(1)} = 0$ with $\phi_F = 0$ (see Fig. 2.1); $\psi_c^{(F)}$ - parameter that determines the blade angle; $m_{F1} = \frac{\omega^{(F)}}{\omega^{(1)}}$ - the ratio by cutting; ΔE_1 and ΔL_1 - corrections of machine-tool settings that are shown in Fig. 2.3.

The determination of the pinion machine-tool settings is based on the equations that relate the parameters of the gear and pinion ellipses, equations of tangency of the pinion and gear tooth surfaces at the main contact point and the equation of meshing by pinion cutting. These settings must be determined for the following 4 cases that are represented in the plane of normals, by Fig. 12.1 and Fig. 12.2, respectively. Figure

12.1(a) corresponds to the case where the gear is left-hand, the gear tooth contacting surface is convex, $r_c^{(F)} > r_c^{(P)}$ and CN > AN. Figure 12.1(b) corresponds to the case where the gear is left-hand, the gear tooth contacting surface is concave, $r_c^{(F)} < r_c^{(P)}$ and CN < AN.

Drawings of Fig. 12.2 correspond to the cases where the gear is right-hand and the gear tooth contacting surface is convex (Fig. 12.2,a) and concave (Fig. 12.2,b). The difference between $r_c^{(P)}$ and $r_c^{(F)}$ with other parameters as given determines the required dimensions of the contacting ellipse.

Determination of the Cutting Ratio m_{F1}

It is mentioned above that the proposed method for generation provides: (i) the simultaneous tangency of four surfaces: Σ_P, Σ_F, Σ_1 and Σ_2, where Σ_P and Σ_F are the gear and pinion generating surfaces and Σ_1 and Σ_2 are the generated pinion and gear tooth surfaces; (ii) the generating gears (cradles) are rotated with the same angular velocities i.e. $\omega^{(P)} = \omega^{(F)}$. This yields the following equation for the pinion cutting ratio

$$m_{F1} = \frac{\omega^{(F)}}{\omega^{(1)}} = \frac{\omega^{(P)}}{\omega^{(2)} m_{12}} = \frac{m_{P2}}{m_{12}}$$

Here:

$$m_{P2} = \frac{\sin\gamma_2}{\cos\Delta_2} \text{ (see equation 8.5)}$$

$$m_{12} = \frac{\omega^{(1)}}{\omega^{(2)}} = \frac{N_2}{N_1}$$

where N_2 and N_1 are the numbers of gear and pinion teeth.

The final expression for the pinion cutting ratio is

$$m_{F1} = \frac{N_1 \sin\gamma_2}{N_2 \cos\Delta_2} \tag{12.1}$$

Determination of b_F

The procedure of computations of b_F is based on the following steps: (i) determination of semiaxes of the gear cradle ellipse, a_p and b_p; (ii) determination of the parameter of orientation of the gear cradle ellipse, δ_p; (iii) determination of the parameter of orientation of the pinion cradle ellipse, δ_F and, (iv) determination of b_F.

Step 1: Determination of semiaxes of the gear cradle ellipse.

The gear cradle ellipse is obtained by intersection of the cylinder of radius b_p (Fig. 2.1) with the plane of normals. The semiminor axis of the cradle ellipse is the cylinder radius b_p. The semimajor axis is represented by the equation

$$a_p = \frac{b_p}{\underset{\sim}{i}_m^{(2)} \cdot \underset{\sim}{i}_n} \tag{12.2}$$

where the unit vector $\underset{\sim}{i}_m^{(2)}$ is collinear to the cylinder axis, $\underset{\sim}{i}_n$ is the unit vector that is perpendicular to the plane of normals. The scalar product $\underset{\sim}{i}_m^{(2)} \cdot \underset{\sim}{i}_n$ may be represented as follows

$$\underset{\sim}{i}_m^{(2)} \cdot \underset{\sim}{i}_n =$$

$$[1\ 0\ 0][L_m(2)_f][L_{fn}] \begin{bmatrix} 1 \\ 0 \\ 0 \end{bmatrix} \tag{12.3}$$

Here, the column matrix represents the unit vector $\underset{\sim}{i}_n$ in coordinate system S_n and the row matrix represents the unit vector $\underset{\sim}{i}_m^{(2)}$ in $S_m^{(2)}$.

Equation (12.3) yields

$$\underset{\sim}{i}_m^{(2)} \cdot \underset{\sim}{i}_n = \cos\Delta_2\cos\eta \tag{12.4}$$

and

$$a_p = \frac{b_p}{\cos\Delta_2\cos\eta} \tag{12.5}$$

Step 2: Determination of orientation of the gear cradle ellipse.

We designate with $\underset{\sim}{b}_p^o$ the unit vector of the minor ellipse axis and with δ_p the angle that is formed by axis y_n and the major ellipse axis (Fig. 12.3). Vectors $\underset{\sim}{b}_p^o$ and $\underset{\sim}{i}_m^{(2)}$ are mutual perpendicular and this yields that

$$[1\ 0\ 0][L_{m_f}^{(2)}]]L_{fn}] \begin{bmatrix} 0 \\ -\sin\delta_p \\ \cos\delta_p \end{bmatrix} = \sin\delta_p\sin\eta\cos\Delta_2 + \cos\delta_p\sin\Delta_2 = 0 \tag{12.6}$$

and

$$\tan\delta_p = -\frac{\tan\Delta_2}{\sin\eta} \tag{12.7}$$

Step 3: Determination of orientation of the pinion cradle ellipse.

The unit vector of minor axis of the pinion cradle ellipse, $\underset{\sim}{b}_F^o$, (Fig. 12.3) is perpendicular to the cylinder axis of radius b_F. Thus

$$\underset{\sim}{i}_m^{(1)} \cdot \underset{\sim}{b}_F^o = 0 \tag{12.8}$$

The matrix representation of equation (12.8) is as follows:

$$[1\ 0\ 0][L_m^{(1)}{}_h][L_{hf}][L_{fn}]\begin{bmatrix} 0 \\ -\sin\delta_F \\ \cos\delta_F \end{bmatrix} = 0 \tag{12.9}$$

Equation (12.9) yields

$$\tan\delta_F = \frac{A}{B} \tag{12.10}$$

where

$$A = \cos\varepsilon\sin\gamma_1 - \cos\gamma_1\tan(\gamma_1 - \Delta_1) \tag{12.11}$$

$$B = \cos\eta\sin\varepsilon + \sin\eta[\cos\varepsilon\cos\gamma_1 + \sin\gamma_1\tan(\gamma_1 - \Delta_1)] \tag{12.12}$$

Step 4: Determination of b_F

It is easy to prove that the ratio between the axes of both ellipses is the same since

$$\frac{b_F}{a_F} = \underset{\sim}{i}_m^{(1)} \cdot \underset{\sim}{i}_n \ , \ \frac{b_P}{a_P} = \underset{\sim}{i}_m^{(2)} \cdot \underset{\sim}{i}_n$$

and

$$\underset{\sim}{i}_m^{(1)} \cdot \underset{\sim}{i}_n = \underset{\sim}{i}_m^{(2)} \cdot \underset{\sim}{i}_n \text{ (see Eq. (10.9))}$$

Thus:

$$a_F = \frac{b_F}{\cos\Delta_2\cos\eta}, \quad a_P = \frac{b_P}{\cos\Delta_2\cos\eta} \tag{12.13}$$

The parameters of both ellipses have been represented by equation (7.19) as follows

$$a_F^2 \sin^2(q - \delta_F) + b_F^2 \cos^2(q - \delta_F) = d_1^2 + d_2^2 \tag{12.14}$$

Equations (7.15), (7.16) and (12.12) yield that

$$d_1^2 + d_2^2 = b_P^2 \left[\cos^2(q - \delta_P) + \frac{\sin^2(q - \delta_P)}{\cos^2\Delta_2 \cos^2\eta} \right] \tag{12.15}$$

where q is the angle that is formed between vector $\overline{DO}$ and axis Y_n (Fig. 7.2). We recall that vector $\overline{DO}$ is collinear to the contact normal. Using equations (12.14) and (12.15), we obtain

$$b_F = b_P \left[\frac{\cos^2(q - \delta_P)\cos^2\Delta_2\cos^2\eta + \sin^2(q - \delta_P)}{\cos^2(q - \delta_F)\cos^2\Delta_2\cos^2\eta + \sin^2(q - \delta_F)} \right]^{1/2} \tag{12.16}$$

Determination of q_F

The main idea of determination of q_F is based on identification in plane $X_m^{(1)} = 0$ of projections of two vectors: $\overline{OC}$ (Fig. 12.1 and Fig. 12.2) and $\underset{\sim}{a}$ that is the unit vector of $\overline{O_m^{(1)} O_s^{(F)}}$ (Fig. 12.4). We recall that points $O_m^{(1)}$ and O lie on the axis of the cradle and $O_s^{(F)}$ and C lie on the axis of the pinion head-cutter (Fig. 12.4). Points O and C are the points of intersection of pinion cradle axis, $X_m^{(1)}$, and the pinion head-cutter axis, $O_s^{(F)}C$, with the plane of normals, Π. Plane Π has been shown in Fig. 6.1.

Unit vectors $\underset{\sim}{i}_m^{(1)}$, $\underset{\sim}{a}$ and $\overline{OC}$ lie in the same plane. Here $\underset{\sim}{i}_m^{(1)}$ is the unit vector of axis $X_m^{(1)}$.

Thus:

$$[\underset{\sim}{a}\ \underset{\sim}{i}_m^{(1)}\ \overline{OC}] = \underset{\sim}{a} \cdot (\underset{\sim}{i}_m^{(1)} \times \overline{OC}) = 0 \qquad (12.17)$$

The determination of the q_F is based on equation (12.17) and the computational procedure may be presented as follows:

Step 1: Representation of vector $\underset{\sim}{a}$ in coordinate system $S_m^{(1)}$

Figure 12.5(a) and Fig. 12.5(b) show the orientation of unit vector $\underset{\sim}{a}$ in plane $X_m^{(1)}$ in two cases where the generating gear is left-hand (generated gear is right-hand) and generating gear right-hand (generated is left-hand), respectively. Vector $\underset{\sim}{a}$ is represented by the following column matrix:

$$\underset{\sim}{a} = \begin{bmatrix} 0 \\ \sin q_F \\ \cos q_F \end{bmatrix} \qquad (12.18)$$

Angle q_F is measured clockwise. This angle is negative if measured in opposite direction as shown in Fig. 2.1.

The generating gear generates the member-gear with the same direction of the spiral (the member-gear is down with the respect to the generating gear as it is shown in Fig. 2.2). The generating gear generates the pinion with the opposite direction of the spiral (the pinion is up with the respect to the generating gear as it is shown in Fig. 2.3).

Step 2: Representation of vector $\overline{OC}$ in coordinate system S_n. Using equations (7.5) and (12.13) we may represent vector $\overline{OC}$ as follows:

$$\overline{OC} = \begin{bmatrix} 0 \\ a_F\cos\delta_F\cos\mu_{F0} - b_F\sin\delta_F\sin\mu_{F0} \\ a_F\sin\delta_F\cos\mu_{F0} + b_F\cos\delta_F\sin\mu_{F0} \end{bmatrix} =$$

$$a_F \begin{bmatrix} 0 \\ \cos\delta_F\cos\mu_{F0} - \sin\delta_F\sin\mu_{F0}\cos\eta\cos\Delta_2 \\ \sin\delta_F\cos\mu_{F0} + \cos\delta_F\sin\mu_{F0}\cos\eta\cos\Delta_2 \end{bmatrix} = \begin{bmatrix} 0 \\ b_2 \\ b_3 \end{bmatrix} \qquad (12.19)$$

The sub-script "F0" in μ_{F0} indicates that the initial position of the contact normal (at the main contact point) is considered.

Step 3: Representation of vector $\overline{OC}$ in coordinate system $S_m^{(1)}$

The coordinate transformation in transition from S_n to $S_m^{(1)}$ is represented by the product of matrices.

$$[L_{m\ h}^{(1)}][L_{hf}][L_{fn}] = \begin{bmatrix} a_{11} & a_{12} & a_{13} \\ a_{21} & a_{22} & a_{23} \\ a_{31} & a_{32} & a_{33} \end{bmatrix} \qquad (12.20)$$

Then vector $\overline{OC}$ may be represented as follows

$$\overline{OC} = \begin{bmatrix} a_{12}b_2 + a_{13}b_3 \\ a_{22}b_2 + a_{23}b_3 \\ a_{32}b_2 + a_{33}b_3 \end{bmatrix} \qquad (12.21)$$

Step 4: Representation of the cross-product $\underset{\sim}{i}_m^{(1)} \times \overline{OC}$.

It is easy to verify that:

$$\underset{\sim}{i}_m^{(1)} \times \overline{OC} = \begin{bmatrix} 0 \\ -(a_{32}b_2 + a_{33}b_3) \\ a_{22}b_2 + a_{23}b_3 \end{bmatrix} \tag{12.22}$$

Step 5: Determination of q_F

Equations (12.17), (12.18) and (12.22) yield

$$-\sin q_F(a_{32}b_2 + a_{33}b_3) + \cos q_F(a_{22}b_2 + a_{23}b_3) = 0$$

Thus

$$\tan q_F = \frac{a_{22}b_2 + a_{23}b_3}{a_{32}b_2 + a_{33}b_3} \tag{12.23}$$

Here:

$$a_{22} = -\sin\varepsilon\cos\gamma_1\sin\eta + \cos\varepsilon\cos\eta \tag{12.24}$$

$$a_{23} = -\sin\varepsilon\sin\gamma_1 \tag{12.25}$$

$$a_{32} = \sin\eta[\cos\varepsilon\cos\gamma_1\sin(\gamma_1 - \Delta_1) - \sin\gamma_1\cos(\gamma_1 - \Delta_1)] + \cos\eta\sin\varepsilon\sin(\gamma_1 - \Delta_1) \tag{12.26}$$

$$a_{33} = \cos\gamma_1\cos(\gamma_1 - \Delta_1) + \cos\varepsilon\sin\gamma_1\sin(\gamma_1 - \Delta_1) \tag{12.27}$$

Expressions of b_2 and b_3 have been represented by the column matrix (12.19) in terms of μ_{FO}. Our purpose is to derive relations between μ_{FO}, μ_{PO} and $y_n^{(N)}$ and $z_n^{(N)}$. Here: μ_{PO} is the parameter of the gear cradle axis for

point A (Fig. 9.1); $y_n^{(N)}$ and $z_n^{(N)}$ are coordinates of the main contact point. Equations (7.17) and (7.18) yield:

$$\tan \mu_{FO} = \frac{\frac{d_2}{d_1} \tan(q - \delta_F) - \cos\eta\cos\Delta_2}{\tan(q - \delta_F) + \frac{d_2}{d_1} \cos\eta\cos\Delta_2} \tag{12.28}$$

Here (see equations (7.15) and (7.16))

$$\frac{d_2}{d_1} = \frac{\tan(q - \delta_P)\tan\mu_{PO} + \cos\eta\cos\Delta_2}{\tan(q - \delta_P) - \cos\eta\cos\Delta_2\tan\mu_{PO}} \tag{12.29}$$

The determination of parameter μ_{PO} is based on the following considerations (Fig. 12.6)

$$\overline{O_n A} = \overline{O_n N} + \overline{NA} \tag{12.30}$$

Equation (12.30) yields

$$y_n^{(A)} - y_n^{(N)} = -\overline{AN} \cdot \cos q$$

$$z_n^{(A)} - z_n^{(N)} = -\overline{AN} \cdot \sin q$$

Thus:

$$\frac{z_n^{(A)} - z_n^{(N)}}{y_n^{(A)} - y_n^{(N)}} - \tan q = 0 \tag{12.31}$$

Using equations (7.4) and (12.5) we get

$$z_n^{(A)} = b_P \left(\frac{\sin\delta_P \cos\mu_{PO}}{\cos\eta\cos\Delta_2} + \cos\delta_P \sin\mu_{PO} \right) \tag{12.32}$$

$$y_n^{(A)} = b_P \left(\frac{\cos\delta_P \cos\mu_{P0}}{\cos\eta \cos\Delta_2} - \sin\delta_P \sin\mu_{P0} \right) \tag{12.33}$$

$y_n^{(N)}$ and $z_n^{(N)}$ are coordinates of the main contact point N in coordinate system S_n,q determines the orientation of the contact normal in plane $x_n = 0$.

Using Eqs. (12.31) - (12.33) we may determine parameter μ_{P0}.

Determination of Relation Between ΔE_1 and ΔL_1

Parameters ΔE_1 and ΔL_1 of the pinion machine-tool settings have been shown in Fig. 2.3. Our goal is to prove that the proposed method for generation relates ΔE_1 and ΔL_1 in a certain way.

Consider the drawing of Fig. 12.7. Point D coincides with the origins: O_h of coordinate system S_h, O_f of coordinate system S_f (Fig. 5.1) and the origin of coordinate system S_n. Point D is also shown in Fig. 9.1. Point O is the point of intersection of the pinion cradle axis with the plane of normals, Π. Vector $\overline{DO}$ must be collinear to the contact normal (Fig. 9.1).

Figure 12.7 shows a plane that is drawn through points $O_m^{(1)}$, D and O. Since vectors $\underset{\sim}{i}_m^{(1)}$, $\overline{O_m^{(1)}D}$ and $\overline{OD}$ lie in the same plane, we have that

$$[\overline{O_m^{(1)}D}\ \overline{DO}\ \underset{\sim}{i}_m] = 0 \tag{12.34}$$

Vector $\overline{O_m^{(1)}D}$ is represented by the column matrix (see Eq. 4.12))

$$\overline{O_m^{(1)}D} = \overline{O_m^{(1)}O_h} = \begin{bmatrix} L\sin\Delta_1 \\ \Delta E_1 \\ \Delta L_1 \end{bmatrix} \tag{12.35}$$

Vector $\overline{DO}$ is collinear to the unit contact normal $\underset{\sim}{n}_f$ and is given by (see

Eq. 4.6))

$$[n_{m(1)}^{(F)}] = \begin{bmatrix} \sin\psi_c^{(F)} \\ \cos\psi_c^{(F)}\sin\tau_F \\ \cos\psi_c^{(F)}\cos\tau_F \end{bmatrix} \tag{12.36}$$

Equations (12.34) - (12.36) yield

$$\begin{vmatrix} L\sin\Delta_1 & \Delta E_1 & \Delta L_1 \\ \sin\psi_c^{(F)} & \cos\psi_c^{(F)}\sin\tau_F & \cos\psi_c^{(F)}\cos\tau_F \\ 1 & 0 & 0 \end{vmatrix} = 0 \tag{12.37}$$

Equation (12.36) results in that

$$\frac{\Delta E_1}{\Delta L_1} = \tan\tau_F \tag{12.38}$$

where

$$\tau_F = \theta_F \pm q_F + \phi_F \tag{12.39}$$

Determination of $\psi_c^{(F)}$, τ_F and ΔE_1

Parameter $\psi_c^{(F)}$ determines the blade angle of the pinion head-cutter. Parameter τ_F with the known value of q_F determines the cone surface parameter θ_F. We may determine $\psi_c^{(F)}$ and τ_F by using the equations of tangency at the main contact point represented as follows:

$$\underset{\sim}{r}^{(P)} = \underset{\sim}{r}^{(F)} \tag{12.40}$$

$$\underset{\sim}{n}^{(P)} = \underset{\sim}{n}^{(F)} \tag{12.41}$$

Equations (12.40) and (12.41) provide the equality of position-vectors and unit surface normals, respectively at the main contact point for the generating surfaces Σ_P and Σ_F. Vector equations (12.40) and (12.41) provide three and two scalar equations, respectively, since $|\underset{\sim}{n}^{(P)}| = |\underset{\sim}{n}^{(F)}| = 1$. Using vector Eq. (12.41) we may determine parameters $\psi_c^{(F)}$ and τ_F. To determine ΔE_1 we need only one scalar equation from the three ones provided by vector equations but the remaining two scalar equations should be checked to ensure that they are satisfied with the determined machine-tool settings.

13. INSTALLMENT OF MACHINE-TOOL SETTINGS

The installment of the eccentric angle, EA, and cradle angle, CA, on the Gleason cutting machine No. 26 and No. 116 provides the required values of q_j and b_j (j = P, F).

Consider that a left-hand gear is generated. Figure 13.1 shows two positions of the eccentric and its center: before and after the installment of the cradle angle, CA. The axis of the cradle is perpendicular to the plane of drawings and pointed to the observer. The axis of the head-cutter passes through the center of the cradle since the eccentric angle is not installed yet. Figure 13.2 shows two positions of the axis of the head-cutter: before and after the installment of the eccentric angle. It is evident that angles q_j, CA and EA are related by the equation

$$q_j = CA + \frac{EA}{2} - 90^\circ \quad (j = P, F) \tag{13.1}$$

$$\frac{b_j}{2} = OO_c \sin \frac{EA}{2} \tag{13.2}$$

where $OO_c = k$ is the given constant value. Figures 13.3 and 13.4 correspond to the installment of a right-hand gear (the generating gear is left-hand). Figure 13.3 shows the installment of the cradle angle (CA). Figure 13.4 shows the installment of the eccentric angle and the relations between angular parameters CA, EA and q_j. Equations (13.1) and (13.2) also for the case of generation of a right-hand gear but the value of q_j is larger than in the case of generation of a left-hand gear (see Fig. 13.2).

The installment of corrections of machine-tool settings ΔE_1 and ΔL_1 are only applied for the generation of the pinion. These corrections are installed on the Gleason's cutting machine by "the change of machine center to back" and "the sliding base".

The correction ΔE_1 represents the shortest distance between the crossed axes of the pinion and the gear; ΔE_1 is called "the offset" in Gleason terminology (Fig. 13.5).

The correction ΔL_1 is installed at the machine as a vector-sum of: (i) the change of machine center to back (CB) and (ii) the sliding base (SB) (Fig. 13.6a,b). The change of machine center to back is directed parallel to the pinion axis and the sliding base is directed parallel to the cradle axis. It is evident that

$$CB = \frac{\Delta L_1}{\cos\gamma_R}, \qquad SB = \Delta L_1 \tan\gamma_R \tag{13.3}$$

Here, γ_R is the root cone angle; CB is the machine center to back; SB is the sliding base.

CONCLUSION

The authors proposed a method for generation of spiral bevel gears with conjugated gear tooth surfaces with the following properties:

(i) The transformation of rotation is performed with zero or almost zero kinematical errors.

(ii) The contact point of gear tooth surfaces (the center of instantaneous contact ellipse) moves in a plane (π) of a constant orientation that passes through the pitch line of the gears.

(iii) The normal to the contacting surfaces moves in the process of motion in plane π keeping its original orientation.

(iv) It is expected that due to the motion of the contact ellipse along but not across the gear tooth surfaces the contact ratio will be increased and the conditions of lubrication improved.

The authors developed a method of parallel motion of a straight line by two ellipses with related dimensions and orientation.

A TCA program for the simulation of meshing and bearing contact for the proposed gears has been developed. The advantage of the proposed gearing is that the gears can be manufactured by the Gleason's equipment.

REFERENCES

D.W. Dudley, 1962 "Bevel and Hypoid Gear Manufacture," Chapter 20 of Gear Handbook: The Design, Manufacture, and Application of Gears by D.W. Dudley, New York: McGraw-Hill, 1962.

"Tooth Contact Analysis, Formulas, and Calculation Procedures," 1964, Distributed by Gleason Machine Division, The Gleason Works, 1000 University Avenue, Rochester, NY 14692, Publication No. SD3115.

"Understanding Tooth Contact Analysis," 1981, Distributed by Gleason Machine Division, The Gleason Works, 1000 University Avenue, Rochester, NY 14692, Publication No. SD3139.

D.P. Townsend, J.J. Coy and B.R. Hatvani, 1976, "OH-58 Helicopter Transmission Failure Analysis," NASA TM-X-71867.

F.L. Litvin, 1968, "The Theory of Gearing," 2d ed. Moscow: Nauka.

F.L. Litvin, P. Rahman, and R.N. Goldrich, 1982, "Mathematical Models for the Synthesis and Optimization of Spiral Bevel Gear Tooth Surfaces for Helicopter Transmissions," NASA CR-3553.

F.L. Litvin and J.J. Coy, "Spiral-Bevel Geometry and Gear Train Precision," in Advanced Power Transmission on Technology, Cleveland, OH: NASA Lewis Research Center, NASA CF-2210, AVRADCOM TR 82-C-16, pp. 335-344.

F.L. Litvin, M.S. Hayasaka, P. Rahman, and J.J. Coy, 1985, "Synthesis and Analysis of Spiral Bevel Gears," in *Design and Synthesis*, Tokyo, Japan, July 11-13, 1984 ed. by H. Yoshikawa, New York: North Holland, pp. 302-305.

F.L. Litvin and Y. Gutman, 1981 "Methods of Synthesis and Analysis for Hypoid Gear-Drives of "Formate" and "Helixform" Parts 1-3, Transactions of the ASME: Journal of Mechanical Design, Vol. 103, pp. 83-113.

F.L. Litvin and Y. Gutman, 1981 "A Method of Local Synthesis of Gears Grounded on the Connections between the Principal and Geodetic Curvatures of Surfaces," Transactions of the ASME: Journal of Mechanical Design, pp. 114-125.

F.L. Litvin, 1977, "Relationships between the Curvatures of Tooth Surfaces in Three-Dimensional Gear Systems," NASA-TM-75130.

F.L. Litvin, W.-J. Tsung, J.J. Coy and C. Heine, 1984, "Generation of Conjugate Spiral Bevel Gears, Journal of Mechanisms, Transmissions and Automation in Design (in press).

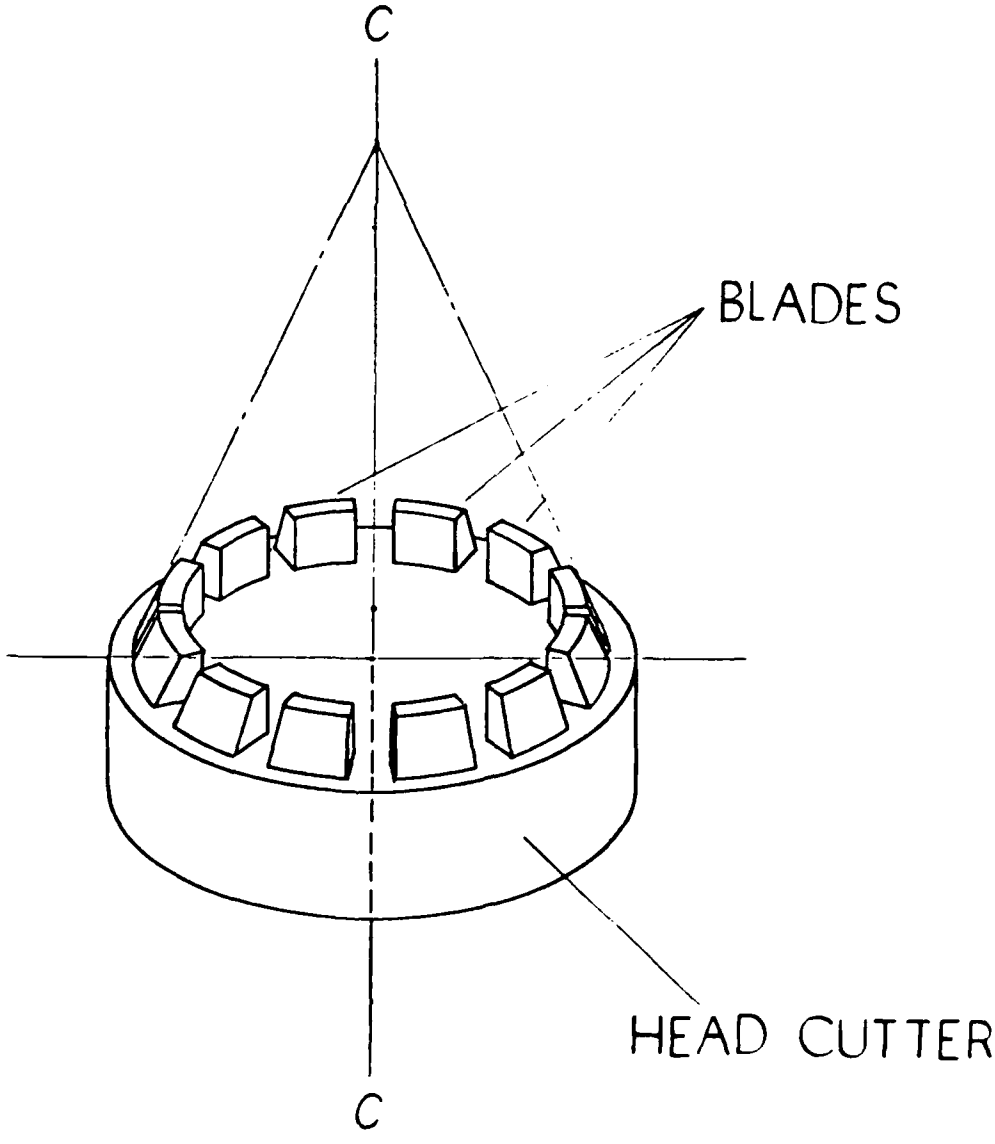

Fig. 1.1

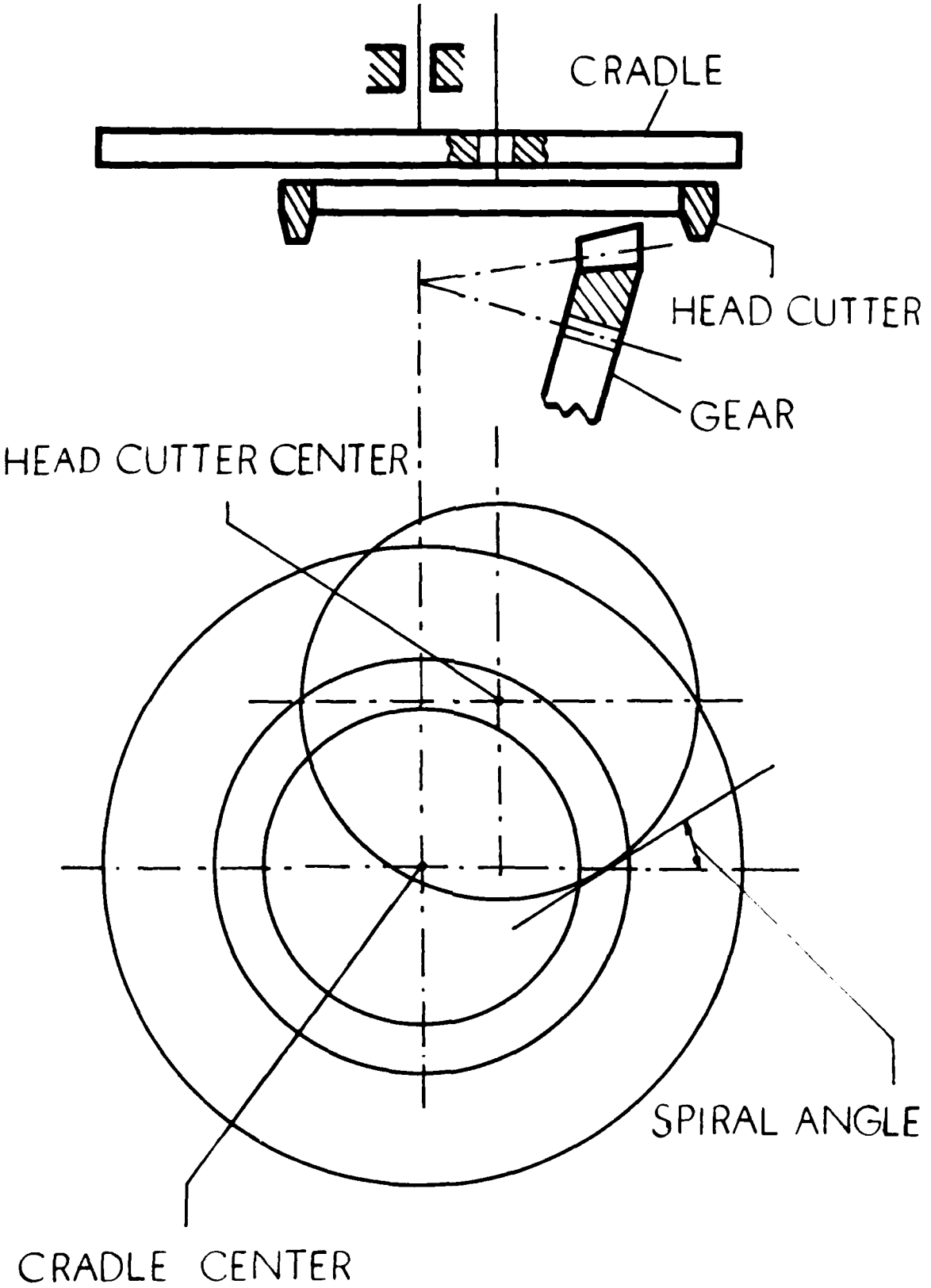
CRADLE
HEAD CUTTER
GEAR
HEAD CUTTER CENTER
SPIRAL ANGLE
CRADLE CENTER

Fig. 1.2

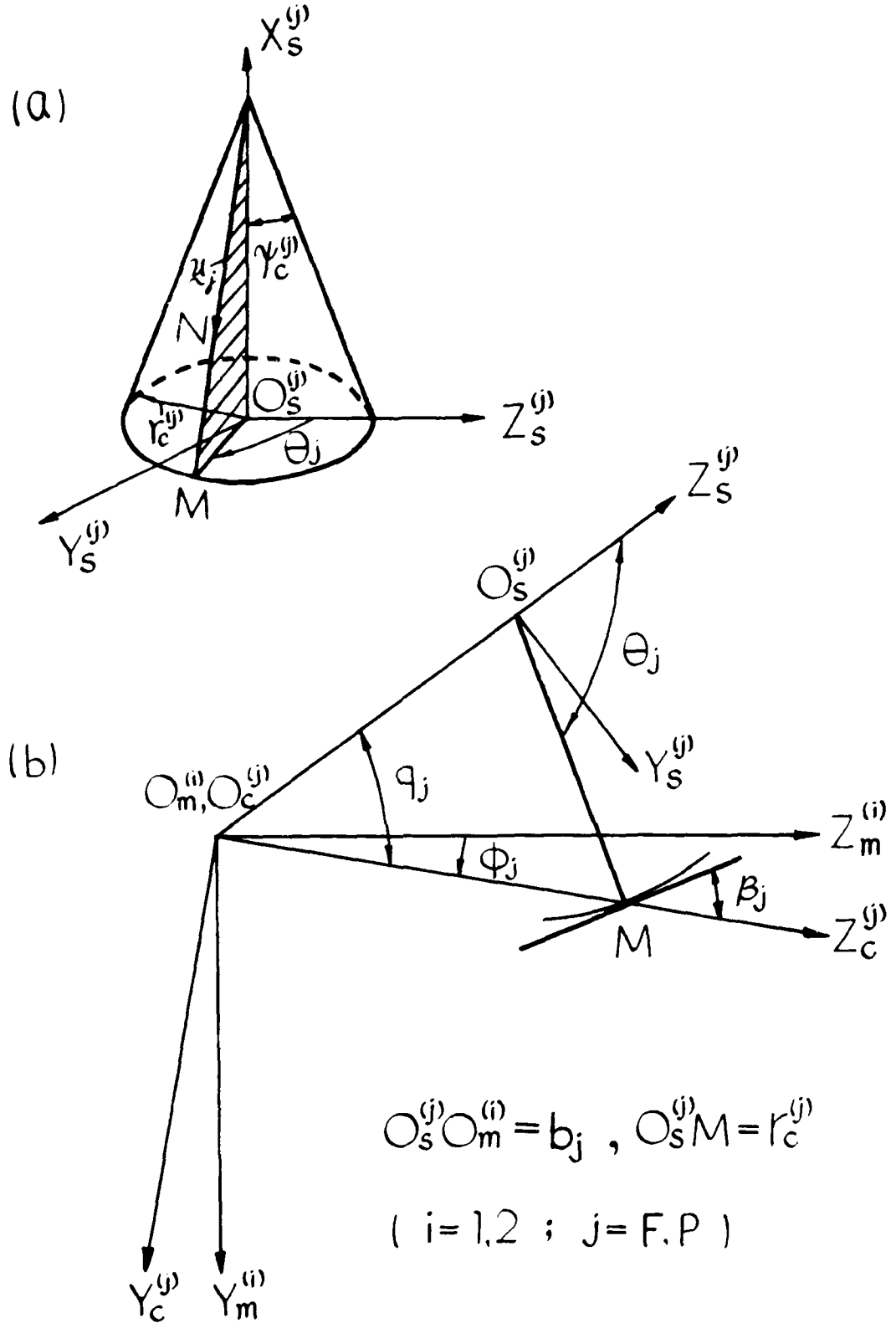
(a)
$X_s^{(j)}$
$\gamma_c^{(j)}$
ℓ_j
N
$O_s^{(j)}$
$r_c^{(j)}$
θ_j
$Z_s^{(j)}$
M
$Y_s^{(j)}$
(b)
$Z_s^{(j)}$
$O_s^{(j)}$
θ_j
$Y_s^{(j)}$
$O_m^{(i)}, O_c^{(j)}$
q_j
$Z_m^{(i)}$
ϕ_j
β_j
M
$Z_c^{(j)}$
$O_s^{(j)} O_m^{(i)} = b_j$, $O_s^{(j)} M = r_c^{(j)}$
(i = 1,2 ; j = F, P)
$Y_c^{(j)}$
$Y_m^{(i)}$

Fig. 2.1

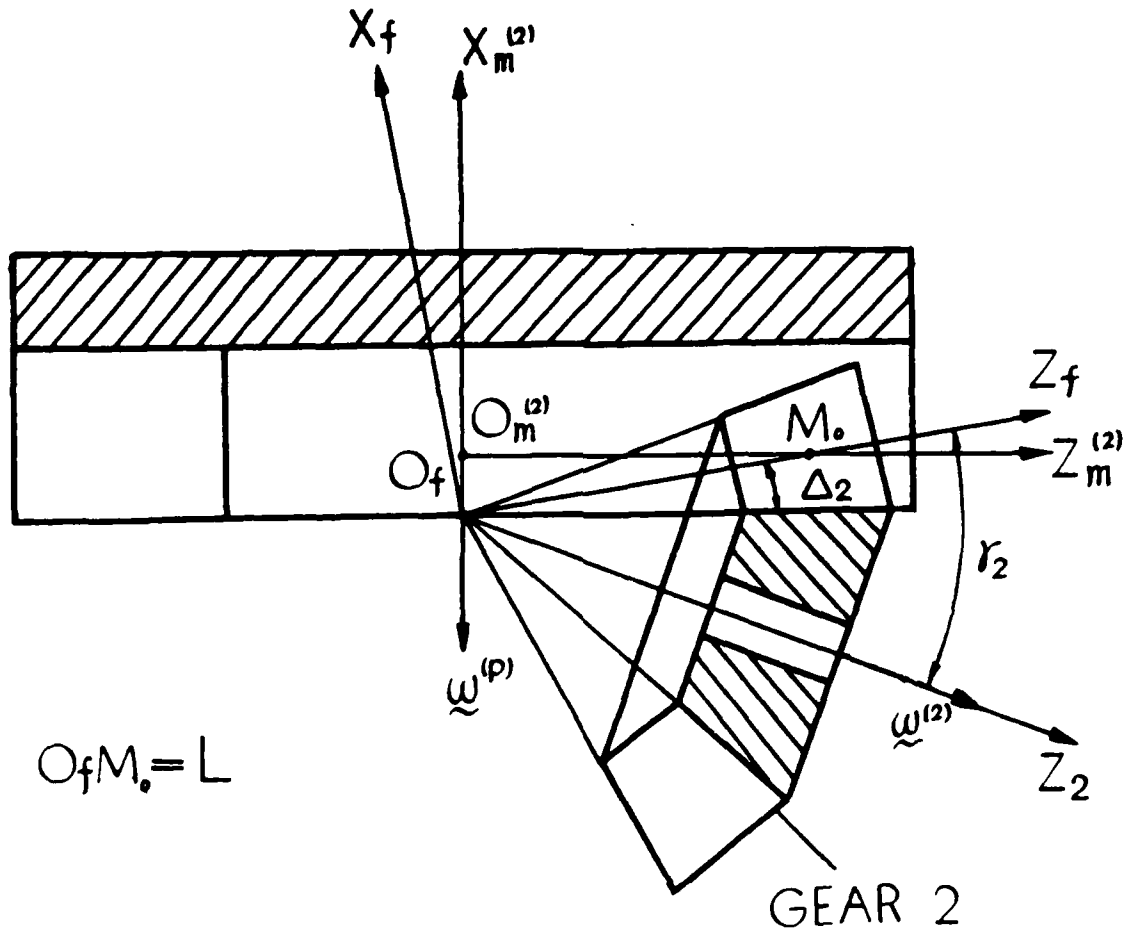
X_f
$X_m^{(2)}$
Z_f
$O_m^{(2)}$
M_o
O_f
$Z_m^{(2)}$
Δ_2
γ_2
$\omega^{(p)}$
$\omega^{(2)}$
$O_fM_o = L$
Z_2
GEAR 2

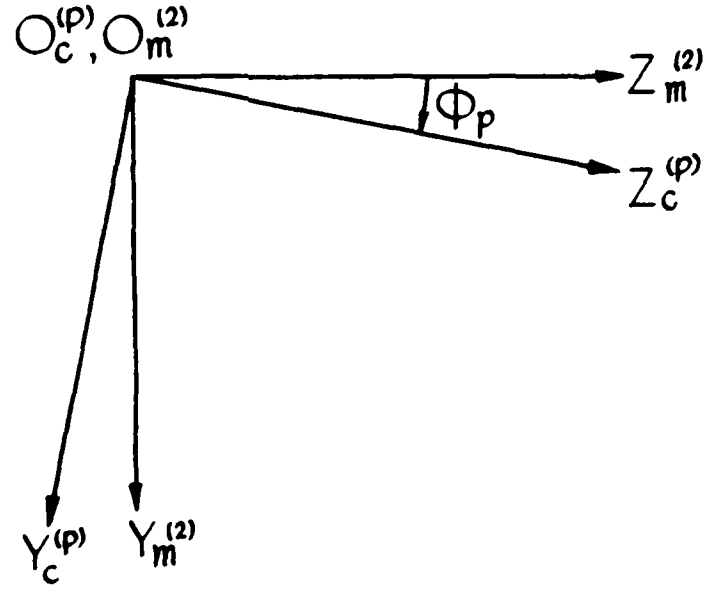
$O_c^{(p)}, O_m^{(2)}$
$Z_m^{(2)}$
Φ_p
$Z_c^{(p)}$
$Y_c^{(p)}$
$Y_m^{(2)}$

Fig. 2.2

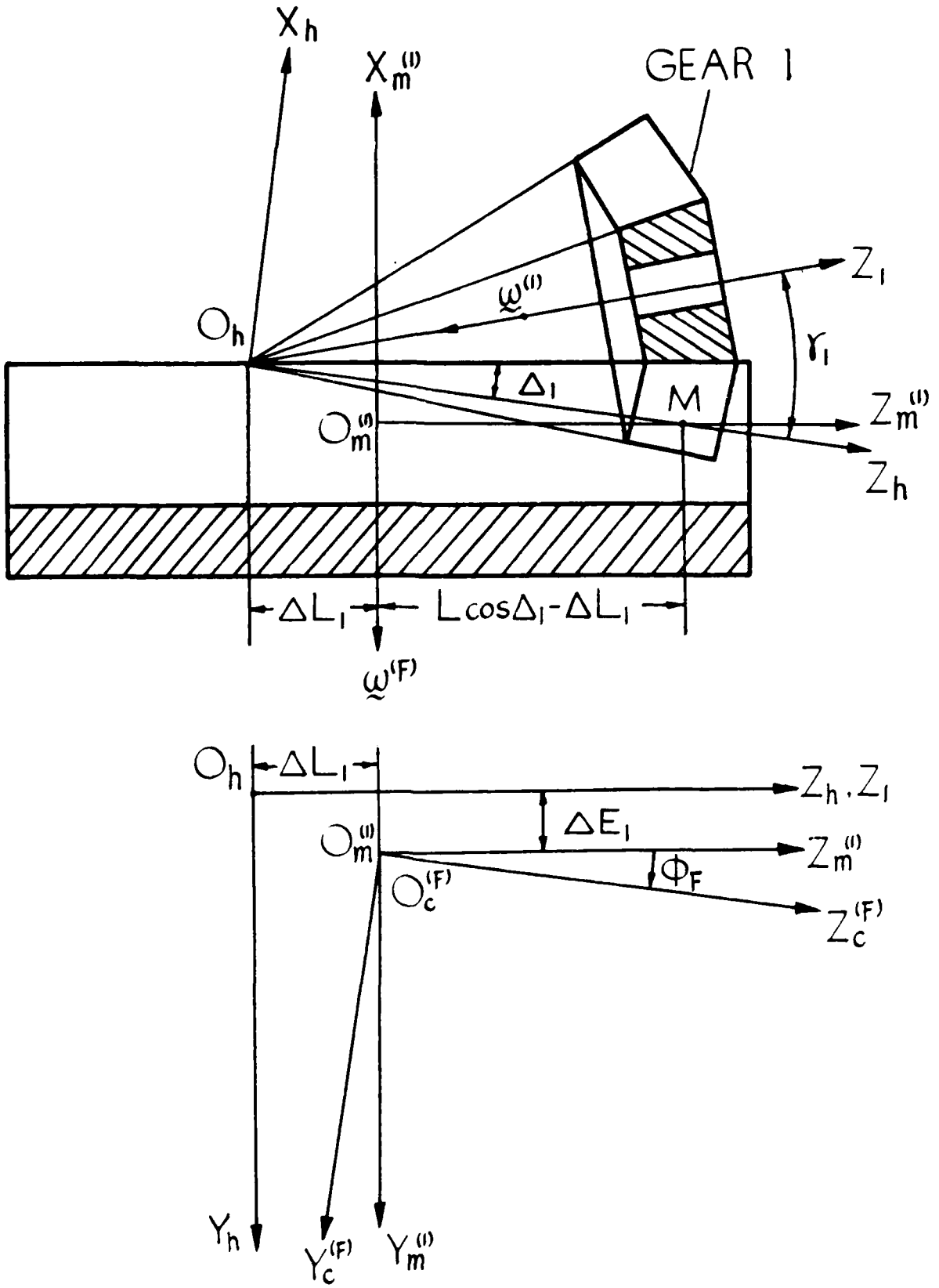
X_h
$X_m^{(1)}$
GEAR 1
Z_1
$\omega^{(1)}$
O_h
γ_1
Δ_1
M
$O_m^{(1)}$
$Z_m^{(1)}$
Z_h
ΔL_1
$L\cos\Delta_1 - \Delta L_1$
$\omega^{(F)}$
O_h
ΔL_1
Z_h, Z_1
ΔE_1
$O_m^{(1)}$
$Z_m^{(1)}$
Φ_F
$O_c^{(F)}$
$Z_c^{(F)}$
Y_h
$Y_c^{(F)}$
$Y_m^{(1)}$

Fig. 2.3

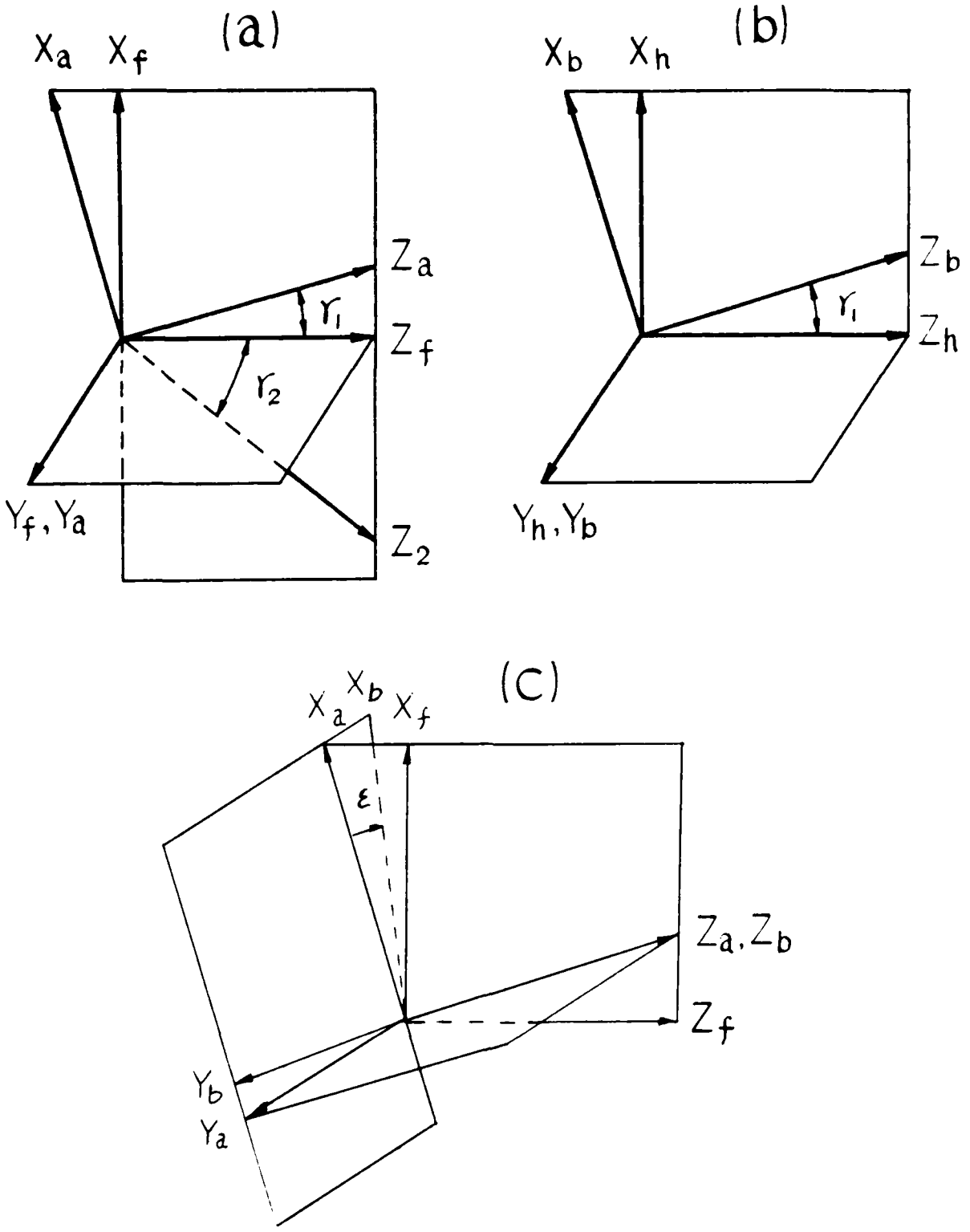
(a)
X_a X_f
Z_a
r_1
Z_f
r_2
Y_f, Y_a
Z_2
(b)
X_b X_h
Z_b
r_1
Z_h
Y_h, Y_b
(C)
X_a X_b X_f
ε
Z_a, Z_b
Z_f
Y_b
Y_a

Fig. 5.1

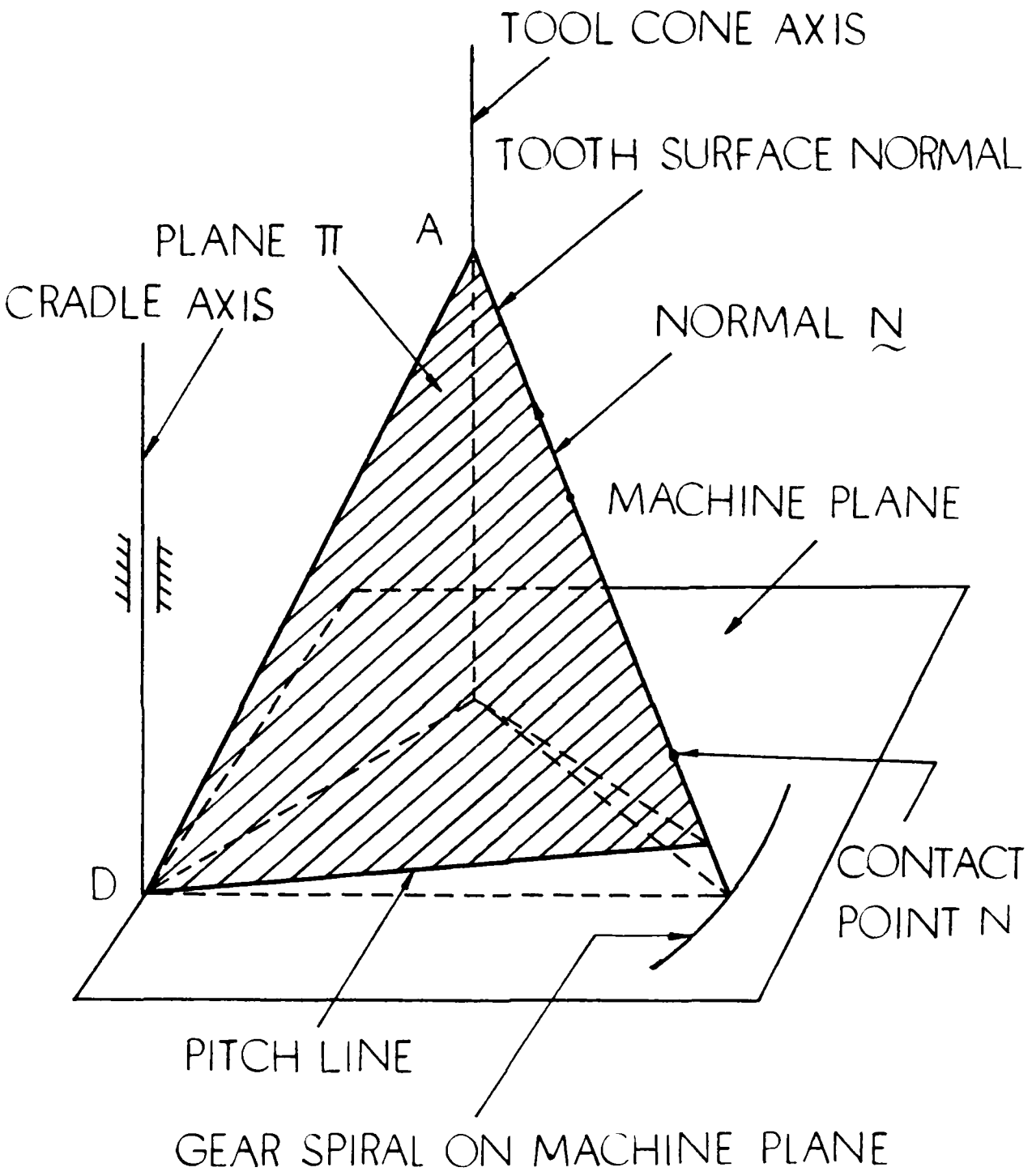
TOOL CONE AXIS
TOOTH SURFACE NORMAL
PLANE π
A
CRADLE AXIS
NORMAL N
MACHINE PLANE
D
CONTACT
POINT N
PITCH LINE
GEAR SPIRAL ON MACHINE PLANE

Fig. 6.1

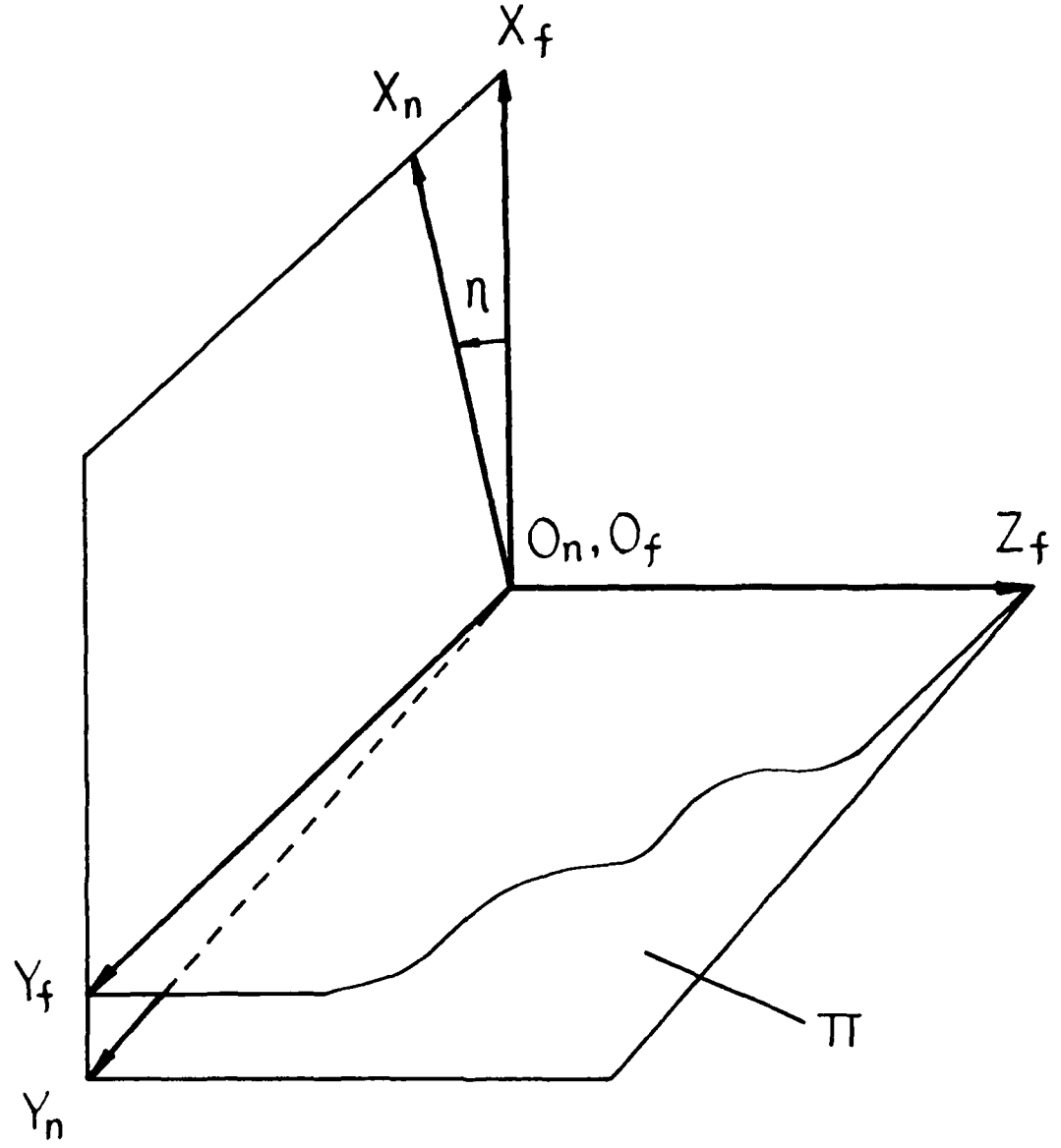

Fig. 6.2

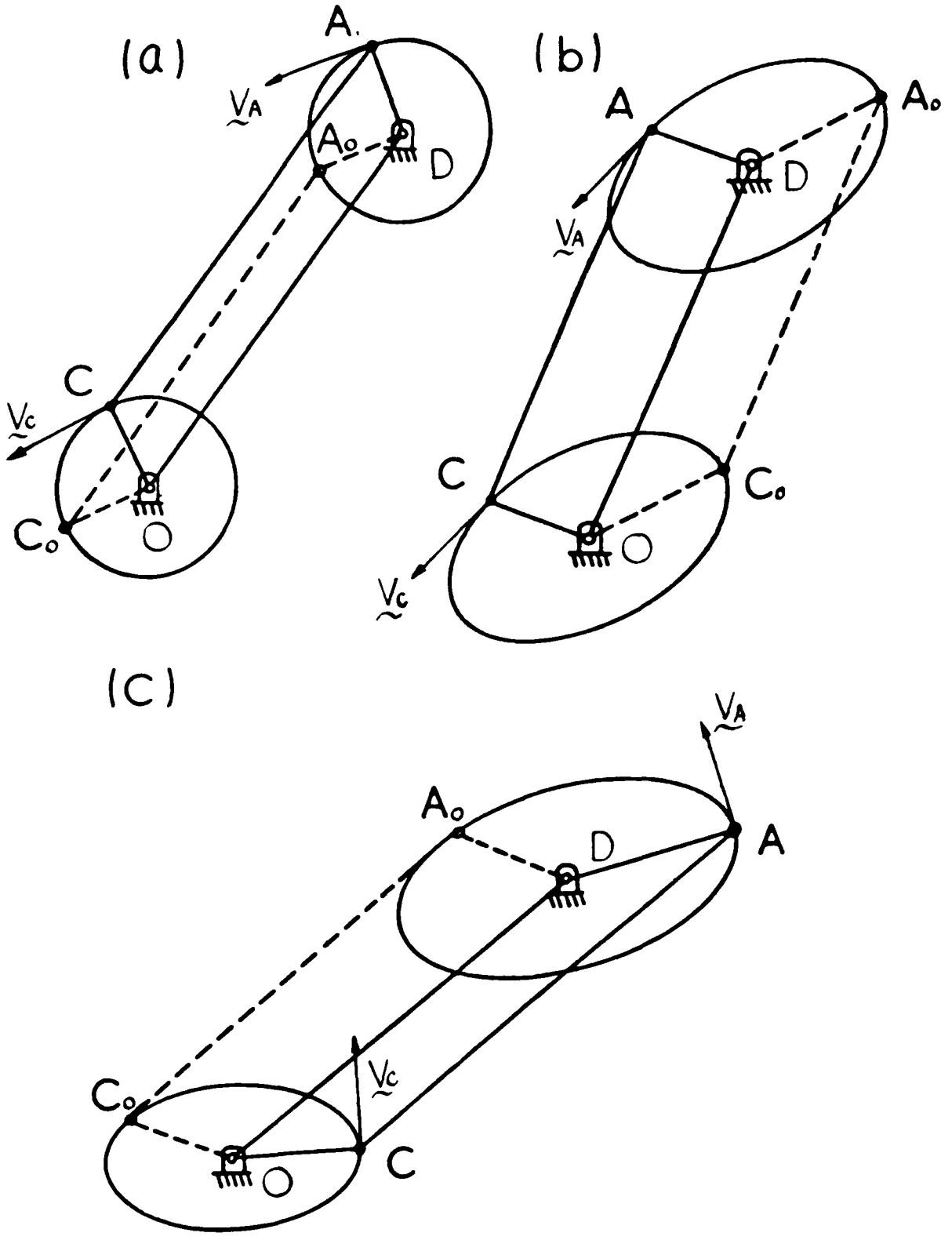

Fig. 7.1

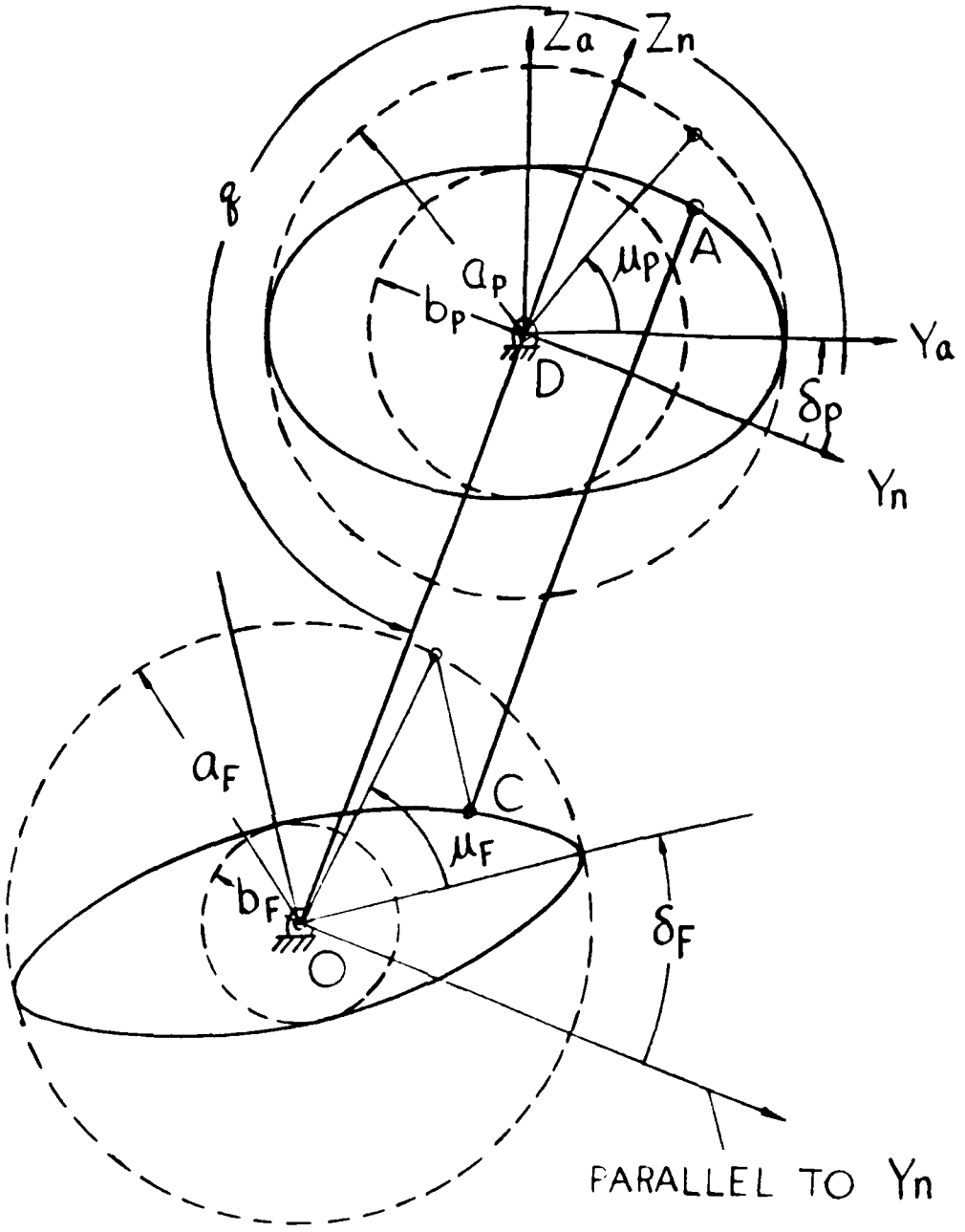
Za
Zn
q
a_P
b_P
μ_P
A
D
Ya
δ_P
Yn
a_F
C
μ_F
b_F
O
δ_F
PARALLEL TO Yn

Fig. 7.2

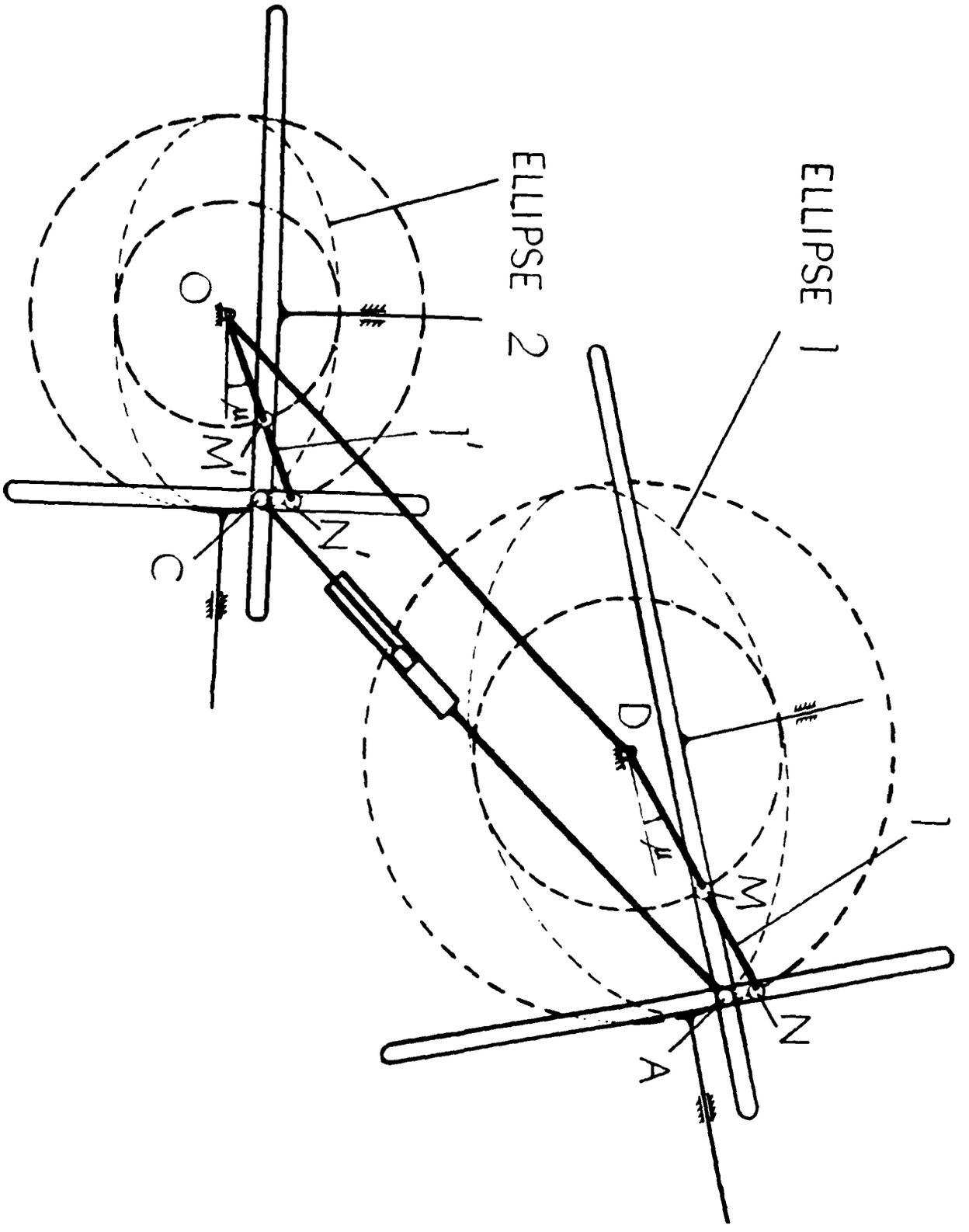

Fig. 7.3

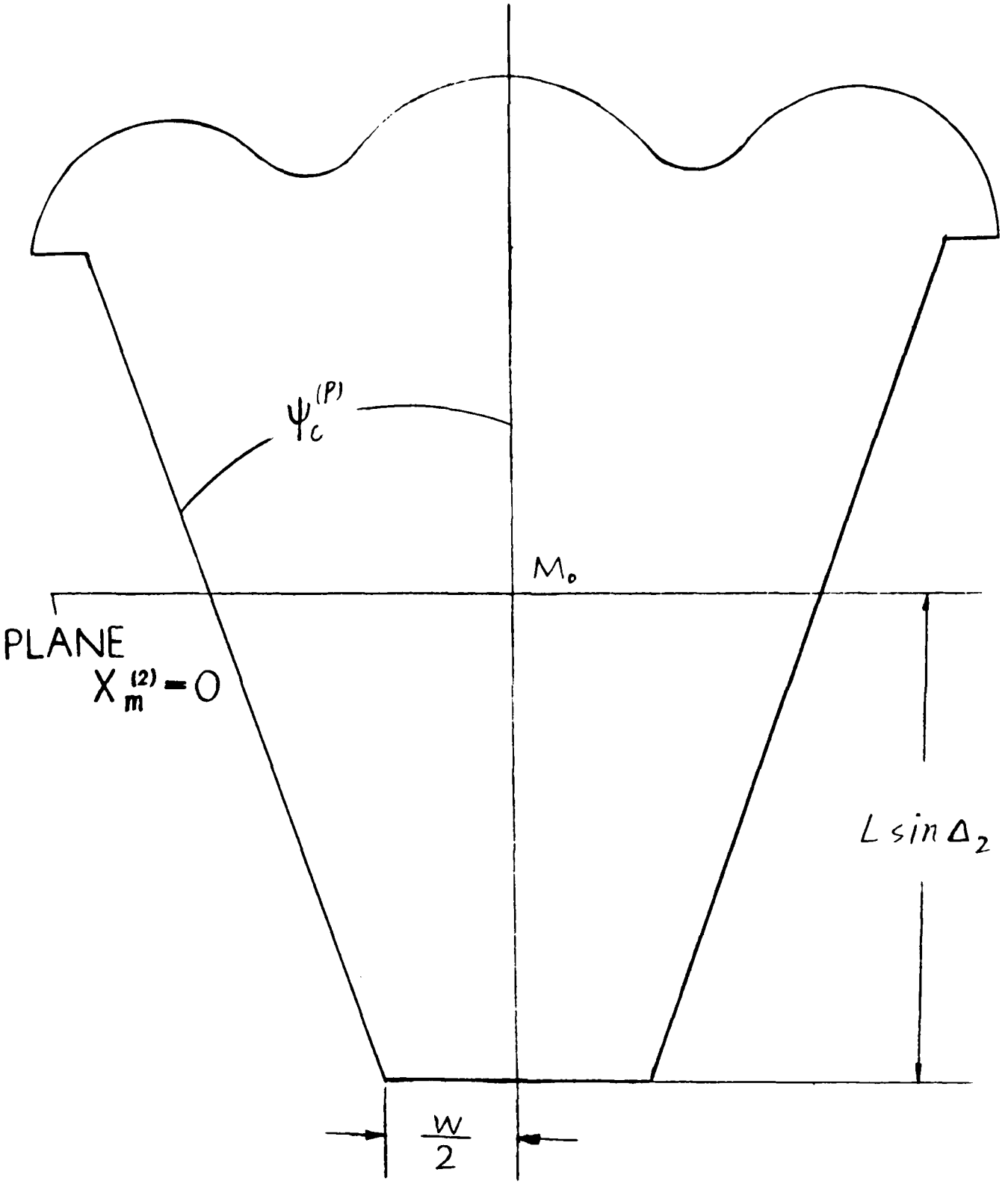

Fig. 8.1

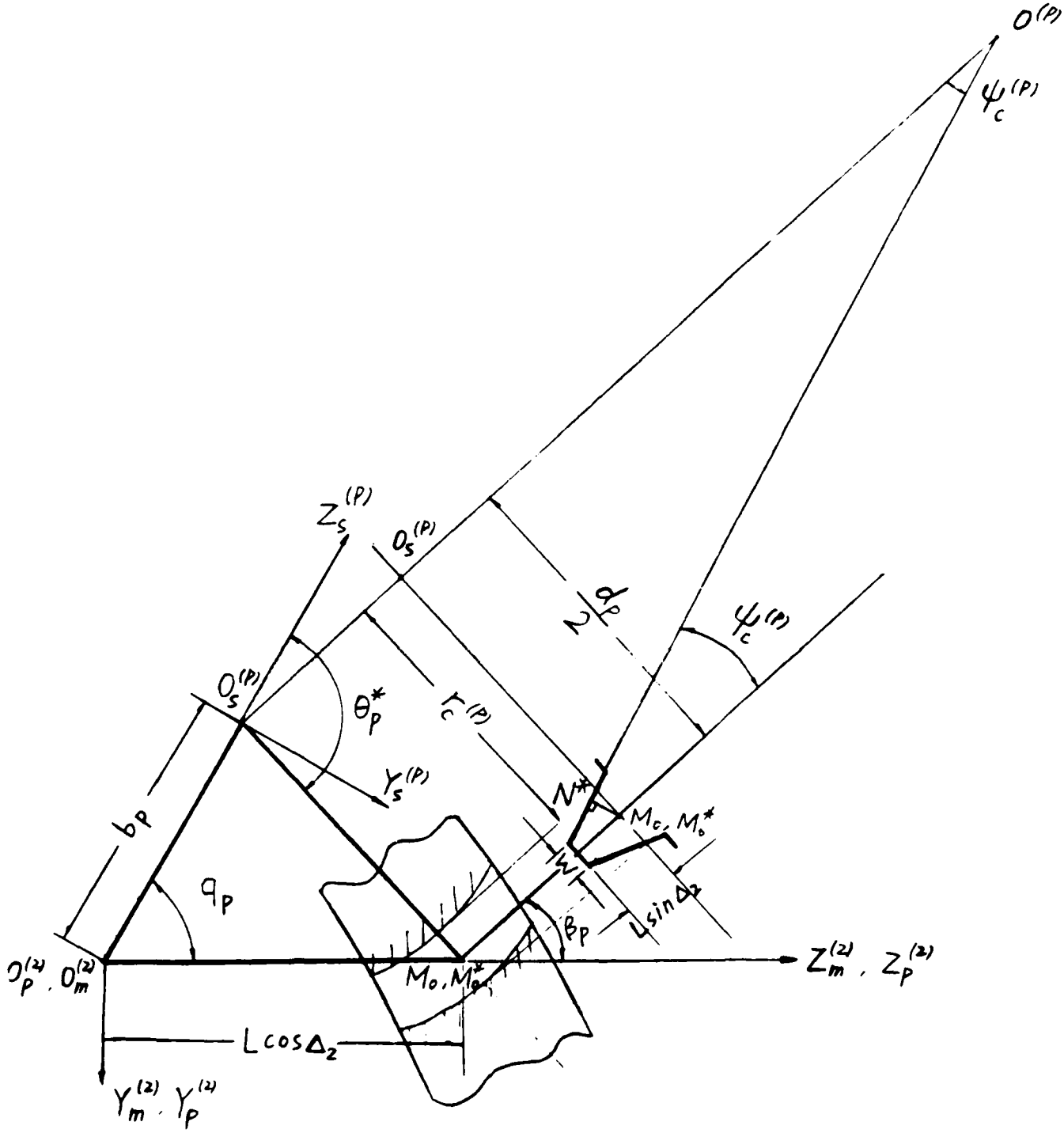
$O^{(P)}$
$\psi_c^{(P)}$
$Z_s^{(P)}$
$O_s^{(P)}$
r_p
$\psi_c^{(P)}$
$O_s^{(P)}$
θ_p^*
$r_c^{(P)}$
$Y_s^{(P)}$
N^*
M_o, M_o^*
b_p
q_p
W_T
$L\sin\Delta_2$
β_p
$O_p^{(2)}, O_m^{(2)}$
M_o, M_o^*
$Z_m^{(2)}, Z_p^{(2)}$
$L\cos\Delta_2$
$Y_m^{(2)}, Y_p^{(2)}$

Fig. 8.2

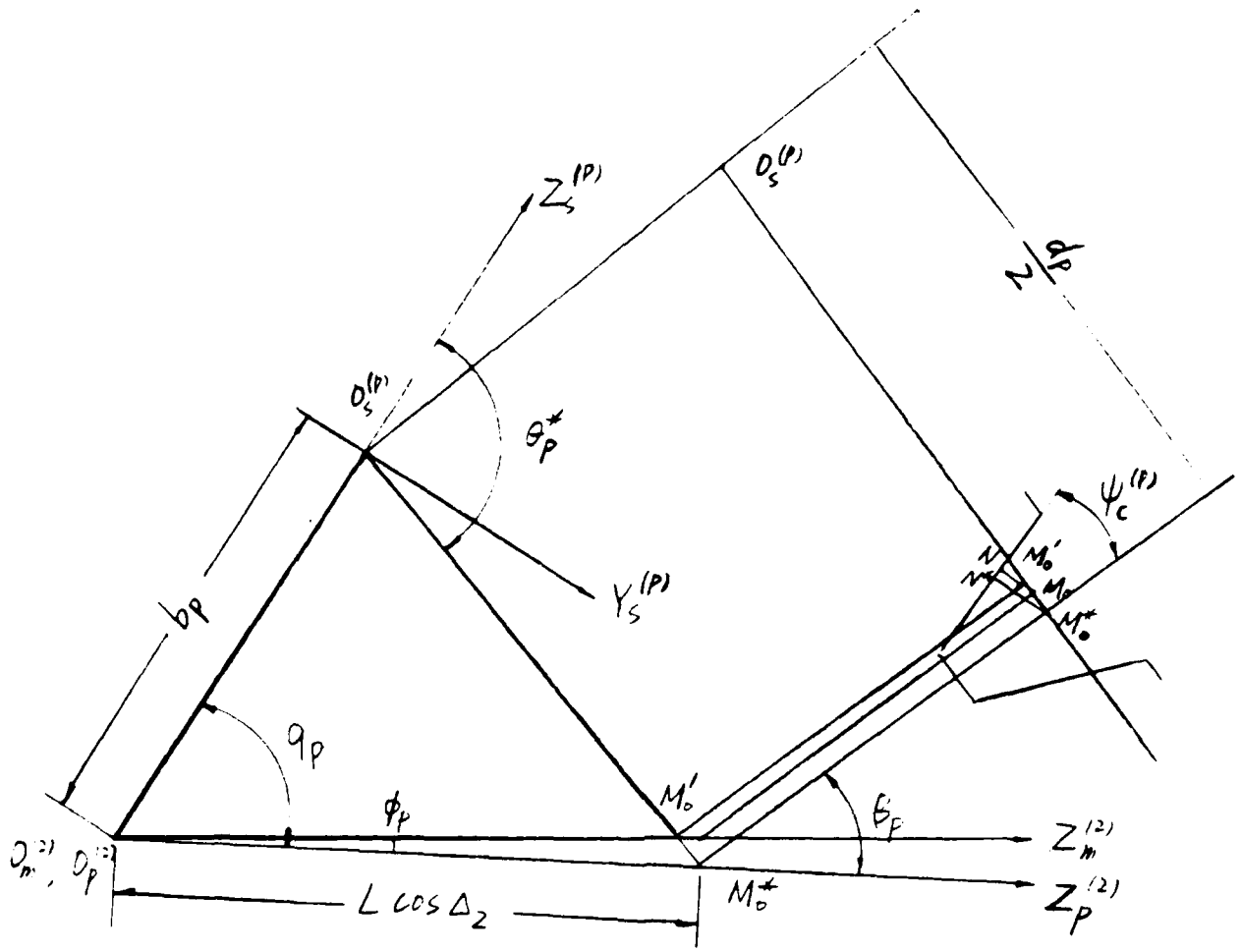

M_o' is the intersection of the pitch line and $\overline{O_s^{(p)} M_o^*}$

Fig. 8.3

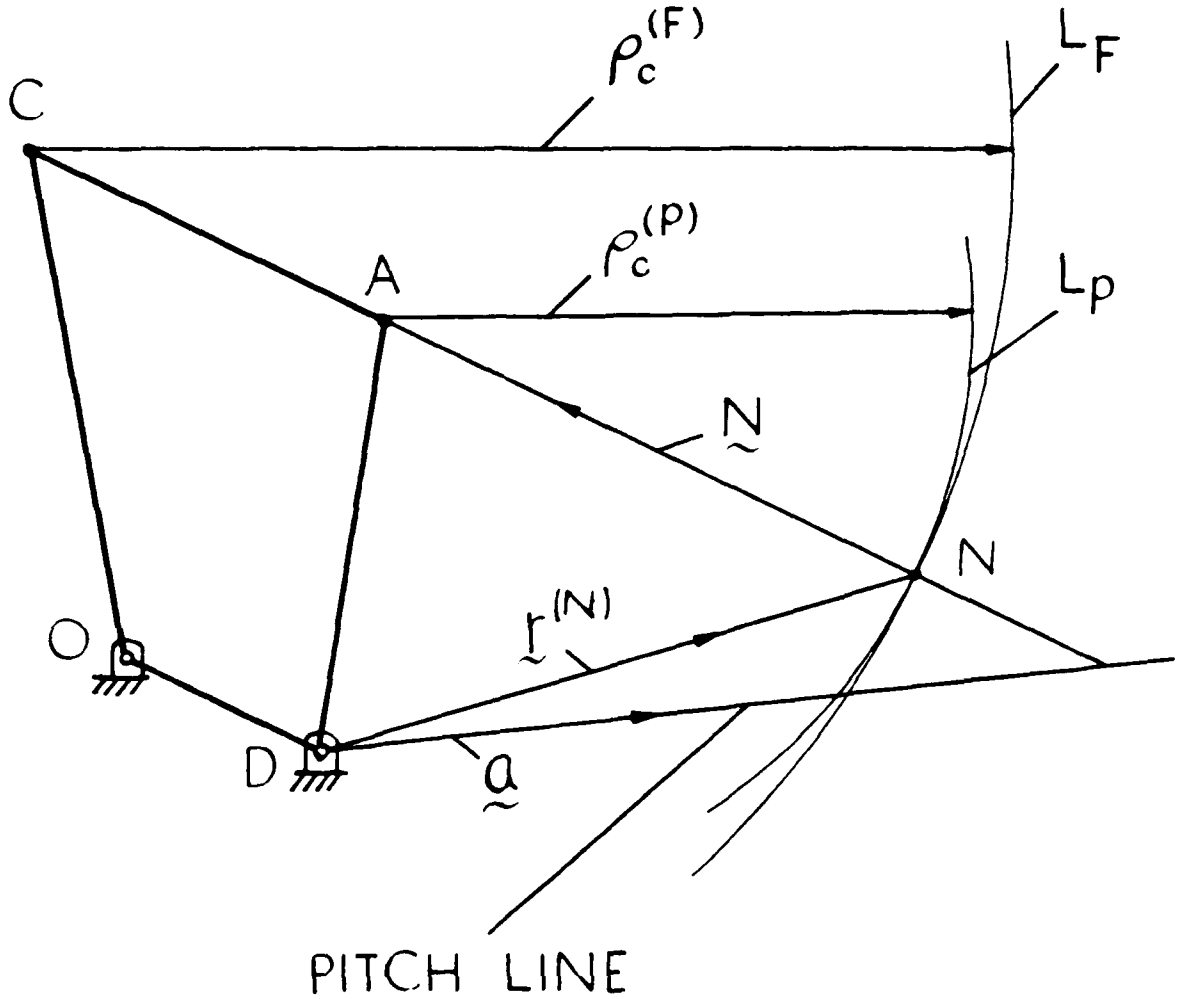
C
$\rho_c^{(F)}$
L_F
A
$\rho_c^{(P)}$
L_p
$\underset{\sim}{N}$
N
O
$\underset{\sim}{r}^{(N)}$
D
$\underset{\sim}{a}$
PITCH LINE

Fig. 9.1

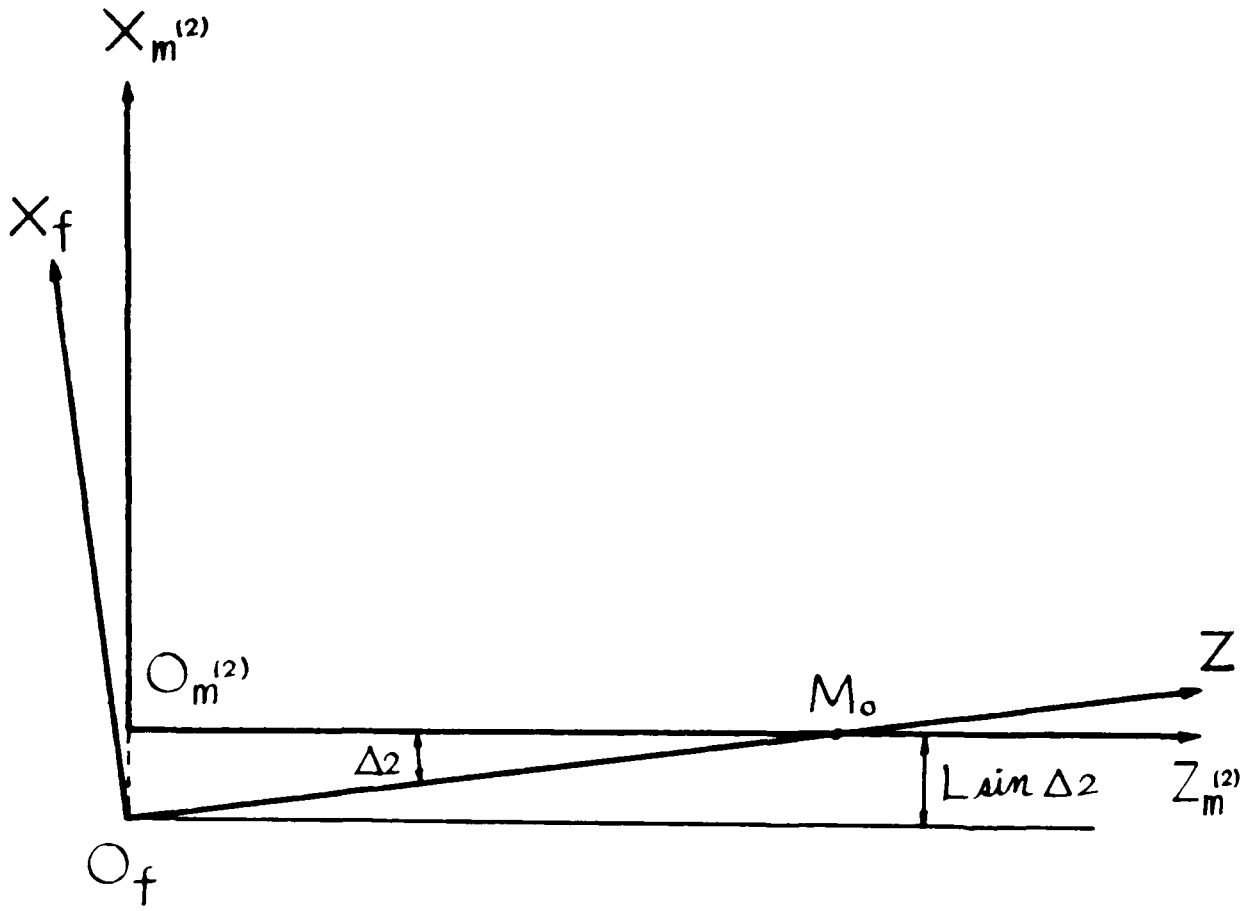

Fig. 11.1

LEFT-HAND GEAR

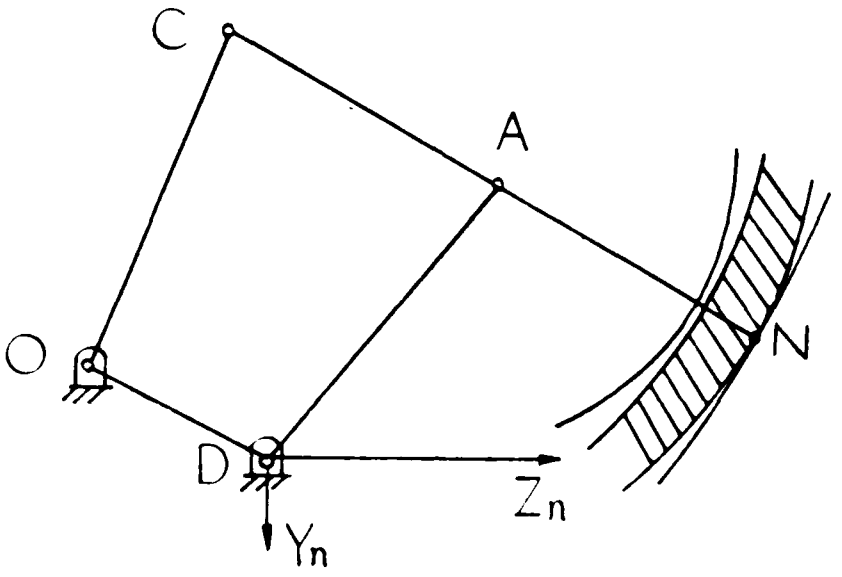

(a) GEAR TOOTH CONVEX SIDE

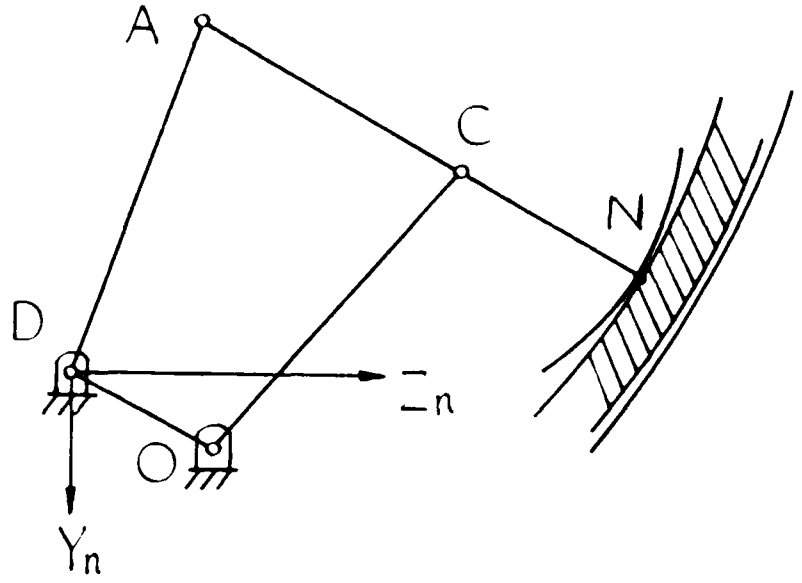

(b) GEAR TOOTH CONCAVE SIDE

Fig. 12.1

RIGHT-HAND GEAR

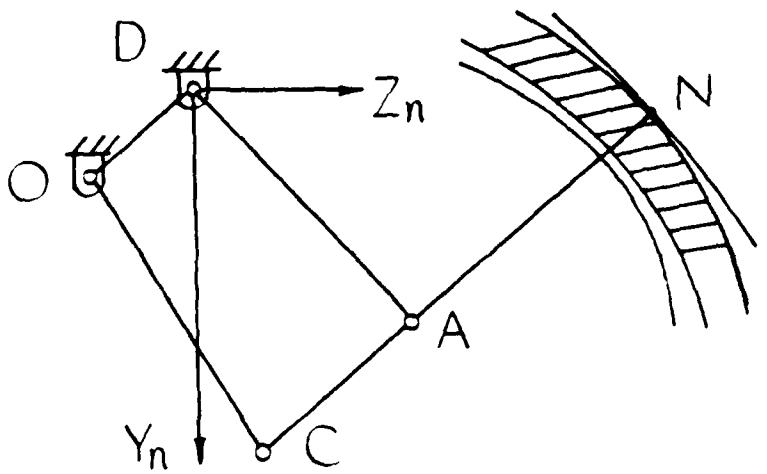

(a) GEAR TOOTH CONVEX SIDE

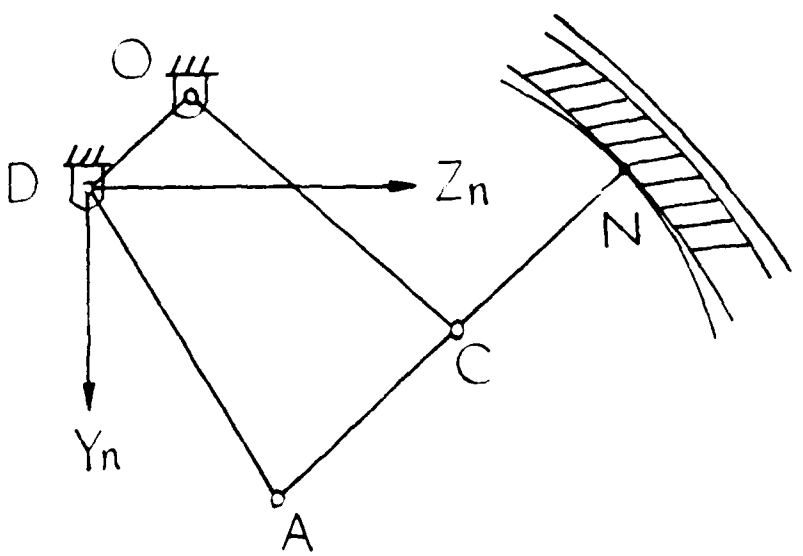

(b) GEAR TOOTH CONCAVE SIDE

Fig. 12.2

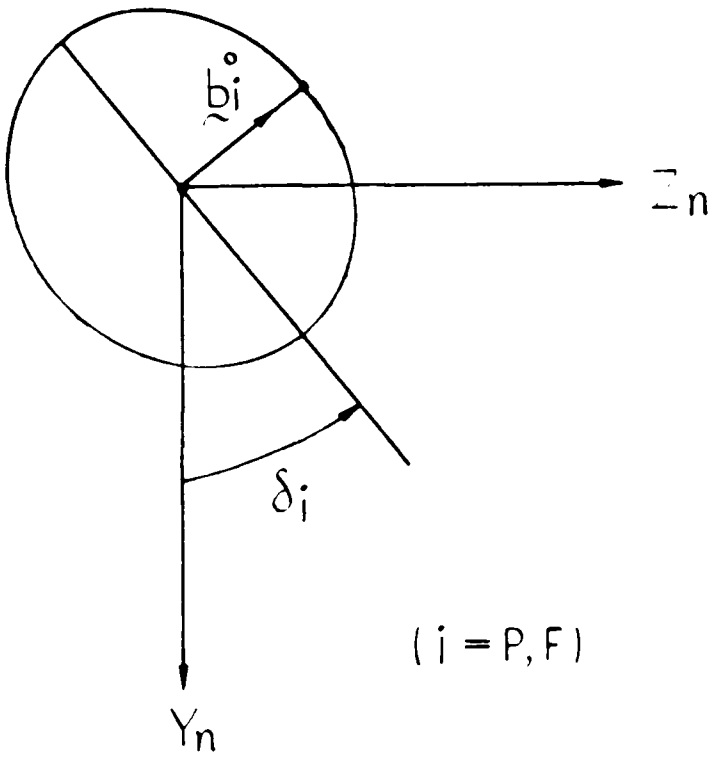

Fig. 12.3

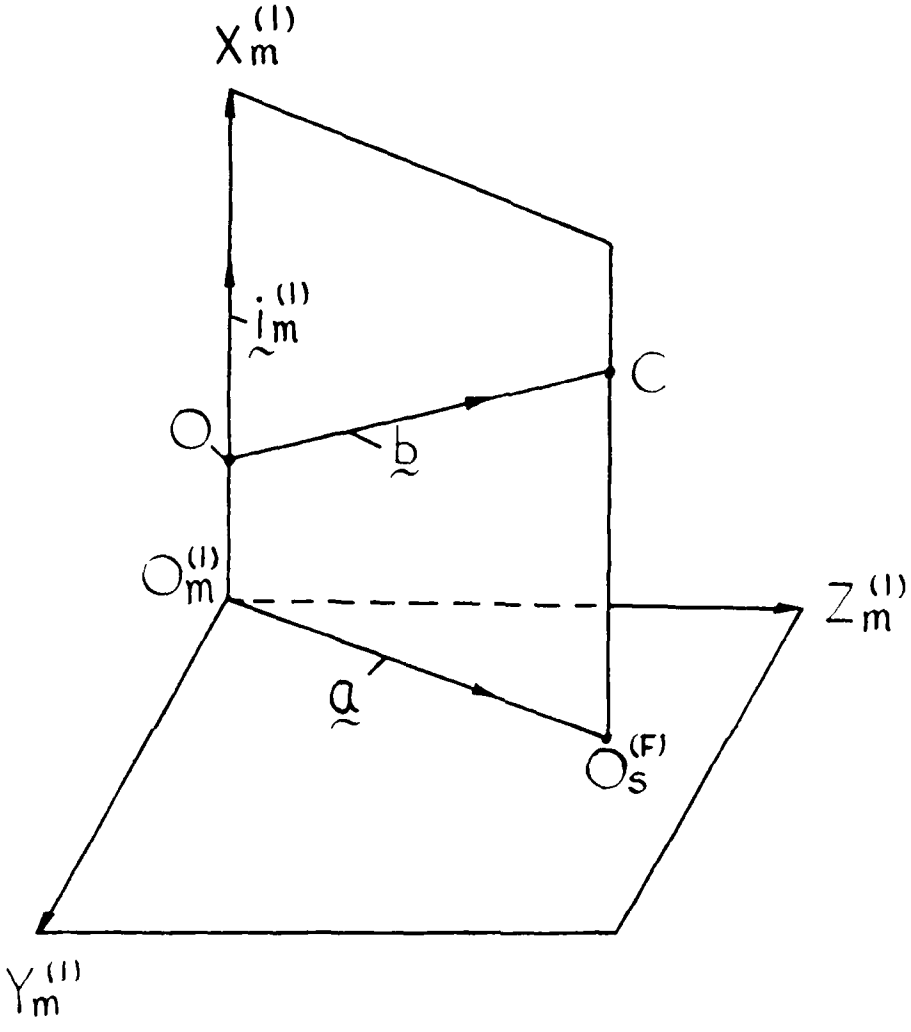
$X_m^{(1)}$
$\underset{\sim}{i}_m^{(1)}$
C
O
$\underset{\sim}{b}$
$O_m^{(1)}$
$Z_m^{(1)}$
$\underset{\sim}{a}$
$O_S^{(F)}$
$Y_m^{(1)}$

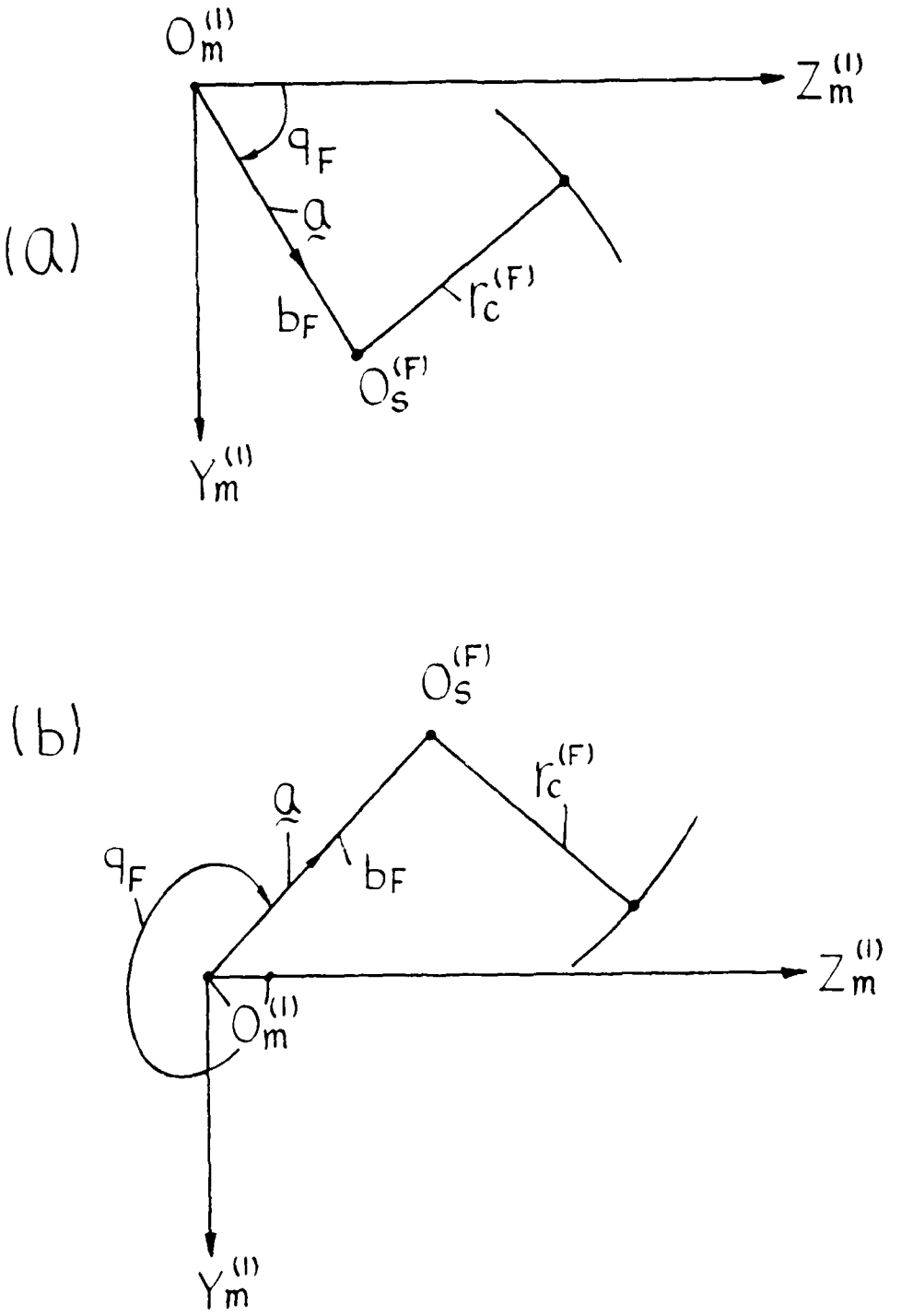
(a)
$O_m^{(1)}$
$Z_m^{(1)}$
q_F
$\underset{\sim}{a}$
b_F
$r_c^{(F)}$
$O_s^{(F)}$
$Y_m^{(1)}$
(b)
$O_s^{(F)}$
$r_c^{(F)}$
$\underset{\sim}{a}$
q_F
b_F
$Z_m^{(1)}$
$O_m^{(1)}$
$Y_m^{(1)}$

Fig. 12.5

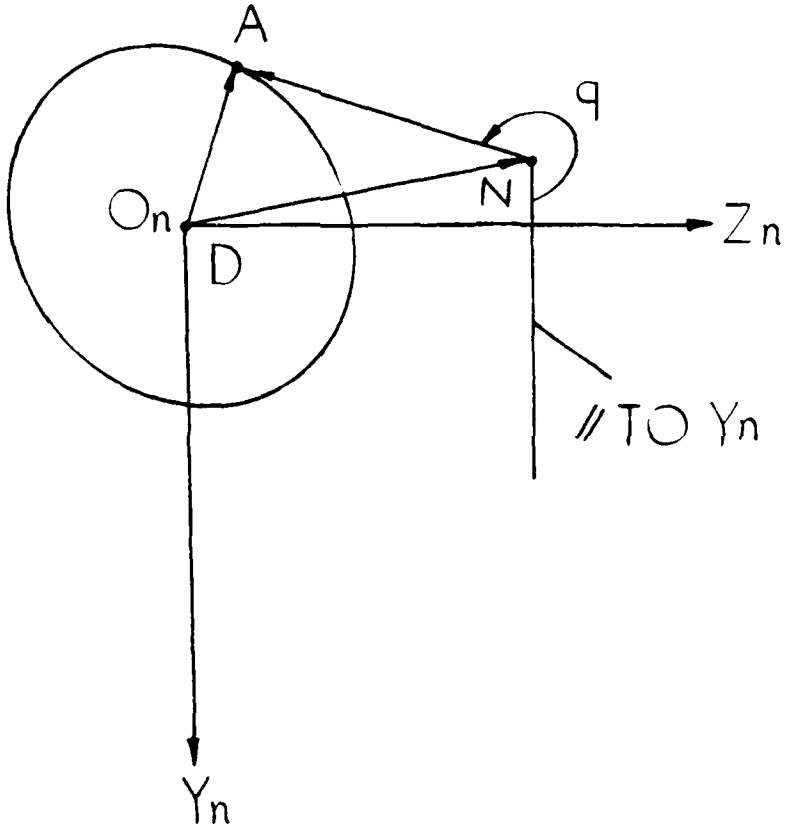

FIG. 12.6

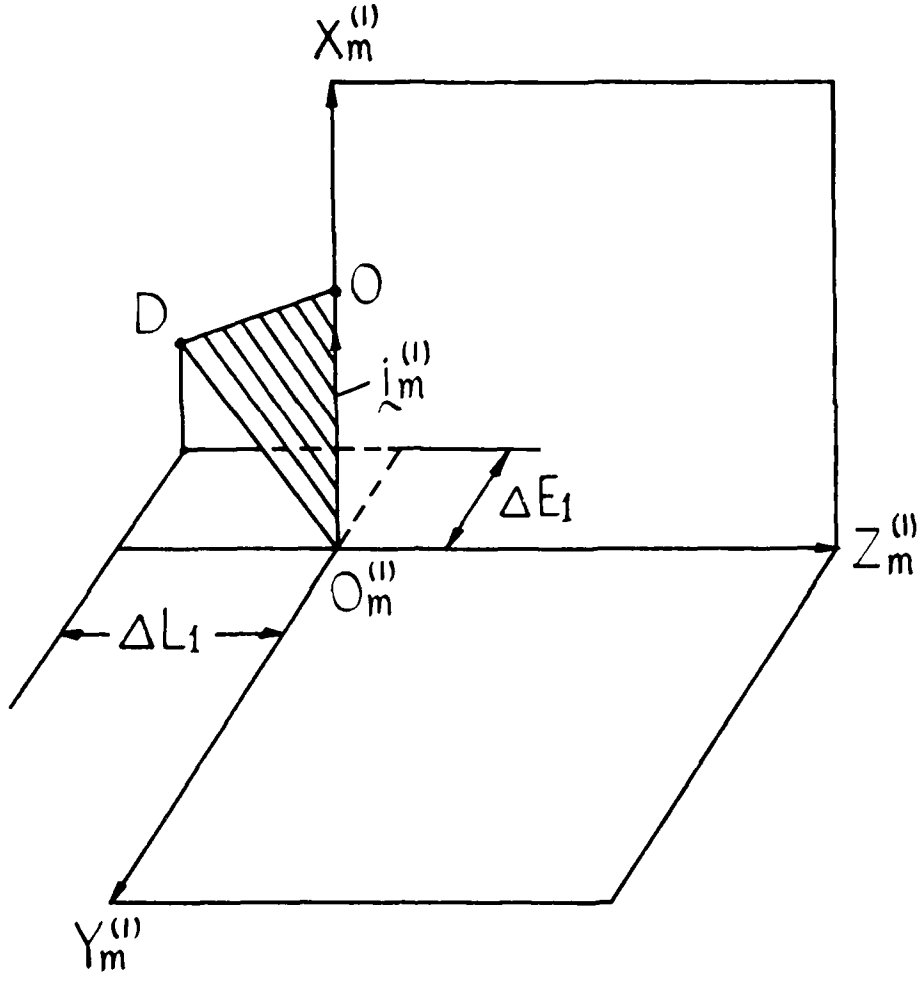

Fig. 12.7

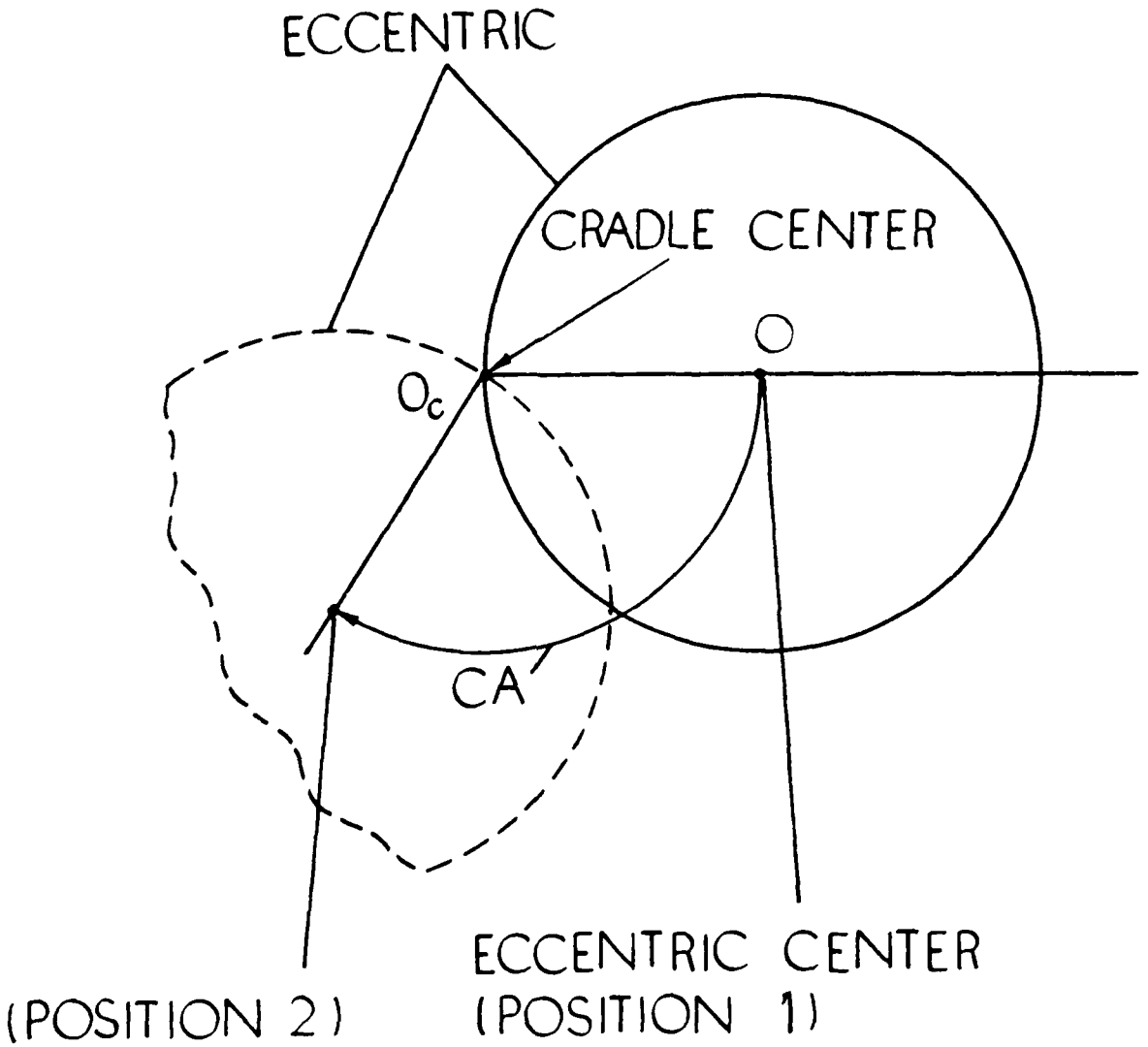
ECCENTRIC
CRADLE CENTER
O
O_c
CA
ECCENTRIC CENTER
(POSITION 1)
(POSITION 2)

Fig. 13.1

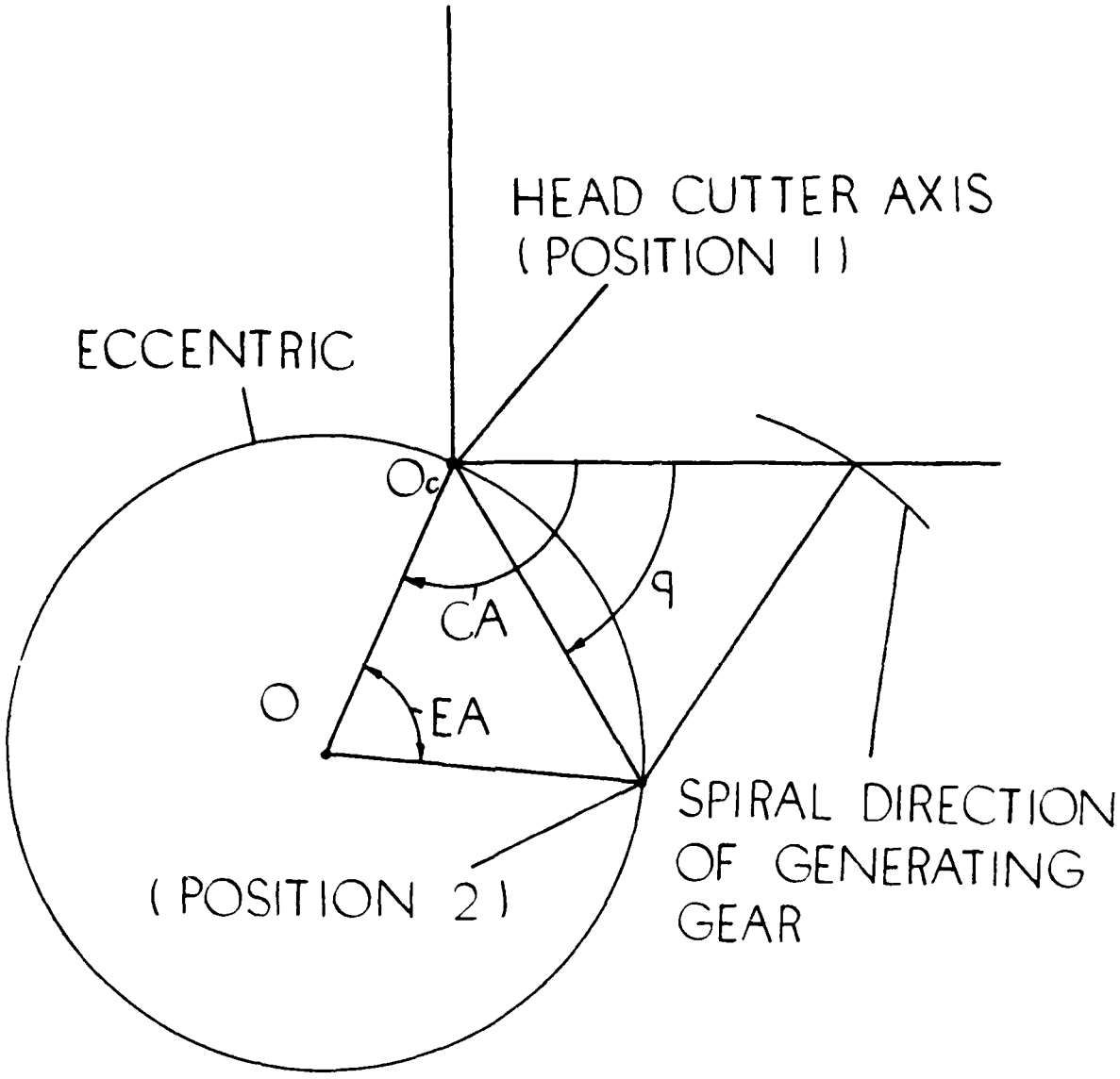
HEAD CUTTER AXIS
(POSITION 1)
ECCENTRIC
O_c
CA
q
O
EA
SPIRAL DIRECTION
OF GENERATING
GEAR
(POSITION 2)

Fig. 13.2

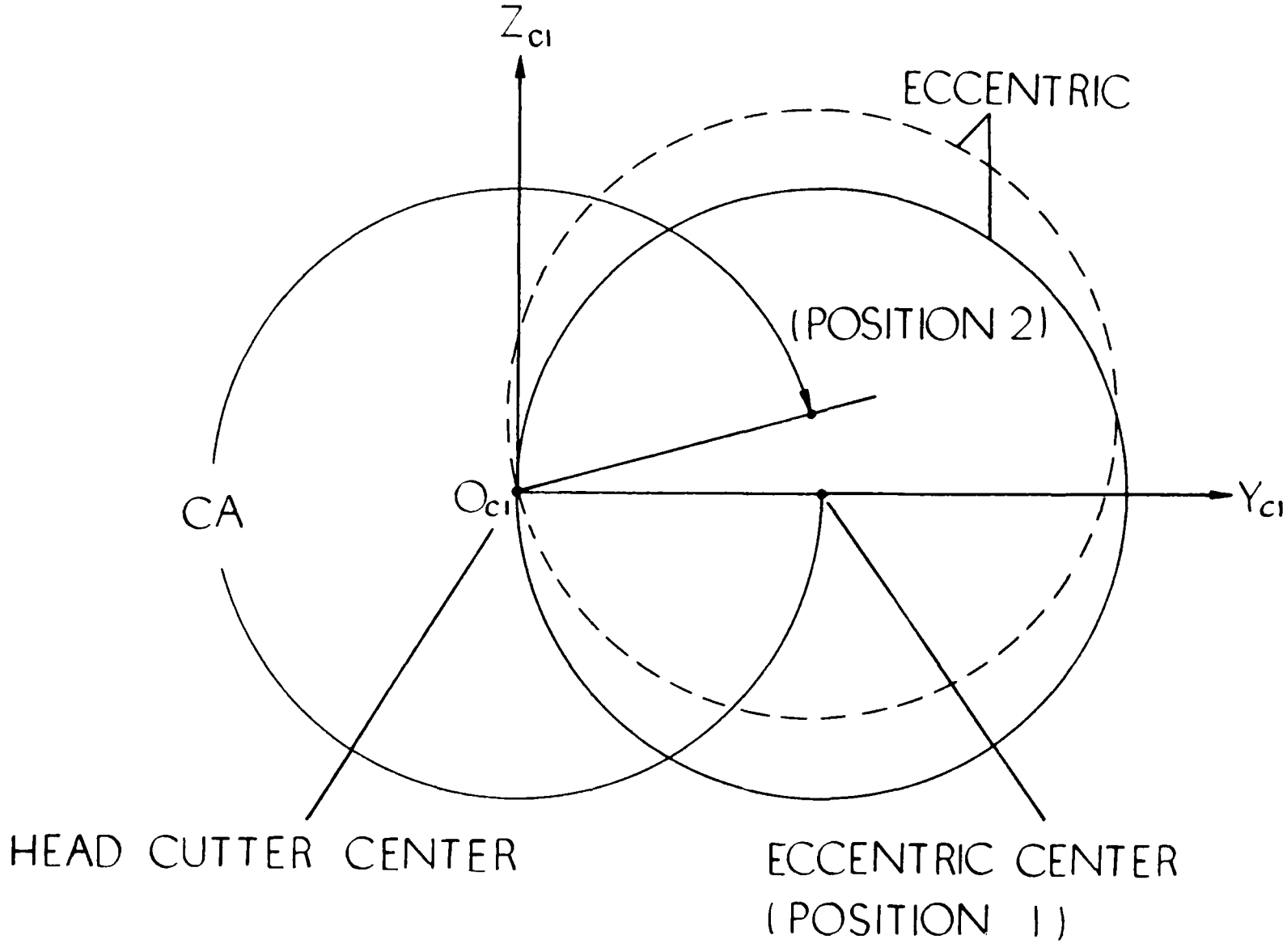
Z_{C1}
ECCENTRIC
(POSITION 2)
CA
O_{C1}
Y_{C1}
HEAD CUTTER CENTER
ECCENTRIC CENTER
(POSITION 1)

Fig. 13.3

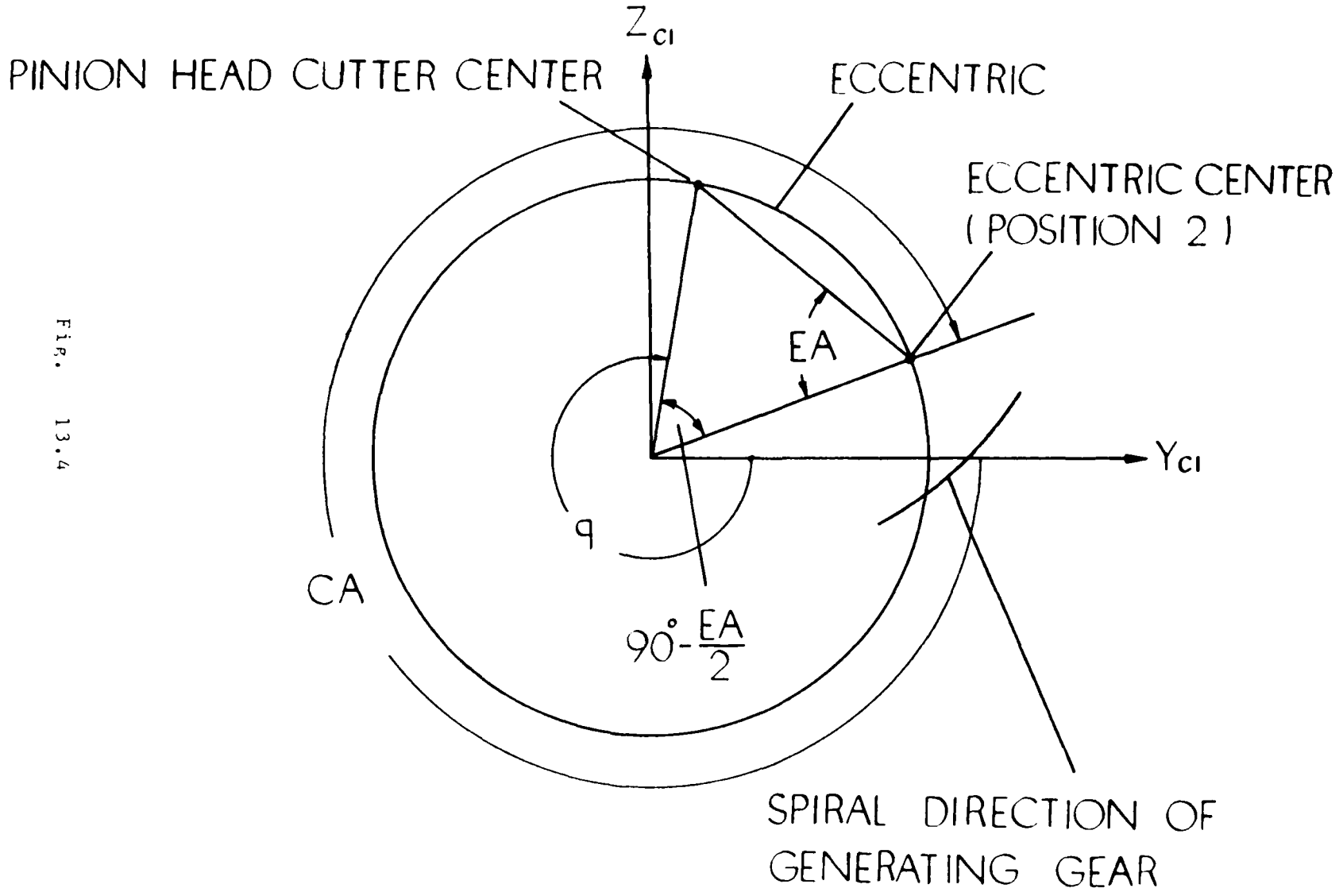
Z_{c1}
PINION HEAD CUTTER CENTER
ECCENTRIC
ECCENTRIC CENTER
(POSITION 2)
EA
Y_{c1}
q
CA
$90°-\frac{EA}{2}$
SPIRAL DIRECTION OF
GENERATING GEAR

Fig. 13.4

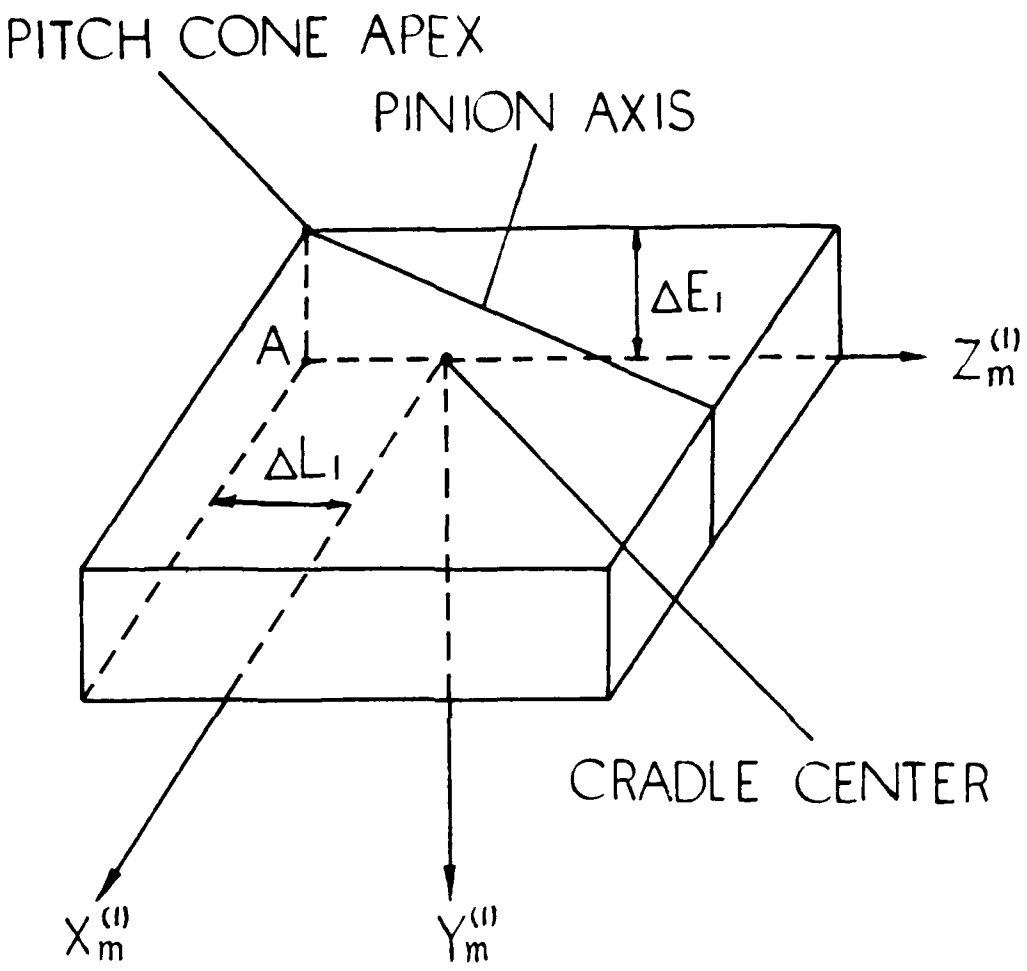
PITCH CONE APEX
PINION AXIS
ΔE1
A
Z(1)m
ΔL1
CRADLE CENTER
X(1)m
Y(1)m

Fig. 13.5

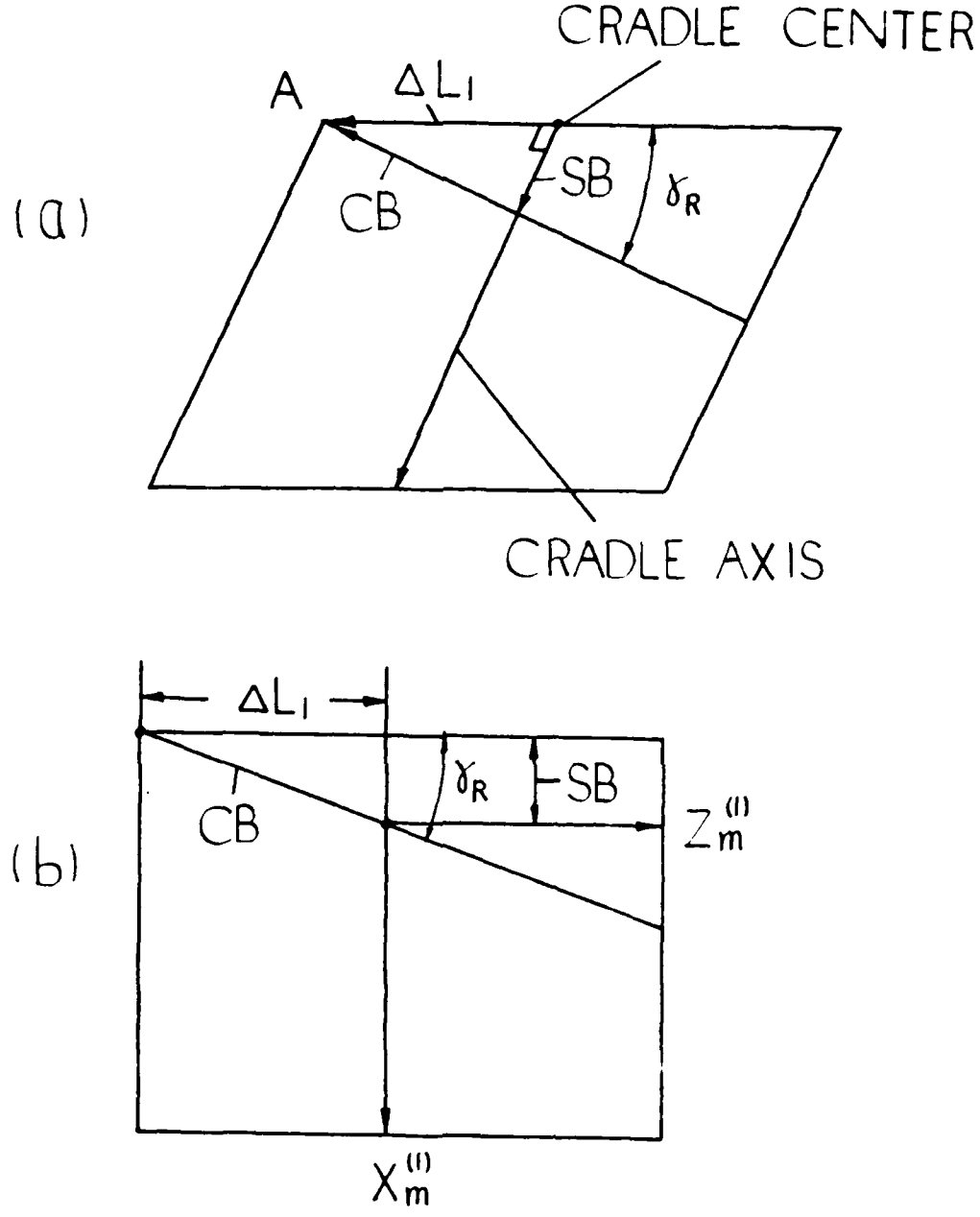

Fig. 13.6

FLOWCHART

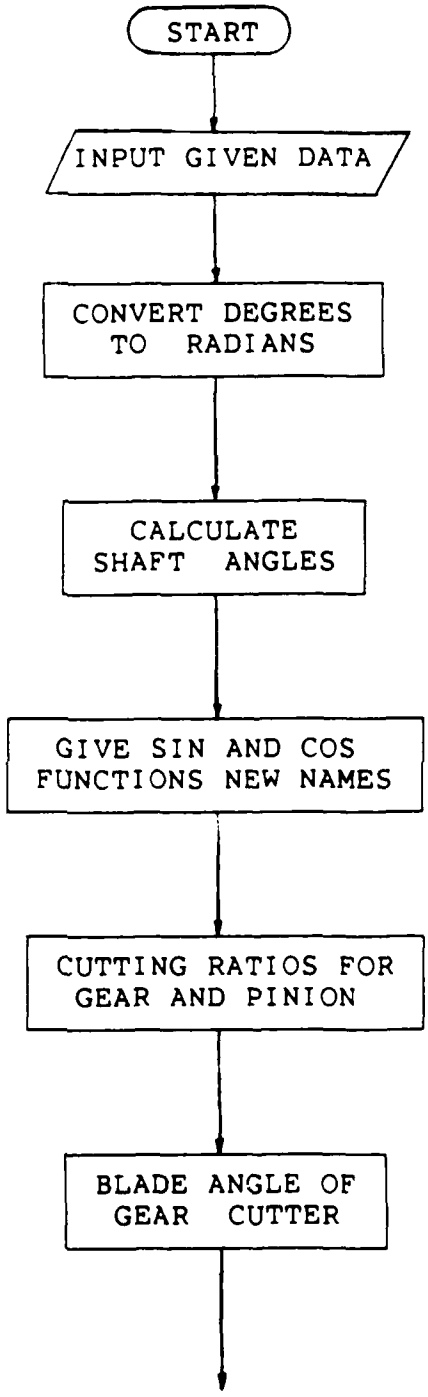
START
INPUT GIVEN DATA
CONVERT DEGREES TO RADIANS
CALCULATE SHAFT ANGLES
GIVE SIN AND COS FUNCTIONS NEW NAMES
CUTTING RATIOS FOR GEAR AND PINION
BLADE ANGLE OF GEAR CUTTER

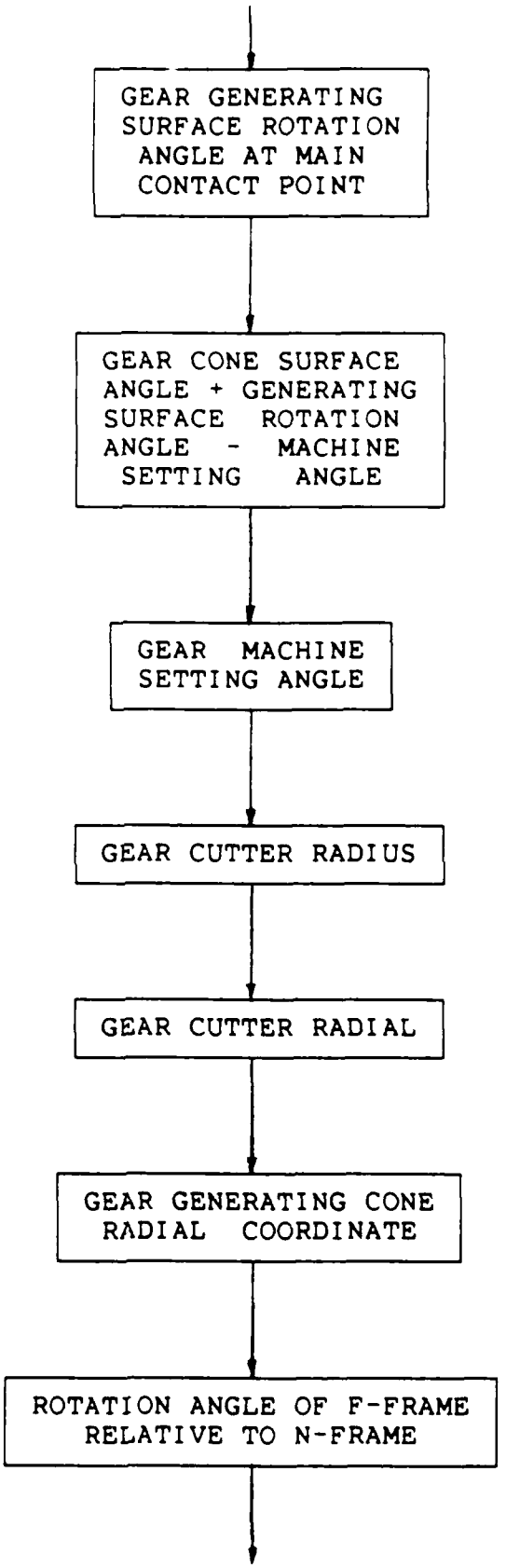
GEAR GENERATING SURFACE ROTATION ANGLE AT MAIN CONTACT POINT
GEAR CONE SURFACE ANGLE + GENERATING SURFACE ROTATION ANGLE - MACHINE SETTING ANGLE
GEAR MACHINE SETTING ANGLE
GEAR CUTTER RADIUS
GEAR CUTTER RADIAL
GEAR GENERATING CONE RADIAL COORDINATE
ROTATION ANGLE OF F-FRAME RELATIVE TO N-FRAME

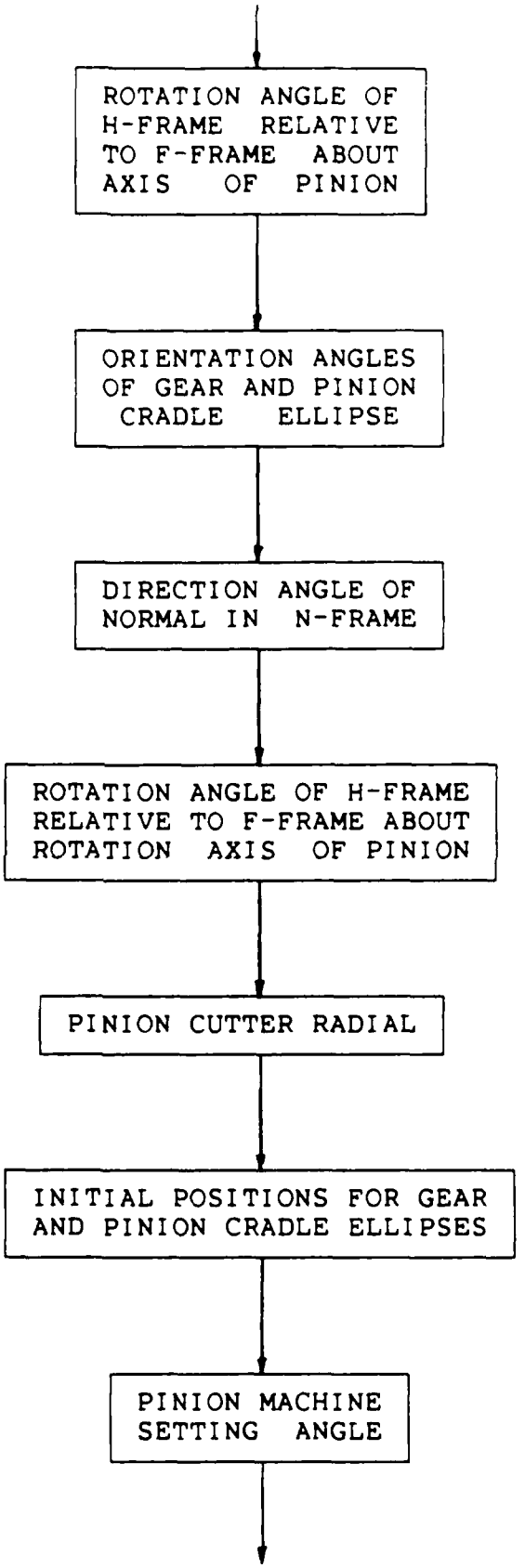
ROTATION ANGLE OF H-FRAME RELATIVE TO F-FRAME ABOUT AXIS OF PINION
ORIENTATION ANGLES OF GEAR AND PINION CRADLE ELLIPSE
DIRECTION ANGLE OF NORMAL IN N-FRAME
ROTATION ANGLE OF H-FRAME RELATIVE TO F-FRAME ABOUT ROTATION AXIS OF PINION
PINION CUTTER RADIAL
INITIAL POSITIONS FOR GEAR AND PINION CRADLE ELLIPSES
PINION MACHINE SETTING ANGLE

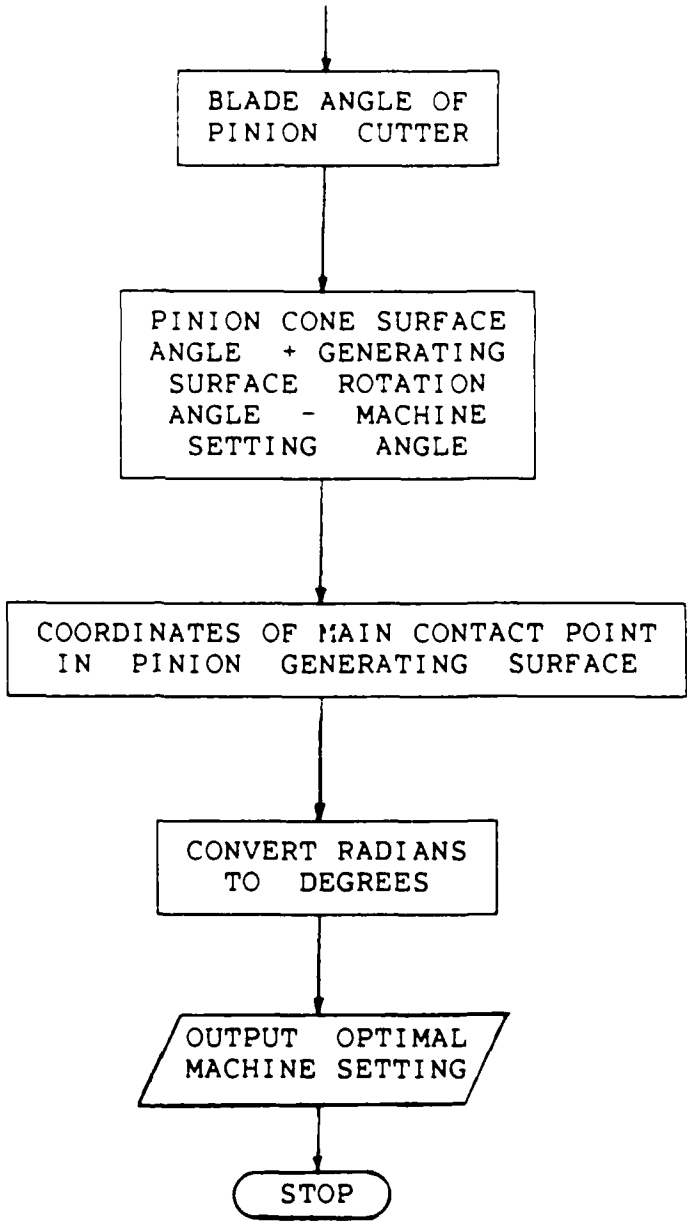
BLADE ANGLE OF PINION CUTTER
PINION CONE SURFACE ANGLE + GENERATING SURFACE ROTATION ANGLE - MACHINE SETTING ANGLE
COORDINATES OF MAIN CONTACT POINT IN PINION GENERATING SURFACE
CONVERT RADIANS TO DEGREES
OUTPUT OPTIMAL MACHINE SETTING
STOP

NUMERICAL EXAMPLE

Basic Machine Settings

		Gear (LH)	Pinion (RH)	
		Both Sides	Concave	Convex
# of Teeth	N	41	10	10
Mean Spiral Angle	β	35°	----	----
Dedendum Angle	Δ	3° 53′	1° 41′	1° 41′
Mean Cone Dist.	L	3.226	----	----
Cutter Radius	r	3.957128371	3.895686894	4.034935029
Cutter Width	W	0.08	----	----
Blade Angle	α	20°	16.7979304880°	23.188994098°
Machine Root Angle	γ_R	72.4097056667°	12.0236276667°	12.0236276667°
Radial	b	3.37751754380	3.31529203349	3.45277453402
Setting Angle	q	73.6837239464°	75.1337128849°	71.9315208492°
Machine Offest	ΔE	0	0.005082532914	-0.009816930736
Mach. Ctr. to Back	X_b	0	-0.00041258199	0.000621[illegible]
Sliding Base	X_s	0	-0.00008594705	0.000[illegible]
Ratio of Roll	m	0.973756061793	0.237501478486	[illegible]
Orientation Angle	ε	----	-0.2690602236[illegible]	[illegible]
Tilt	i	0		
Swivel	j	0		

AD-A184 437 GENERATION OF SPIRAL BEVEL GEARS WITH CONJUGATE TOOTH SURFACES AND TOOTH (U) ILLINOIS UNIV AT CHICAGO CIRCLE DEPT OF MECHANICAL ENGINEERIN F L LITVIN ET AL 2/2

UNCLASSIFIED AUG 87 NASA-CR-4088 NAG3-48 F/G 13/9 NL

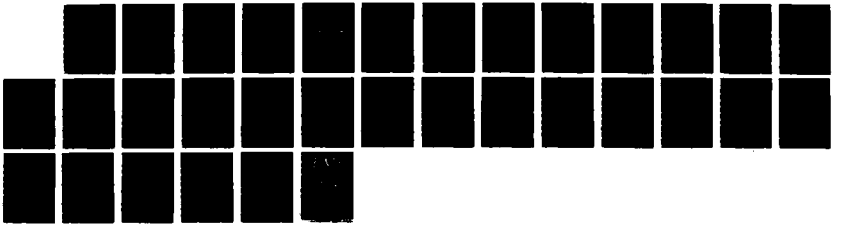

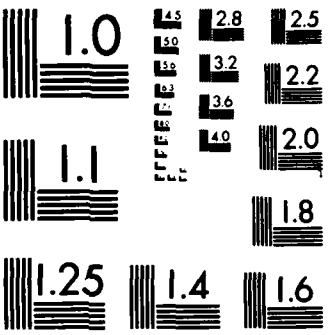

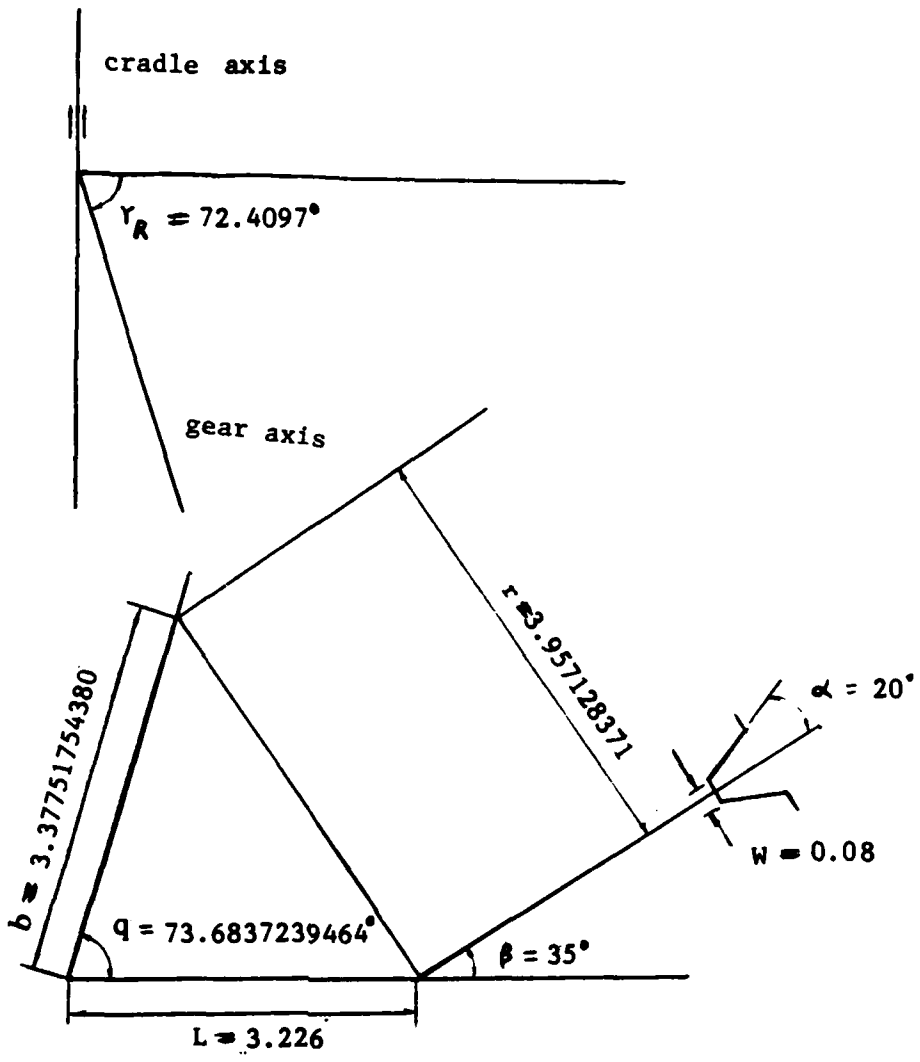
cradle axis
γ_R = 72.4097°
gear axis
r = 3.957128371
α = 20°
W = 0.08
b = 3.3775174380
q = 73.6837239464°
β = 35°
L = 3.226

GEAR (LH)

PINION (CONCAVE)

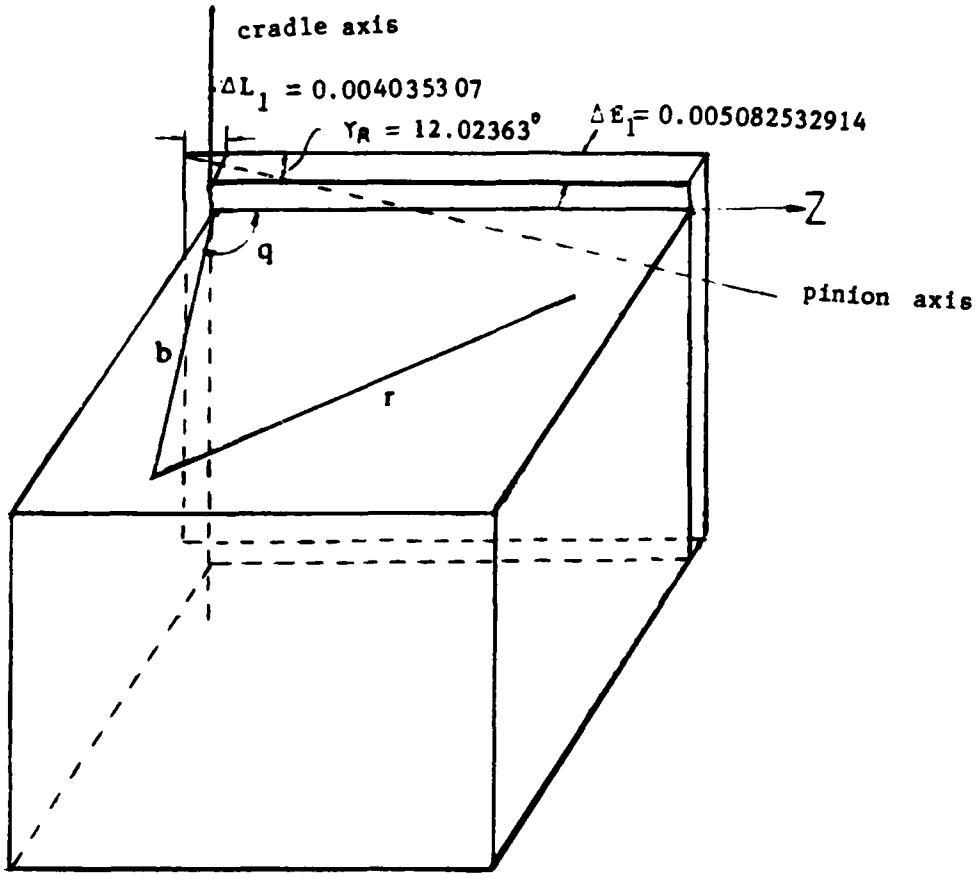

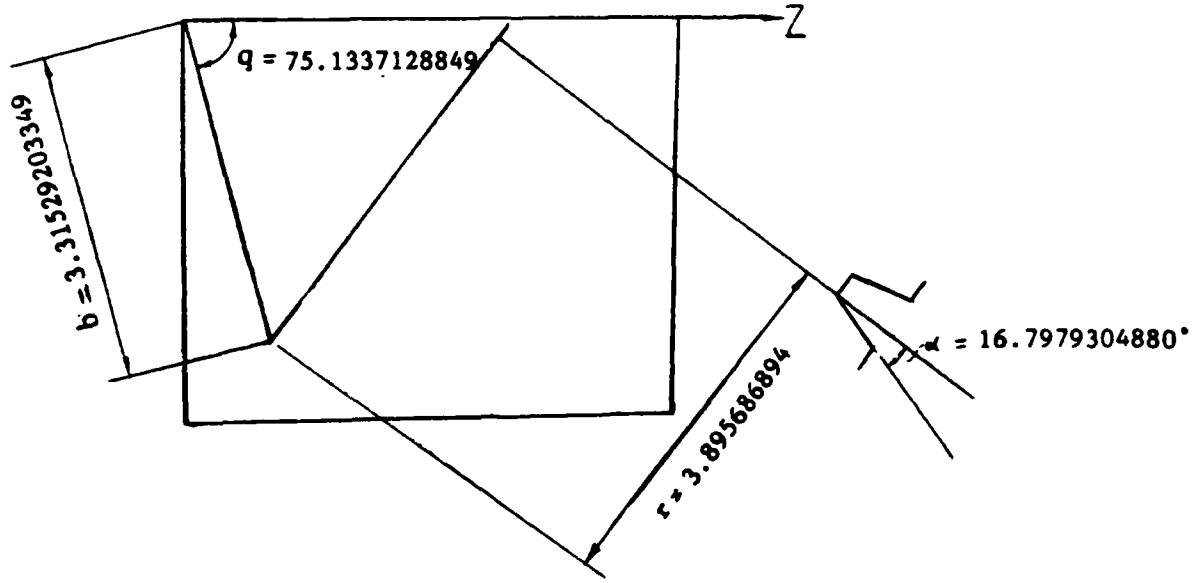

PINION (CONVEX)

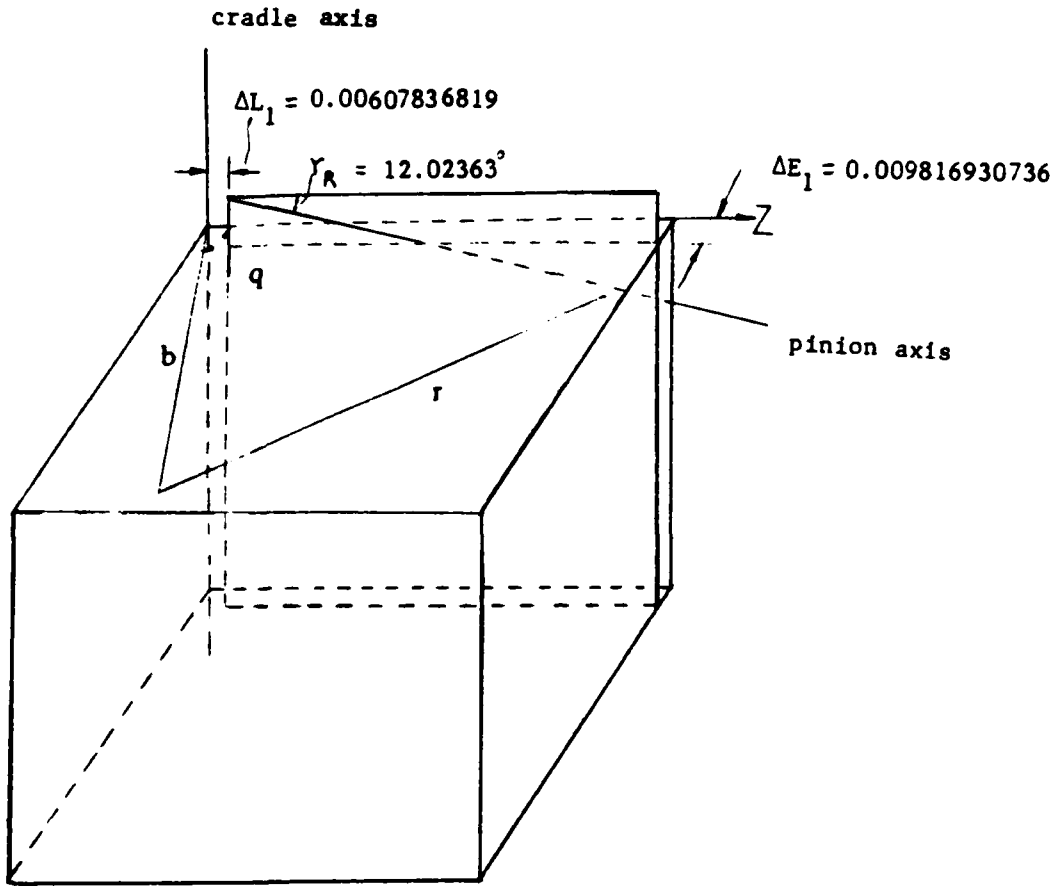

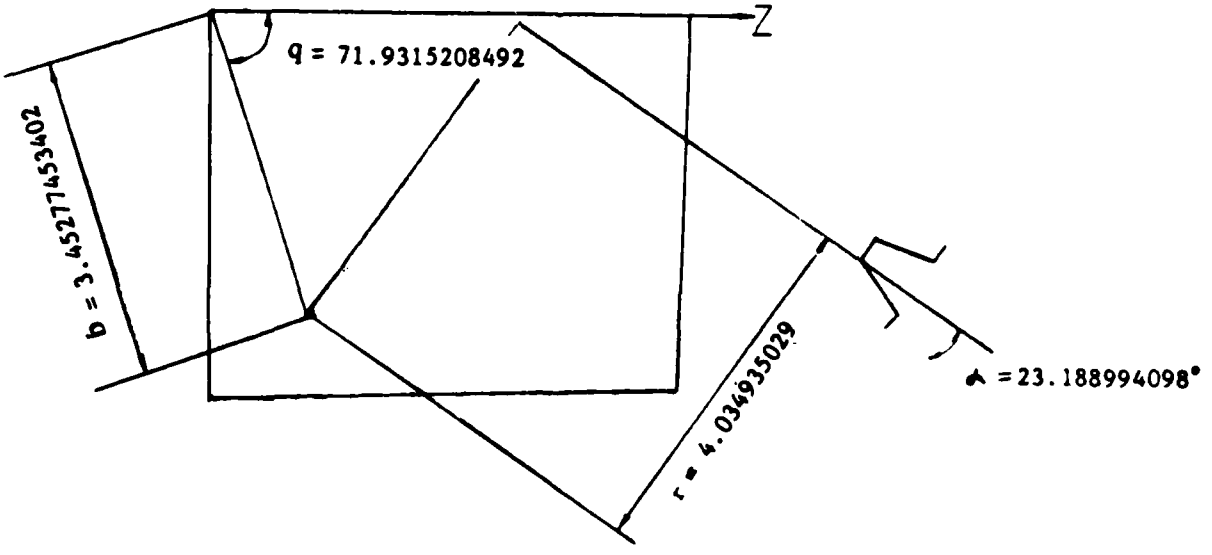

TOOTH CONTACT ANALYSIS

GEAR - CONVEX

GEAR - CONCAVE

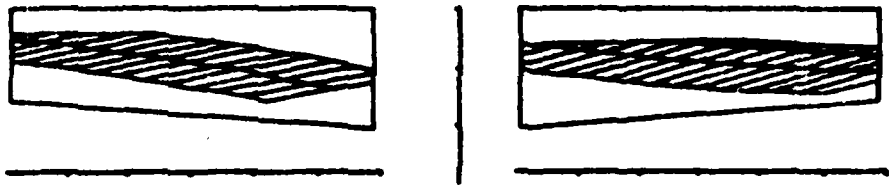

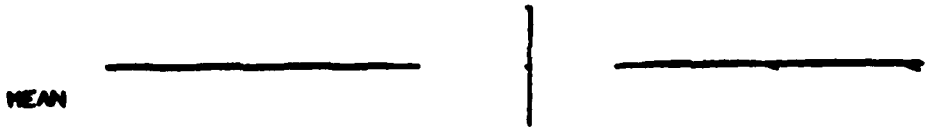

```
C...  ************************************************************
C...  *                                                          *
C...  *                                                          *
C...  *      MACHINE SETTINGS OF CONJUGATE SPIRAL BEVEL GEAR     *
C...  *                                                          *
C...  *                AUTHORS: FAYDOR    LITVIN                 *
C...  *                         WEI-JIUNG  TSUNG                 *
C...  *                         HONG-TAO     LEE                 *
C...  *                                                          *
C...  *                                                          *
C...  ************************************************************
C
C PURPOSE
C
C     To find the machine setting parameters for the generation of
C     spiral bevel gears.
C
C NOTE
C
C     This program is written in FORTRAN 77.  It can be compiled by
C     V compiler in IBM mainframe or FORTRAN compiler in VAX system.
C
C DESCRIPTION OF INPUT PARAMETERS
C
C...  JJ          : JJ=1 for left-hand gear, JJ=2 for right-hand gear
C...  TN1         : teeth number of pinion
C...  TN2         : teeth number of gear
C...  D1DG, D1MIN : dedendum angle of pinion (degree and arc minute,
C...                respectively)
C...  D2DG, D2MIN : dedendum angle of gear (degree and arc minute,
C...                respectively)
C...  GAMADG      : shaft angle (degree)
C...  BPDG        : mean spiral angle (degree)
C...  RL          : mean cone distance
C...  W           : point width for gear finishing
C...  ALFAP       : blade angle of gear cutter (degree)
C...  RCF1        : pinion cutter radius for pinion concave side
C...  RCF2        : pinion cutter radius for pinion convex side
C...  DUP1        : a chosen value for pinion concave side to locate the
C                   main contact point at the desired location
C...  DUP2        : a chosen value for pinion convex side to locate the
C                   main contact point at the desired location
C...  DUPFEP      : a chosen value for pinion concave side to get the
C                   desired direction of the contact path
C
C DESCRIPTION OF OUTPUT PARAMETERS
C
C... PHPDG        : blade angle of gear cutter (degree)
C... PHFDG        : blade angle of pinion cutter (degree)
C... RCP          : radius of gear cutter (measured on cradle plane)
C... RCF          : radius of pinion cutter (measured on cradle plane)
C... TPDG         : the difference between the sum of gear cone surface
C                   angle coordinate and generating surface rotation
C                   angle, and machine setting angle (degree) [see
C                   equation (4.18) in report]
```

```
C... TFDG          : the difference between the sum of pinion cone
C                    surface angle coordinate and generating surface
C                    rotation angle, and machine setting angle (degree)
C...                 [see equation (4.3) in report]
C... BP            : radial of gear cutter
C... BF            : radial of pinion cutter
C... QPDG          : machine setting angle of gear
C... QFDG          : machine setting angle of pinion
C... MP2           : ratio of cradle angular velocity for cutting the
C                    gear and gear angular velocity
C... MF1           : ratio of cradle angular velocity for cutting the
C                    pinion and pinion angular velocity
C... DE1           : machine offset for cutting the pinion
C... DL1           : vector-sum of (1) the change of machine center to
C                    back and (2) the sliding base
C... FEE0DG        : generating surface rotation angle at initial main
C                    contact point
C... DELTADG       : rotation angle of frame h relative to frame f about
C                    Z1
C
      IMPLICIT REAL*8(A-H,O-Z)
C
C INPUT THE DESIGN DATA
C
      DATA JJ/1/
      DATA TN1,TN2/10.D00,41.D00/
      DATA D1DG,D1MIN/1.D00,41.D00/
      DATA D2DG,D2MIN/3.D00,53.D00/
      DATA GAMADG,BPDG/90.D00,35.D00/
      DATA RL/3.226D00/
      DATA W/0.08D00/
      DATA ALFAP/20.D00/
      DATA RCF1/3.86707929616D00/
      DATA RCF2/4.05714282715D00/
      DATA DUP1/0.042787628358701D00/
      DATA DUP2/-0.037763737441601 6731D00/
      DATA DUPFEP/-0.526309620098410257D00/
C
C CONVERT DEGREES TO RADIANS
C
      CNST=4.D00*DATAN(1.D00)/180.D00
      D1=(D1DG+D1MIN/60.D00)*CNST
      D2=(D2DG+D2MIN/60.D00)*CNST
      BP=BPDG*CNST
C
C CALCULATE GAMA1 AND GAMA2
C
      GAMA=GAMADG*CNST
      RM12=TN2/TN1
      RM21=TN1/TN2
      GMA1=DATAN(DSIN(GAMA)/(RM12+DCOS(GAMA)))
      GMA2=DATAN(DSIN(GAMA)/(RM21+DCOS(GAMA)))
      IF(GMA1 .LT. 0.)THEN
       GMA1=180.*CNST+GMA1
      END IF
```

```
      IF(GMA2 .LT. 0.)THEN
       GMA2=180.*CNST+GMA2
      END IF
C
C SUBSTITUTE SIN AND COS FUNCTION BY A SHORT NAME
C
      SNBP=DSIN(BP)
      CSBP=DCOS(BP)
      SND1=DSIN(D1)
      CSD1=DCOS(D1)
      SNR1D1=DSIN(GMA1-D1)
      CSR1D1=DCOS(GMA1-D1)
      SNR1D2=DSIN(GMA1+D2)
      CSR1D2=DCOS(GMA1+D2)
      SNR2D2=DSIN(GMA2-D2)
      CSR2D2=DCOS(GMA2-D2)
      CSD2=DCOS(D2)
      SND2=DSIN(D2)
      CSGM1=DCOS(GMA1)
      SNGM1=DSIN(GMA1)
      CSGM2=DCOS(GMA2)
      SNGM2=DSIN(GMA2)
C
C CALCULATE CUTTING RATIOS
C
      RMP2=SNGM2/CSD2
      RMF1=TN1*SNGM2/(TN2*CSD2)
C
C II=1: THE PINION CONCAVE PART ANALYSIS, II=2: THE PINION CONVEX PART
C ANALYSIS
C
      DO 10000 II=1,2
      IF(II .EQ. 1)THEN
       RCF=RCF1
       DUP=DUP1
       ELSE
       RCF=RCF2
       DUP=DUP2
      END IF
C
C CALCULATE PHP
C
      IF(II .EQ .1)THEN
       PHP=ALFAP*CNST
       ELSE
       PHP=(180.D00-ALFAP)*CNST
       END IF
      SNPHP=DSIN(PHP)
      CSPHP=DCOS(PHP)
C
C CALCULATE FEEP AT INITIAL MAIN CONTACT POINT
C
      A=CSD2*SNPHP-SND2*CSPHP*SNBP+DUP*SNBP/RL
      IF(JJ .EQ. 2)THEN
       A=-A
```

```
      END IF
      B=DUP*CSBP/RL-SND2*CSPHP*CSBP
      C=SND2*CSPHP*CSBP
      D=DSQRT(A*A+B*B-C*C)
      E=C-B
      F1=DATAN((-A+D)/E)
      F2=DATAN((-A-D)/E)
      IF(DABS(F1) .LT. DABS(F2))THEN
       FEE=2.D00*F1
       ELSE
       FEE=2.D00*F2
      END IF
      CSFEE=DCOS(FEE)
      SNFEE=DSIN(FEE)
C
C CALCULATE TP
C
      IF(JJ .EQ. 1)THEN
       TP=90.D00*CNST-BP+FEE
       ELSE
       TP=270.D00*CNST+BP+FEE
      END IF
      SNTP=DSIN(TP)
      CSTP=DCOS(TP)
C
C CALCULATE QP
C
      IF(II .EQ. 1)THEN
       IF(JJ .EQ. 1)THEN
        D=DUPFEP*SNBP*SNTP+RL*CSD2*SNPHP*CSBP*SNFEE+RL*SND2*CSPHP
     #    *CSBP*CSBP
        ELSE
        D=DUPFEP*SNBP*SNTP-RL*CSD2*SNPHP*CSBP*SNFEE+RL*SND2*CSPHP
     #    *CSBP*CSBP
       END IF
       E=DUPFEP*CSBP*SNTP+RL*CSD2*SNPHP*CSBP*CSFEE-RL*SND2*CSPHP
     #   *SNBP*CSBP
       QP=DATAN(-E/D)
       IF(QP .LT. 0.D00)THEN
        QP=180.D00*CNST+QP
       END IF
      END IF
      IF(JJ .EQ. 1)THEN
       SNQPFE=DSIN(QP-FEE)
       CSQPFE=DCOS(QP-FEE)
       THP=90.D00*CNST+QP-BP
       ELSE
       SNQPFE=DSIN(QP+FEE)
       CSQPFE=DCOS(QP+FEE)
       THP=270.D00*CNST-QP+BP
      END IF
      SNTHP=DSIN(THP)
C
C CALCULATE RCP
C
```

```
      CM0=RL*CSD2*DSIN(QP)/DCOS(BP-QP)
      IF(II .EQ. 1)THEN
       RCP=CM0-W/2.0D00-RL*SND2*SNPHP/CSPHP
       ELSE
       RCP=CM0+W/2.D00-RL*SND2*SNPHP/CSPHP
      END IF
C
C CALCULATE RBP
C
      RBP=RL*CSD2*CSBP/DCOS(BP-QP)
C
C CALCULATE UP
C
      UP=(RCP*CSPHP/SNPHP+RL*SND2)*CSPHP+RBP*(SNPHP*SNQPFE-CSPHP*
     #    SNTHP*SND2/CSD2)/SNTP
C
C CALCULATE RN
C
      AN=-SNPHP*CSD2+CSPHP*CSTP*SND2
      BN=CSPHP*SNTP
      RN=DATAN(AN/BN)
      SNRN=DSIN(RN)
      CSRN=DCOS(RN)
C
C CALCULATE DLTA
C
      A=CSGM1
      B=-SNRN/CSRN
      C=(SNGM1*SNR1D1-CSD2)/CSR1D1
      X1=-B+DSQRT(A**2+B**2-C**2)
      X2=-B-DSQRT(A**2+B**2-C**2)
      Y=C-A
      AE=X1/Y
      BE=X2/Y
      DLT2A=DATAN(AE)
      DLT2B=DATAN(BE)
      IF(DABS(DLT2A).LT.DABS(DLT2B))THEN
       DLTA=DLT2A*2.D00
       ELSE
       DLTA=DLT2B*2.D00
      END IF
      SNDLTA=DSIN(DLTA)
      CSDLTA=DCOS(DLTA)
C
C CALCULATE DETAP
C
      A01=SND2/CSD2
      B01=-SNRN
      DETAP=DATAN(A01/B01)
C
C CALCULATE DTAF
C
      A211=CSGM1*SNR1D1/CSR1D1-CSDLTA*SNGM1
      B211=-(SNDLTA*CSRN+SNRN*(CSDLTA*CSGM1+SNGM1*SNR1D1/CSR1D1))
      DETAF=DATAN(A211/B211)
```

```
      CSDTAF=DCOS(DETAF)
      SNDTAF=DSIN(DETAF)
C
C CALCULATE Q
C
C calculate normal vector at main contact point in F coordinate system
C
      RNXF2=SNPHP*CSD2-CSPHP*CSTP*SND2
      RNYF2=CSPHP*SNTP
      RNZF2=SNPHP*SND2+CSPHP*CSTP*CSD2
C
C calculate normal vector at main contact point in N coordinate system
C
      RNYN2=-SNRN*RNXF2+CSRN*RNYF2
      RNZN2=RNZF2
C
      Q=DATAN2(-RNZN2,-RNYN2)
      QAP=Q-DETAP
      QAF=Q-DETAF
      SNQAP=DSIN(QAP)
      CSQAP=DCOS(QAP)
      SNQAF=DSIN(QAF)
      CSQAF=DCOS(QAF)
C
C CALCULATE BF
C
      BF=DSQRT((CSQAP**2*CSD2**2*CSRN**2+SNQAP**2)
     #     /(CSQAF**2*CSD2**2*CSRN**2+SNQAF**2))*RBP
C
C CALCULATE PO
C
      RAP=RBP/(CSD2*CSRN)
C
C calculute coordinate of main contact point in M coordinate system
C
      RMXM2=RCP*CSPHP/SNPHP-UP*CSPHP
      RMYM2=UP*SNPHP*SNTP-RBP*SNQPFE
      RMZM2=UP*SNPHP*CSTP+RBP*CSQPFE
C
C calculute coordinate of main contact point in F coordinate system
C
      RMXF2=CSD2*RMXM2-SND2*RMZM2+RL*SND2*CSD2
      RMYF2=RMYM2
      RMZF2=SND2*RMXM2+CSD2*RMZM2+RL*SND2*SND2
C
C calculute coordinate of main contact point in N coordinate system
C
      RMXN2=CSRN*RMXF2+SNRN*RMYF2
      RMYN2=-SNRN*RMXF2+CSRN*RMYF2
      RMZN2=RMZF2
C
      AG=-RAP*SNQAP
      BG=RBP*CSQAP
      CG=RMYN2*DSIN(Q)-RMZN2*DCOS(Q)
      G11=-BG+DSQRT(AG**2+BG**2-CG**2)
```

```
      G22=-BG-DSQRT(AG**2+BG**2-CG**2)
      G33=CG-AG
      P01=DATAN(G11/G33)
      P02=DATAN(G22/G33)
      IF(DABS(P01).LT.DABS(P02))THEN
       P0=P02*2.D00
       ELSE
       P0=P01*2.D00
       END IF
      SNP0=DSIN(P0)
      CSP0=DCOS(P0)
C
C CALCULATE F0
C
      AF=BF/(CSD2*CSRN)
      RNF=BF**2
      RMF=AF**2
      DD11=RAP*SNQAP*CSP0-RBP*CSQAP*SNP0
      DD22=RAP*SNQAP*SNP0+RBP*CSQAP*CSP0
      SSS=(AF*SNQAF)**2+(BF*CSQAF)**2
      CSF0=(AF*DD11*SNQAF+BF*DD22*CSQAF)/SSS
      SNF0=(AF*DD22*SNQAF-BF*DD11*CSQAF)/SSS
      F0=DATAN2(SNF0,CSF0)
C
C CALCULATE QF
C
      AA22=-SNDLTA*CSGM1*SNRN+CSDLTA*CSRN
      AA23=-SNDLTA*SNGM1
      AA32=SNRN*(CSDLTA*CSGM1*SNR1D1-SNGM1*CSR1D1)+CSRN*SNDLTA*SNR1D1
      AA33=CSGM1*CSR1D1+CSDLTA*SNGM1*SNR1D1
      BB22=AF*(CSDTAF*CSF0-SNDTAF*SNF0*CSRN*CSD2)
      BB33=AF*(SNDTAF*CSF0+CSDTAF*SNF0*CSRN*CSD2)
      UUU=-(AA22*BB22+AA23*BB33)
      DDD=AA32*BB22+AA33*BB33
      QFFE=DATAN2(UUU,DDD)
      QF=QFFE
      SNQF=DSIN(QF)
      CSQF=DCOS(QF)
      SNQFFE=DSIN(QFFE)
      CSQFFE=DCOS(QFFE)
C
C calculate normal vector at main contact point in H coordinate system
C
      RNXH2=(CSDLTA*CSGM1*CSGM1+SNGM1*SNGM1)*RNXF2-SNDLTA*CSGM1*RNYF2
     #      +CSGM1*SNGM1*(1.D00-CSDLTA)*RNZF2
      RNYH2=SNDLTA*CSGM1*RNXF2+CSDLTA*RNYF2-SNDLTA*SNGM1*RNZF2
      RNZH2=CSGM1*SNGM1*(1.D00-CSDLTA)*RNXF2+SNDLTA*SNGM1*RNYF2+
     #      (CSDLTA*SNGM1*SNGM1+CSGM1*CSGM1)*RNZF2
C
C CALCULATE PHF
C
      PHF=DASIN(CSD1*RNXH2-SND1*RNZH2)
      IF(II .EQ. 2)THEN
       PHF=180.D00*CNST-PHF
      END IF
```

```
      SNPHF=DSIN(PHF)
      CSPHF=DCOS(PHF)
C
C CALCULATE TF
C
      IF(II .EQ. 2)THEN
       TF=DATAN2(-RNYH2,-SND1*RNXH2-CSD1*RNZH2)
       ELSE
       TF=DATAN2(RNYH2,SND1*RNXH2+CSD1*RNZH2)
      END IF
      SNTF=DSIN(TF)
      CSTF=DCOS(TF)
C
C     CALCULATE THF
C
      THF=TF+QFFE
      SNTHF=DSIN(THF)
      CSTHF=DCOS(THF)
C
C CALCULATE UF
C
C calculute coordinate of main contact point in H coordinate system
C
      RMXH2=(CSDLTA*CSGM1*CSGM1+SNGM1*SNGM1)*RMXF2-SNDLTA*CSGM1*RMYF2
     #      +CSGM1*SNGM1*(1.D00-CSDLTA)*RMZF2
      RMYH2=SNDLTA*CSGM1*RMXF2+CSDLTA*RMYF2-SNDLTA*SNGM1*RMZF2
      RMZH2=CSGM1*SNGM1*(1.D00-CSDLTA)*RMXF2+SNDLTA*SNGM1*RMYF2+
     #      (CSDLTA*SNGM1*SNGM1+CSGM1*CSGM1)*RMZF2
C
      UF=(RCF*CSPHF/SNPHF-RMXH2*CSD1+RMZH2*SND1-RL*SND1)/CSPHF
C
C CALCULATE DE1,DL1
C
      DE1=RMYH2-UF*SNPHF*SNTF+BF*SNQFFE
      DL1=DE1*CSTF/SNTF
C
C CONVERT RADIANS TO DEGREES
C
      PHPDG=PHP/CNST
      TPDG=TP/CNST
      QPDG=QP/CNST
      RNDG=RN/CNST
      DLTADG=DLTA/CNST
      DTAPDG=DETAP/CNST
      DTAFDG=DETAF/CNST
      QDG=Q/CNST
      PODG=PO/CNST
      FODG=FO/CNST
      QFDG=QF/CNST
      PHFDG=PHF/CNST
      TFDG=TF/CNST
      FEEDG=FEE/CNST
      WRITE(6,60000)
      WRITE(6,60001)
      WRITE(6,60002)
```

```
      IF(II.EQ.1) THEN
       WRITE(6,60003)
       ELSE
       WRITE(6,60004)
      END IF
      WRITE(6,60002)
      WRITE(6,60001)
      WRITE(6,60000)
      WRITE(6,90001)
      WRITE(6,90002)PHPDG,PHFDG,RCP,RCF,TPDG,TFDG
      WRITE(6,90003)RBP,BF,QPDG,QFDG,RMP2,RMF1,DE1,DL1,FEEDG,DLTADG
      WRITE(6,1)RNDG
      WRITE(6,20001)
      WRITE(6,20002)DTAPDG,P0DG,RBP,RAP
      WRITE(6,20003)
10000 WRITE(6,20004)DTAFDG,F0DG,BF,AF
90003 FORMAT(1H ,'BP    =',G18.12,15X,'BF    =',G18.12,/
     #       1H ,'QPDG  =',G18.12,15X,'QFDG  =',G18.12,/
     #       1H ,'MP2   =',G18.12,15X,'MF1   =',G18.12,/
     #       1H ,'DE1   =',G18.12,15X,'DL1   =',G18.12,/
     #       1H ,'FEE0DG=',G18.12,15X,'DELTA =',G18.12/)
    1 FORMAT(1H ,'ROTATION ANGLE OF RN =',G18.12/)
20001 FORMAT(1H ,'   GEAR CRADLE ELLIPSE PARAMETER   '/)
20002 FORMAT(1H ,'GEAR ELLIPSE ORIENTATION=',G24.17,/
     #       1H ,'INITIAL          POSITION=',G24.17,/
     #       1H ,'MINOR AXIS=',G24.17,5X,'MAJOR AXIS=',G24.17/)
20003 FORMAT(1H ,'   PINION CRADLE ELLIPSE PARAMETER   '/)
20004 FORMAT(1H ,'PINION ELLIPSE ORIENTATION=',G24.17,/
     #       1H ,'INITIAL          POSITION=',G24.17,/
     #       1H ,'MINOR AXIS=',G24.17,5X,'MAJOR AXIS=',G24.17/)
60000 FORMAT(1H1,' ')
60001 FORMAT(1H ,'*************************************************')
60002 FORMAT(1H ,'*                                               *')
60003 FORMAT(1H ,'*        CONCAVE PINION PART ANALYSIS           *')
60004 FORMAT(1H ,'*        CONVEX  PINION PART ANALYSIS           *')
90001 FORMAT(1H ,'GEAR PARAMETER',27X,'PINION PARAMETER')
90002 FORMAT(1H ,'PHPDG =',G18.12,15X,'PHFDG =',G18.12,/
     #       1H ,'RCP   =',G18.12,15X,'RCF   =',G18.12,/
     #       1H ,'TPDG  =',G18.12,15X,'TFDG  =',G18.12)
      END
```

```
C...  ************************************************************
C...  *                                                          *
C...  *       TOOTH CONTACT ANALYSIS OF SPIRAL BEVEL GEAR        *
C...  *                                                          *
C...  *               AUTHORS: FAYDOR     LITVIN                 *
C...  *                        WEI-JIUNG   TSUNG                 *
C...  *                        HONG-TAO      LEE                 *
C...  *                                                          *
C...  *                                                          *
C...  ************************************************************
C
C PURPOSE
C
C     Tooth contact analysis of spiral bevel gears
C
C NOTE
C
C     This program is written in FORTRAN 77.  It can be compiled by
C     V compiler in IBM mainframe.
C
C     This program calls ZSPOW, a subroutine of IMSL package.
C
C DESCRIPTION OF INPUT PARAMETERS
C
C...  JJ          : JJ=1 for left-hand gear, JJ=2 for right-hand gear
C...  II          : II=1 for pinion concave side, II=2 for pinion convex
C                   side
C...  TN1         : teeth number of pinion
C...  TN2         : teeth number of gear
C...  D1DG, D1MIN : dedendum angle of pinion (degree and arc minute,
C...                respectively)
C...  D2DG, D2MIN : dedendum angle of gear (degree and arc minute,
C...                respectively)
C...  GAMADG      : shaft angle (degree)
C...  RL          : mean cone distance
C...  PHPDG       : blade angle of gear cutter (degree)
C...  PHFDG       : blade angle of pinion cutter (degree)
C...  RCP         : radius of gear cutter (measured on cradle plane)
C...  RCF         : radius of pinion cutter (measured on cradle plane)
C...  TPDG        : the difference between the sum of gear cone surface
C                   angle coordinate and generating surface rotation
C                   angle, and machine setting angle (degree) [see
C                   equation (4.18) in report]
C...  TFDG        : the difference between the sum of pinion cone
C                   surface angle coordinate and generating surface
C                   rotation angle, and machine setting angle (degree)
C...                [see equation (4.3) in report]
C...  BP          : radial of gear cutter
C...  BF          : radial of pinion cutter
C...  QPDG        : machine setting angle of gear
C...  QFDG        : machine setting angle of pinion [ALWAYS consider it
C                   as a POSITIVE input even it is negative gotten from
C                   the output of maching setting program
C...  MP2         : ratio of cradle angular velocity for cutting the
C                   gear and gear angular velocity
```

```
C...  MF1          : ratio of cradle angular velocity for cutting the
C                    pinion and pinion angular velocity
C...  DE1          : machine offset for cutting the pinion
C...  DL1          : vector-sum of (1) the change of machine center to
C                    back and (2) the sliding base
C...  FEE0DG       : generating surface rotation angle at initial main
C                    contact point
C...  DELTADG      : rotation angle of frame h relative to frame f about
C                    Z1
C...  DFEPDG       : increment of FEPDG
C
      IMPLICIT REAL*8(A-H,O-Z)
      INTEGER NSIG,IER,ITMAX,M,MLOOP,N1,N2,N5,NSIG1
      REAL*8 PAR5(5),X(5),FNORM5,WK5(75),MP2,MF1
      EXTERNAL FCN1,FCN2
      COMMON/A1/CNST
      COMMON/A2/DE1,DL1,RCP,RL,RCF,PHFDG
      COMMON/A3/SNPHF,CSPHF,SNR1D1,CSR1D1,SNBP,CSBP,SNR1D2,CSR1D2
      COMMON/A4/W,ECENDG,DISTEC
      COMMON/A5/SNGM1,CSGM1,GMA1,SNGM2,CSGM2,SND2,CSD2,SND1,CSD1
      COMMON/A6/SNTP,CSTP,TP,TPDG,SNTF,CSTF,TF,TFDG
      COMMON/A7/SNDLTA,CSDLTA,SNPHP,CSPHP,SNR2D2,CSR2D2,DLTADG
      COMMON/A12/UF,BF,RBP,UP,RMF1,RMP2
      COMMON/A14/SNRN,CSRN,RNDG,RN
      COMMON/A18/SNQP,CSQP,QPDG,SNQF,CSQF,QFDG,QP,QF,QP0,QF0
      COMMON/A27/XF1,YF1,ZF1,XF2,YF2,ZF2
      COMMON/A32/AYN,AZN,BYN,BZN,CYN,CZN,DYN,DZN,RMYN,RMZN
      COMMON/A33/PHP1,PHF1,PHP2,PHF2,PHP1DG,PHF1DG,PHP2DG,PHF2DG
      COMMON/A34/FE1,SNFE1,CSFE1,FE2,SNFE2,CSFE2,FEP,FE221,FE111,
     #           FEPDG,FEFDG,F111DG,F221DG
      COMMON/A35/SNTHP,CSTHP,SNTHF,CSTHF,THPDG,THFDG
      COMMON/A36/RK12,RK22,RK11,RK21,UTX11,UTX12,UTY11,UTY12,UTZ11,
     #           UTZ12,UTX21,UTX22,UTY21,UTY22,UTZ21,UTZ22
      COMMON/A37/RNXF2,RNYF2,RNZF2,RNXF1,RNYF1,RNZF1
      COMMON/A38/DEF,SIGMDG,ALPHDG,AXISA,AXISB,ERROR
      COMMON/A40/GMENRA,PMENR1,PMENR2
      COMMON/A49/SNQAP,CSQAP,SNQAF,CSQAF
      COMMON/A55/DETAP,DETAF,SNDTAP,CSDTAP,SNDTAF,CSDTAF,DTAPDG,DTAFDG
      COMMON/A77/Q,QDG,P0DG,F0DG,PMIN,PMAX,FMIN,FMAX
C
C INPUT DATA
C
      JJ=1
      II=1
      TN1=10.D00
      TN2=41.D00
      D1DG=1.D00
      D1MIN=41.D00
      D2DG=3.D00
      D2MIN=53.D00
      GAMADG=90.D00
      RL=3.226D00
      PHPDG=20.0D00
      PHFDG=16.7979304880D00
      RCP=3.83760775903D00
```

```
      RCF=3.86707929616D00
      TPDG=53.0019620800D00
      TFDG=51.5519731416D00
      BP=3.37751754380D00
      BF=3.31529203349D00
      QPDG=73.6837239464D00
      QFDG=77.1317508049D00
      MP2=.973756061793D00
      MF1=.237501478486D00
      DE1=0.508253291408D-02
      DL1=0.403530720434D-02
      FEP0DG=-1.9980379199559D00
      DLTADG=-.269060223623D00
      DFEPDG=1.00D00
C
C END OF INPUT DATA
C
      DEF=0.00025D00
      N5=5
      NSIG1=12
      ITMAX=200
      RBP=BP
      RMP2=MP2
      RMF1=MF1
C...
C...  CONVERT DEGREE TO RADIANS
C...
      CNST=4.D00*DATAN(1.D00)/180.D00
      GAMA=GAMADG*CNST
      QP=QPDG*CNST
      PHP=PHPDG*CNST
      PHF=PHFDG*CNST
      TP=TPDG*CNST
      TF=TFDG*CNST
      DLTA=DLTADG*CNST
      QF=QFDG*CNST
      FEP0=FEP0DG*CNST
      FEF0=0.D00
      D1=(D1DG+D1MIN/60.D00)*CNST
      D2=(D2DG+D2MIN/60.D00)*CNST
      RM12=TN2/TN1
      RM21=TN1/TN2
      GMA1=DATAN(DSIN(GAMA)/(RM12+DCOS(GAMA)))
      GMA2=DATAN(DSIN(GAMA)/(RM21+DCOS(GAMA)))
      M=(360.D00/(2.0D00*TN2))/DFEPDG
      CALL HEAD1(JJ,II)
C...
C...  SUBSTITUTE SIN AND COS FUNCTION BY A SHORT NAME
C...
      SND1=DSIN(D1)
      CSD1=DCOS(D1)
      SNR1D1=DSIN(GMA1-D1)
      CSR1D1=DCOS(GMA1-D1)
      SNR1D2=DSIN(GMA1+D2)
      CSR1D2=DCOS(GMA1+D2)
```

```
      SNR2D2=DSIN(GMA2-D2)
      CSR2D2=DCOS(GMA2-D2)
      CSD2=DCOS(D2)
      SND2=DSIN(D2)
      CSGM1=DCOS(GMA1)
      SNGM1=DSIN(GMA1)
      CSGM2=DCOS(GMA2)
      SNGM2=DSIN(GMA2)
      SNPHP=DSIN(PHP)
      CSPHP=DCOS(PHP)
      SNQP=DSIN(QP)
      CSQP=DCOS(QP)
      SNTP=DSIN(TP)
      CSTP=DCOS(TP)
      SNDLTA=DSIN(DLTA)
      CSDLTA=DCOS(DLTA)
      SNQF=DSIN(QF)
      CSQF=DCOS(QF)
      SNPHF=DSIN(PHF)
      CSPHF=DCOS(PHF)
      SNTF=DSIN(TF)
      CSTF=DCOS(TF)
C...
C...                TOOTH CONTACT ANALYSIS
C...  DETERMINATION OF THE KINEMATICAL ERROR, BEARING CONTACT
C...
      TP0=TP
      TF0=TF
      QP0=QP
      QF0=QF
      RINITP=M*DFEPDG
      FEP=-RINITP*CNST+FEP0
C...  INITIAL GUASS FOR ZSPOW
      X(1)=TF0
      X(2)=TP0
      X(3)=-RINITP*CNST+FEF0
      X(4)=0.0D00*CNST
      X(5)=0.0D00*CNST
      MLOOP=M*2+1
      MLOOP0=M+1
      DO 99 J=1,MLOOP0
      IF(JJ .EQ. 1)THEN
      CALL ZSPOW(FCN1,NSIG1,N5,ITMAX,PAR5,X,FNORM5,WK5,IER)
      ELSE
      CALL ZSPOW(FCN2,NSIG1,N5,ITMAX,PAR5,X,FNORM5,WK5,IER)
      END IF
      CALL ANGLE(X(1))
      CALL ANGLE(X(2))
      CALL ANGLE(X(3))
      CALL ANGLE(X(4))
      CALL ANGLE(X(5))
      FEF=X(3)
      FE2=(FEP-FEP0)/RMP2
      FE1=(FEF-FEF0)/RMF1
      FE111=X(4)
```

```
      FE221=X(5)
      FE2PR=FE2-FE221
      FE1PR=FE1-FE111
      FEPDG=FEP/CNST
      FE1PRD=FE1PR/CNST
      FE2PRD=FE2PR/CNST
      FEP=FEP+DFEPDG*CNST
99    CONTINUE
      FE1PR0=FE1PR
      FE2PR0=FE2PR
      RINITP=M*DFEPDG
      FEP=-RINITP*CNST+FEP0
      QP0=QP0
      QF0=QF0
C...  INITIAL GUASS FOR ZSPOW
      X(1)=TF0
      X(2)=TP0
      X(3)=-RINITP*CNST+FEF0
      X(4)=0.0D00*CNST
      X(5)=0.0D00*CNST
      MLOOP=M*2+1
      DO 88 J=1,MLOOP
      IF(JJ .EQ. 1)THEN
      CALL ZSPOW(FCN1,NSIG1,N5,ITMAX,PAR5,X,FNORM5,WK5,IER)
      ELSE
      CALL ZSPOW(FCN2,NSIG1,N5,ITMAX,PAR5,X,FNORM5,WK5,IER)
      END IF
      CALL ANGLE(X(1))
      CALL ANGLE(X(2))
      CALL ANGLE(X(3))
      CALL ANGLE(X(4))
      CALL ANGLE(X(5))
      FEF=X(3)
      FE2=(FEP-FEP0)/RMP2
      FE1=(FEF-FEF0)/RMF1
      SNFE1=DSIN(FE1)
      CSFE1=DCOS(FE1)
      SNFE2=DSIN(FE2)
      CSFE2=DCOS(FE2)
      SNTF=DSIN(X(1))
      CSTF=DCOS(X(1))
      SNTP=DSIN(X(2))
      CSTP=DCOS(X(2))
      FE111=X(4)
      FE221=X(5)
      FE2PR=FE2-FE221
      FE1PR=FE1-FE111
      ERROR=(FE2PR*3600.D00-FE2PR0*3600.D00-(FE1PR*3600.D00-FE1PR0*
     #      3600.D00)*TN1/TN2)/CNST
      TFDG=X(1)/CNST
      TPDG=X(2)/CNST
      FEFDG=X(3)/CNST
      FEPDG=FEP/CNST
      F111DG=FE111/CNST
      F221DG=FE221/CNST
```

```
      FE1PRD=FE1PR/CNST
      FE2PRD=FE2PR/CNST
C...
C...  DETERMINATION OF THE BEARING CONTACT
C...
      CALL FNORM(DN1XTH,DN1XFE,DN1YTH,DN1YFE,DN1ZTH,DN1ZFE)
      CALL PNORM(DN2XTH,DN2XFE,DN2YTH,DN2YFE,DN2ZTH,DN2ZFE)
      CALL DUP(UPP,DUPTHP,DUPFEP)
      CALL DUF(UFF,DUFTHF,DUFFEF)
      CALL DR2(UPP,DUPTHP,DUPFEP,DX2THP,DX2FEP,DY2THP,DY2FEP,
     #         DZ2THP,DZ2FEP)
      CALL DR1(UFF,DUFTHF,DUFFEF,DX1THF,DX1FEF,DY1THF,DY1FEF,
     #         DZ1THF,DZ1FEF)
      CALL PC(DN2XTH,DN2XFE,DX2THP,DX2FEP,DN2YTH,DN2YFE,DY2THP,
     #        DY2FEP,X12,X22,RK12,RK22)
      CALL PC(DN1XTH,DN1XFE,DX1THF,DX1FEF,DN1YTH,DN1YFE,DY1THF,
     #        DY1FEF,X11,X21,RK11,RK21)
      CALL PD(DX2THP,DX2FEP,DY2THP,DY2FEP,DZ2THP,DZ2FEP,X12,
     #        PDX12,PDY12,PDZ12)
      CALL PD(DX2THP,DX2FEP,DY2THP,DY2FEP,DZ2THP,DZ2FEP,X22,
     #        PDX22,PDY22,PDZ22)
      CALL PD(DX1THF,DX1FEF,DY1THF,DY1FEF,DZ1THF,DZ1FEF,X11,
     #        PDX11,PDY11,PDZ11)
      CALL PD(DX1THF,DX1FEF,DY1THF,DY1FEF,DZ1THF,DZ1FEF,X21,
     #        PDX21,PDY21,PDZ21)
      CALL UNIT(PDX11,PDY11,PDZ11,UNIT11,UX11,UY11,UZ11)
      CALL UNIT(PDX21,PDY21,PDZ21,UNIT21,UX21,UY21,UZ21)
      CALL UNIT(PDX12,PDY12,PDZ12,UNIT12,UX12,UY12,UZ12)
      CALL UNIT(PDX22,PDY22,PDZ22,UNIT22,UX22,UY22,UZ22)
      CALL UTRAN1(UX11,UY11,UZ11,UTX11,UTY11,UTZ11)
      CALL UTRAN1(UX21,UY21,UZ21,UTX21,UTY21,UTZ21)
      CALL UTRAN2(UX12,UY12,UZ12,UTX12,UTY12,UTZ12)
      CALL UTRAN2(UX22,UY22,UZ22,UTX22,UTY22,UTZ22)
      CALL AXIS(SIGMDG,AXISA,AXISB,ALPH,ALPHDG)
      CALL WRITE2
      FEP=FEP+DFEPDG*CNST
   88 CONTINUE
      STOP
      END
C...
C...  *****   SUBROUTINE ANGLE    *****
C...
      SUBROUTINE ANGLE(X)
      IMPLICIT REAL*8(A-H,O-Z)
      COMMON/A1/CNST
      CNST2=2.D00*CNST*180.D00
      M=X/CNST2
      RM=M
      X=X-RM*CNST2
      RETURN
      END
C...
C...  *****   SUBROUTINE FCN1   *****
C...
      SUBROUTINE FCN1(X,F,N5,PAR5)
```

```
      IMPLICIT REAL*8(A-H,O-Z)
      INTEGER N5
      REAL*8 X(N5),F(N5),PAR5(N5)
      COMMON/A1/CNST
      COMMON/A2/DE1,DL1,RCP,RL,RCF,PHFDG
      COMMON/A3/SNPHF,CSPHF,SNR1D1,CSR1D1,SNBP,CSBP,SNR1D2,CSR1D2
      COMMON/A5/SNGM1,CSGM1,GMA1,SNGM2,CSGM2,SND2,CSD2,SND1,CSD1
      COMMON/A6/SNTP,CSTP,TP,TPDG,SNTF,CSTF,TF,TFDG
      COMMON/A7/SNDLTA,CSDLTA,SNPHP,CSPHP,SNR2D2,CSR2D2,DLTADG
      COMMON/A12/UF,BF,RBP,UP,RMF1,RMP2
      COMMON/A18/SNQP,CSQP,QPDG,SNQF,CSQF,QFDG,QP,QF,QP0,QF0
      COMMON/A27/XF1,YF1,ZF1,XF2,YF2,ZF2
      COMMON/A34/FE1,SNFE1,CSFE1,FE2,SNFE2,CSFE2,FEP,FE221,FE111,
     #           FEPDG,FEFDG,F111DG,F221DG
      COMMON/A35/SNTHP,CSTHP,SNTHF,CSTHF,THPDG,THFDG
      COMMON/A37/RNXF2,RNYF2,RNZF2,RNXF1,RNYF1,RNZF1
      QF=QF0-X(3)
      SNQF=DSIN(QF)
      CSQF=DCOS(QF)
      QP=QP0-FEP
      SNQP=DSIN(QP)
      CSQP=DCOS(QP)
      FE111=X(4)
      FE221=X(5)
      SN221=DSIN(FE221)
      CS221=DCOS(FE221)
      SN111=DSIN(FE111)
      CS111=DCOS(FE111)
      SNTF=DSIN(X(1))
      CSTF=DCOS(X(1))
      SNTP=DSIN(X(2))
      CSTP=DCOS(X(2))
      THF=X(1)+QF
      THP=X(2)+QP
      THFDG=THF/CNST
      THPDG=THP/CNST
      SNTHF=DSIN(THF)
      CSTHF=DCOS(THF)
      SNTHP=DSIN(THP)
      CSTHP=DCOS(THP)
      UF1=((RCF*CSPHF/SNPHF-RL*SND1-DL1*SNR1D1/CSR1D1)*CSPHF*SNTF+
     #     BF*(SNPHF*SNQF+CSPHF*SNTHF*(RMF1-SNR1D1)/CSR1D1)-DE1*(
     #     SNPHF-CSPHF*CSTF*SNR1D1/CSR1D1))/SNTF
      XH1=(CSGM1*CSR1D1*CS111+SNGM1*SNR1D1)*(RCF*CSPHF/SNPHF-UF1*
     #     CSPHF-RL*SND1)+BF*(CSGM1*(SNQF*SN111-CSQF*CS111*
     #     SNR1D1)+SNGM1*CSQF*CSR1D1)+DL1*(SNGM1*CSR1D1-CSGM1*
     #     SNR1D1*CS111)-SN111*DE1*CSGM1-UF1*SNPHF*(CSGM1*(SNTF*
     #     SN111+CSTF*CS111*SNR1D1)-SNGM1*CSTF*CSR1D1)
      YH1=CSR1D1*SN111*(RCF*CSPHF/SNPHF-UF1*CSPHF-RL*SND1)-BF*(
     #     SNQF*CS111+CSQF*SN111*SNR1D1)-DL1*SNR1D1*SN111+DE1*
     #     CS111+UF1*SNPHF*(SNTF*CS111-CSTF*SN111*SNR1D1)
      ZH1A=(CSGM1*SNR1D1-SNGM1*CSR1D1*CS111)*(RCF*CSPHF/SNPHF-UF1*
     #     CSPHF)+RL*SND1*(SNGM1*CSR1D1*CS111-CSGM1*SNR1D1)-BF*(SNGM1
     #     *(SNQF*SN111-CSQF*CS111*SNR1D1)-CSGM1*CSQF*CSR1D1)+
     #     DL1*(SNGM1*SNR1D1*CS111+CSGM1*CSR1D1)+DE1*SN111*SNGM1
```

```
      ZH1=ZH1A+UF1*SNPHF*(SNGM1*(SNTF*SN111+CSTF*CS111*SNR1D1)+CSGM1*
     #     CSTF*CSR1D1)
      XF1=(CSDLTA*CSGM1**2+SNGM1**2)*XH1+SNDLTA*CSGM1*YH1+(1.0D00-
     #     CSDLTA)*CSGM1*SNGM1*ZH1
      YF1=-SNDLTA*CSGM1*XH1+CSDLTA*YH1+SNDLTA*SNGM1*ZH1
      ZF1=(1.0D00-CSDLTA)*CSGM1*SNGM1*XH1-SNDLTA*SNGM1*YH1+
     #     (CSDLTA*SNGM1**2+CSGM1**2)*ZH1
      XF2A=RBP*(CSPHP*SNTHP*SND2/CSD2-SNPHP*SNQP)*(CSPHP*CSR2D2
     #     *CSGM2*CS221/SNTP+CSPHP*SNR2D2*SNGM2/SNTP-SNR2D2*SNPHP*
     #     CSGM2*CS221*CSTP/SNTP+SNPHP*CSR2D2*SNGM2*CSTP/SNTP-SNPHP*
     #     CSGM2*SN221)+CSPHP*CSGM2*(RCP*CSPHP+RL*SNPHP*SND2)*(SNTP*
     #     SN221+CSTP*CS221*SNR2D2)
      XF2=XF2A+RBP*CSGM2*(SNQP*SN221+CSQP*CS221*SNR2D2)+RL*SND2*
     #     (CSGM2*CSR2D2*CS221+SNGM2*SNR2D2)-RBP*CSR2D2*CSQP*SNGM2
     #     +CSGM2*CSPHP*CSR2D2*CS221*(RCP*SNPHP-RL*CSPHP*SND2)-RCP*
     #     CSPHP*SNGM2*(CSPHP*CSR2D2*CSTP-SNPHP*SNR2D2)-RL*CSPHP*SND2
     #     *SNGM2*(SNPHP*CSR2D2*CSTP+CSPHP*SNR2D2)
      YF2=CSPHP*CSR2D2*SN221*(RL*CSPHP*SND2-RCP*SNPHP)+RBP*(SNPHP*
     #     SNQP-CSPHP*SNTHP*SND2/CSD2)*(SNPHP*CS221-SNPHP*SNR2D2*
     #     SN221*CSTP/SNTP+CSPHP*CSR2D2*SN221/SNTP)-RBP*(SNQP*CS221
     #     +CSQP*SN221*SNR2D2)-RL*SND2*SN221*CSR2D2+CSPHP*(RCP*
     #     CSPHP+RL*SNPHP*SND2)*(SNTP*CS221-CSTP*SNR2D2*SN221)
      ZF2A=RBP*(SNPHP*SNQP-CSPHP*SNTHP*SND2/CSD2)*(CSPHP*SNR2D2*
     #     CSGM2/SNTP-CSPHP*CSR2D2*SNGM2*CS221/SNTP+SNR2D2*SNPHP*
     #     SNGM2*CS221*CSTP/SNTP+SNPHP*CSR2D2*CSGM2*CSTP/SNTP+SNPHP*
     #     SNGM2*SN221)-RBP*SNGM2*(SNQP*SN221-CSQP*CS221*SNR2D2)
     #     +RBP*CSR2D2*CSQP*CSGM2
      ZF2=ZF2A+SNGM2*CSPHP*(SNTP*SN221+CSTP*SNR2D2*CS221)*(RCP*CSPHP
     #     +RL*SNPHP*SND2)+SNGM2*CSR2D2*CS221*(RCP*CSPHP*SNPHP-RL*
     #     SND2*CSPHP**2)+RCP*CSGM2*CSPHP*(CSPHP*CSR2D2*CSTP-SNPHP*
     #     SNR2D2)+RL*CSPHP*SND2*CSGM2*(CSPHP*SNR2D2+SNPHP*CSR2D2*
     #     CSTP)+RL*SND2*(SNGM2*CSR2D2*CS221-SNR2D2*CSGM2)
      RNXF2=CSPHP*CSGM2*SNTP*SN221+SNPHP*(SNGM2*SNR2D2+CSGM2*CSR2D2*
     #      CS221)-CSPHP*CSTP*(SNGM2*CSR2D2-CSGM2*SNR2D2*CS221)
      RNYF2=CSPHP*CS221*SNTP-SN221*(SNPHP*CSR2D2+CSPHP*SNR2D2*CSTP)
      RNZF2=CSPHP*CSTP*(CSGM2*CSR2D2+SNGM2*SNR2D2*CS221)+SNPHP*(
     #      SNGM2*CSR2D2*CS221-CSGM2*SNR2D2)+CSPHP*SNGM2*SN221*SNTP
      RNXH1=-CSPHF*CSGM1*SNTF*SN111+SNPHF*(SNGM1*SNR1D1+CSGM1*
     #       CSR1D1*CS111)+CSPHF*CSTF*(SNGM1*CSR1D1-CSGM1*SNR1D1*
     #       CS111)
      RNYH1=CSPHF*SNTF*CS111+SN111*(SNPHF*CSR1D1-CSPHF*SNR1D1*CSTF)
      RNZH1=CSPHF*CSTF*(CSGM1*CSR1D1+SNGM1*SNR1D1*CS111)+SNPHF*(
     #       CSGM1*SNR1D1-SNGM1*CSR1D1*CS111)+CSPHF*SNGM1*SNTF*SN111
      RNXF1=(CSDLTA*CSGM1**2+SNGM1**2)*RNXH1+SNDLTA*CSGM1*RNYH1+
     #       (1.D00-CSDLTA)*CSGM1*SNGM1*RNZH1
      RNYF1=-SNDLTA*CSGM1*RNXH1+CSDLTA*RNYH1+SNDLTA*SNGM1*RNZH1
      RNZF1=(1.D00-CSDLTA)*CSGM1*SNGM1*RNXH1-SNDLTA*SNGM1*RNYH1+
     #       (CSDLTA*SNGM1**2+CSGM1**2)*RNZH1
      F(1)=XF1-XF2
      F(2)=YF1-YF2
      F(3)=ZF1-ZF2
      F(4)=RNXF1-RNXF2
      F(5)=RNYF1-RNYF2
      RETURN
      END
```

```
C...
C...   *****    SUBROUTINE FCN2    *****
C...
       SUBROUTINE FCN2(X,F,N5,PAR5)
       IMPLICIT REAL*8(A-H,O-Z)
       INTEGER N5
       REAL*8 X(N5),F(N5),PAR5(N5)
       COMMON/A1/CNST
       COMMON/A2/DE1,DL1,RCP,RL,RCF,PHFDG
       COMMON/A3/SNPHF,CSPHF,SNR1D1,CSR1D1,SNBP,CSBP,SNR1D2,CSR1D2
       COMMON/A5/SNGM1,CSGM1,GMA1,SNGM2,CSGM2,SND2,CSD2,SND1,CSD1
       COMMON/A6/SNTP,CSTP,TP,TPDG,SNTF,CSTF,TF,TFDG
       COMMON/A7/SNDLTA,CSDLTA,SNPHP,CSPHP,SNR2D2,CSR2D2,DLTADG
       COMMON/A12/UF,BF,RBP,UP,RMF1,RMP2
       COMMON/A18/SNQP,CSQP,QPDG,SNQF,CSQF,QFDG,QP,QF,QP0,QF0
       COMMON/A27/XF1,YF1,ZF1,XF2,YF2,ZF2
       COMMON/A34/FE1,SNFE1,CSFE1,FE2,SNFE2,CSFE2,FEP,FE221,FE111,
      #           FEPDG,FEFDG,F111DG,F221DG
       COMMON/A35/SNTHP,CSTHP,SNTHF,CSTHF,THPDG,THFDG
       QF=QF0+X(3)
       SNQF=DSIN(QF)
       CSQF=DCOS(QF)
       QP=QP0+FEP
       SNQP=DSIN(QP)
       CSQP=DCOS(QP)
       FE111=X(4)
       FE221=X(5)
       SN221=DSIN(FE221)
       CS221=DCOS(FE221)
       SN111=DSIN(FE111)
       CS111=DCOS(FE111)
       SNTF=DSIN(X(1))
       CSTF=DCOS(X(1))
       SNTP=DSIN(X(2))
       CSTP=DCOS(X(2))
       THF=X(1)-QF
       THP=X(2)-QP
       THFDG=THF/CNST
       THPDG=THP/CNST
       SNTHF=DSIN(THF)
       CSTHF=DCOS(THF)
       SNTHP=DSIN(THP)
       CSTHP=DCOS(THP)
       UF1=((RCF*CSPHF/SNPHF-RL*SND1-DL1*SNR1D1/CSR1D1)*CSPHF*SNTF+
      #     BF*(-SNPHF*SNQF+CSPHF*SNTHF*(RMF1-SNR1D1)/CSR1D1)-DE1*(
      #     SNPHF-CSPHF*CSTF*SNR1D1/CSR1D1))/SNTF
        XH1=(CSGM1*CSR1D1*CS111+SNGM1*SNR1D1)*(RCF*CSPHF/SNPHF-UF1*
      #     CSPHF-RL*SND1)+BF*(CSGM1*(-SNQF*SN111-CSQF*CS111*
      #     SNR1D1)+SNGM1*CSQF*CSR1D1)+DL1*(SNGM1*CSR1D1-CSGM1*
      #     SNR1D1*CS111)-SN111*DE1*CSGM1-UF1*SNPHF*(CSGM1*(SNTF*
      #     SN111+CSTF*CS111*SNR1D1)-SNGM1*CSTF*CSR1D1)
        YH1=CSR1D1*SN111*(RCF*CSPHF/SNPHF-UF1*CSPHF-RL*SND1)-BF*(
      #     -SNQF*CS111+CSQF*SN111*SNR1D1)-DL1*SNR1D1*SN111+DE1*
      #     CS111+UF1*SNPHF*(SNTF*CS111-CSTF*SN111*SNR1D1)
        ZH1A=(CSGM1*SNR1D1-SNGM1*CSR1D1*CS111)*(RCF*CSPHF/SNPHF-UF1*
```

```
#     CSPHF)+RL*SND1*(SNGM1*CSR1D1*CS111-CSGM1*SNR1D1)-BF*(SNGM1
#     *(-SNQF*SN111-CSQF*CS111*SNR1D1)-CSGM1*CSQF*CSR1D1)+
#     DL1*(SNGM1*SNR1D1*CS111+CSGM1*CSR1D1)+DE1*SN111*SNGM1
 ZH1=ZH1A+UF1*SNPHF*(SNGM1*(SNTF*SN111+CSTF*CS111*SNR1D1)+CSGM1*
#     CSTF*CSR1D1)
 XF1=(CSDLTA*CSGM1**2+SNGM1**2)*XH1+SNDLTA*CSGM1*YH1+(1.0D00-
#     CSDLTA)*CSGM1*SNGM1*ZH1
 YF1=-SNDLTA*CSGM1*XH1+CSDLTA*YH1+SNDLTA*SNGM1*ZH1
 ZF1=(1.0D00-CSDLTA)*CSGM1*SNGM1*XH1-SNDLTA*SNGM1*YH1+
#     (CSDLTA*SNGM1**2+CSGM1**2)*ZH1
 XF2A=RBP*(CSPHP*SNTHP*SND2/CSD2+SNPHP*SNQP)*(CSPHP*CSR2D2
#     *CSGM2*CS221/SNTP+CSPHP*SNR2D2*SNGM2/SNTP-SNR2D2*SNPHP*
#     CSGM2*CS221*CSTP/SNTP+SNPHP*CSR2D2*SNGM2*CSTP/SNTP-SNPHP*
#     CSGM2*SN221)+CSPHP*CSGM2*(RCP*CSPHP+RL*SNPHP*SND2)*(SNTP*
#     SN221+CSTP*CS221*SNR2D2)
 XF2=XF2A+RBP*CSGM2*(-SNQP*SN221+CSQP*CS221*SNR2D2)+RL*SND2*
#     (CSGM2*CSR2D2*CS221+SNGM2*SNR2D2)-RBP*CSR2D2*CSQP*SNGM2
#     +CSGM2*CSPHP*CSR2D2*CS221*(RCP*SNPHP-RL*CSPHP*SND2)-RCP*
#     CSPHP*SNGM2*(CSPHP*CSR2D2*CSTP-SNPHP*SNR2D2)-RL*CSPHP*SND2
#     *SNGM2*(SNPHP*CSR2D2*CSTP+CSPHP*SNR2D2)
 YF2=CSPHP*CSR2D2*SN221*(RL*CSPHP*SND2-RCP*SNPHP)+RBP*(-SNPHP*
#     SNQP-CSPHP*SNTHP*SND2/CSD2)*(SNPHP*CS221-SNPHP*SNR2D2*
#     SN221*CSTP/SNTP+CSPHP*CSR2D2*SN221/SNTP)-RBP*(-SNQP*CS221
#     +CSQP*SN221*SNR2D2)-RL*SND2*SN221*CSR2D2+CSPHP*(RCP*
#     CSPHP+RL*SNPHP*SND2)*(SNTP*CS221-CSTP*SNR2D2*SN221)
 ZF2A=RBP*(-SNPHP*SNQP-CSPHP*SNTHP*SND2/CSD2)*(CSPHP*SNR2D2*
#     CSGM2/SNTP-CSPHP*CSR2D2*SNGM2*CS221/SNTP+SNR2D2*SNPHP*
#     SNGM2*CS221*CSTP/SNTP+SNPHP*CSR2D2*CSGM2*CSTP/SNTP+SNPHP*
#     SNGM2*SN221)-RBP*SNGM2*(-SNQP*SN221-CSQP*CS221*SNR2D2)
#     +RBP*CSR2D2*CSQP*CSGM2
 ZF2=ZF2A+SNGM2*CSPHP*(SNTP*SN221+CSTP*SNR2D2*CS221)*(RCP*CSPHP
#     +RL*SNPHP*SND2)+SNGM2*CSR2D2*CS221*(RCP*CSPHP*SNPHP-RL*
#     SND2*CSPHP**2)+RCP*CSGM2*CSPHP*(CSPHP*CSR2D2*CSTP-SNPHP*
#     SNR2D2)+RL*CSPHP*SND2*CSGM2*(CSPHP*SNR2D2+SNPHP*CSR2D2*
#     CSTP)+RL*SND2*(SNGM2*CSR2D2*CS221-SNR2D2*CSGM2)
 RNXF2=CSPHP*CSGM2*SNTP*SN221+SNPHP*(SNGM2*SNR2D2+CSGM2*CSR2D2*
#      CS221)-CSPHP*CSTP*(SNGM2*CSR2D2-CSGM2*SNR2D2*CS221)
 RNYF2=CSPHP*CS221*SNTP-SN221*(SNPHP*CSR2D2+CSPHP*SNR2D2*CSTP)
 RNZF2=CSPHP*CSTP*(CSGM2*CSR2D2+SNGM2*SNR2D2*CS221)+SNPHP*(
#      SNGM2*CSR2D2*CS221-CSGM2*SNR2D2)+CSPHP*SNGM2*SN221*SNTP
 RNXH1=-CSPHF*CSGM1*SNTF*SN111+SNPHF*(SNGM1*SNR1D1+CSGM1*
#       CSR1D1*CS111)+CSPHF*CSTF*(SNGM1*CSR1D1-CSGM1*SNR1D1*
#       CS111)
 RNYH1=CSPHF*SNTF*CS111+SN111*(SNPHF*CSR1D1-CSPHF*SNR1D1*CSTF)
 RNZH1=CSPHF*CSTF*(CSGM1*CSR1D1+SNGM1*SNR1D1*CS111)+SNPHF*(
#       CSGM1*SNR1D1-SNGM1*CSR1D1*CS111)+CSPHF*SNGM1*SNTF*SN111
 RNXF1=(CSDLTA*CSGM1**2+SNGM1**2)*RNXH1+SNDLTA*CSGM1*RNYH1+
#       (1.D00-CSDLTA)*CSGM1*SNGM1*RNZH1
 RNYF1=-SNDLTA*CSGM1*RNXH1+CSDLTA*RNYH1+SNDLTA*SNGM1*RNZH1
 RNZF1=(1.D00-CSDLTA)*CSGM1*SNGM1*RNXH1-SNDLTA*SNGM1*RNYH1+
#       (CSDLTA*SNGM1**2+CSGM1**2)*RNZH1
 F(1)=XF1-XF2
 F(2)=YF1-YF2
 F(3)=ZF1-ZF2
 F(4)=RNXF1-RNXF2
```

```
      F(5)=RNYF1-RNYF2
      RETURN
      END
C...
C...  *****   SUBROUTINE FNORM   *****
C...
      SUBROUTINE FNORM(DN1XTH,DN1XFE,DN1YTH,DN1YFE,DN1ZTH,DN1ZFE)
      IMPLICIT REAL*8(A-H,O-Z)
      COMMON/A3/SNPHF,CSPHF,SNR1D1,CSR1D1,SNBP,CSBP,SNR1D2,CSR1D2
      COMMON/A6/SNTP,CSTP,TP,TPDG,SNTF,CSTF,TF,TFDG
      COMMON/A12/UF,BF,RBP,UP,RMF1,RMP2
      COMMON/A34/FE1,SNFE1,CSFE1,FE2,SNFE2,CSFE2,FEP,FE221,FE111,
     #           FEPDG,FEFDG,F111DG,F221DG
      DN1XTH=-CSPHF*SNFE1*CSTF+CSPHF*CSFE1*SNR1D1*SNTF
      DN1XFE=-SNPHF*SNFE1*CSR1D1/RMF1-CSPHF*(CSFE1*SNTF/RMF1+SNFE1*
     #       CSTF)-CSPHF*SNR1D1*(-SNFE1*CSTF/RMF1-CSFE1*SNTF)
      DN1YTH=CSPHF*CSFE1*CSTF+CSPHF*SNFE1*SNR1D1*SNTF
      DN1YFE=SNPHF*CSFE1*CSR1D1/RMF1+CSPHF*(-SNFE1*SNTF/RMF1+CSFE1*
     #       CSTF)-CSPHF*SNR1D1*(CSFE1*CSTF/RMF1-SNFE1*SNTF)
      DN1ZTH=-CSPHF*CSR1D1*SNTF
      DN1ZFE=-CSPHF*CSR1D1*SNTF
      RETURN
      END
C...
C...  *****   SUBROUTINE PNORM   *****
C...
      SUBROUTINE PNORM(DN2XTH,DN2XFE,DN2YTH,DN2YFE,DN2ZTH,DN2ZFE)
      IMPLICIT REAL*8(A-H,O-Z)
      COMMON/A6/SNTP,CSTP,TP,TPDG,SNTF,CSTF,TF,TFDG
      COMMON/A7/SNDLTA,CSDLTA,SNPHP,CSPHP,SNR2D2,CSR2D2,DLTADG
      COMMON/A12/UF,BF,RBP,UP,RMF1,RMP2
      COMMON/A34/FE1,SNFE1,CSFE1,FE2,SNFE2,CSFE2,FEP,FE221,FE111,
     #           FEPDG,FEFDG,F111DG,F221DG
      DN2XTH=CSPHP*(SNFE2*CSTP-CSFE2*SNR2D2*SNTP)
      DN2XFE=-SNFE2*CSR2D2*SNPHP/RMP2+CSPHP*(CSFE2*SNTP/RMP2+SNFE2*
     #       CSTP)+CSPHP*SNR2D2*(-SNFE2*CSTP/RMP2-CSFE2*SNTP)
      DN2YTH=CSFE2*CSPHP*CSTP+SNFE2*SNR2D2*CSPHP*SNTP
      DN2YFE=-CSFE2*CSR2D2*SNPHP/RMP2+CSPHP*(-SNFE2*SNTP/RMP2+
     #       CSFE2*CSTP)-CSPHP*SNR2D2*(CSFE2*CSTP/RMP2-SNFE2*SNTP)
      DN2ZTH=-CSPHP*CSR2D2*SNTP
      DN2ZFE=-CSPHP*CSR2D2*SNTP
      RETURN
      END
C...
C...  *****   SUBROUTINE DUP   *****
C...
      SUBROUTINE DUP(UPP,DUPTHP,DUPFEP)
      IMPLICIT REAL*8(A-H,O-Z)
      COMMON/A2/DE1,DL1,RCP,RL,RCF,PHFDG
      COMMON/A5/SNGM1,CSGM1,GMA1,SNGM2,CSGM2,SND2,CSD2,SND1,CSD1
      COMMON/A6/SNTP,CSTP,TP,TPDG,SNTF,CSTF,TF,TFDG
      COMMON/A7/SNDLTA,CSDLTA,SNPHP,CSPHP,SNR2D2,CSR2D2,DLTADG
      COMMON/A12/UF,BF,RBP,UP,RMF1,RMP2
      COMMON/A18/SNQP,CSQP,QPDG,SNQF,CSQF,QFDG,QP,QF,QPO,QFO
      COMMON/A35/SNTHP,CSTHP,SNTHF,CSTHF,THPDG,THFDG
```

```
      UPP=RBP*(SNPHP*SNQP-CSPHP*SNTHP*SND2/CSD2)/SNTP+CSPHP*(RCP*
     #    CSPHP/SNPHP+RL*SND2)
      DUPTHP=RBP*SNQP*(-SNPHP*CSTP+CSPHP*SND2/CSD2)/SNTP**2
      DUPFEP=-RBP*SNTHP*(SNPHP-CSPHP*CSTP*SND2/CSD2)/SNTP**2
      RETURN
      END
C...
C...  *****   SUBROUTINE DUF   *****
C...
      SUBROUTINE DUF(UFF,DUFTHF,DUFFEF)
      IMPLICIT REAL*8(A-H,O-Z)
      COMMON/A2/DE1,DL1,RCP,RL,RCF,PHFDG
      COMMON/A3/SNPHF,CSPHF,SNR1D1,CSR1D1,SNBP,CSBP,SNR1D2,CSR1D2
      COMMON/A5/SNGM1,CSGM1,GMA1,SNGM2,CSGM2,SND2,CSD2,SND1,CSD1
      COMMON/A6/SNTP,CSTP,TP,TPDG,SNTF,CSTF,TF,TFDG
      COMMON/A12/UF,BF,RBP,UP,RMF1,RMP2
      COMMON/A18/SNQP,CSQP,QPDG,SNQF,CSQF,QFDG,QP,QF,QP0,QF0
      COMMON/A35/SNTHP,CSTHP,SNTHF,CSTHF,THPDG,THFDG
      UFF=(BF*(SNPHF*SNQF+CSPHF*SNTHF*(RMF1/CSR1D1-SNR1D1/CSR1D1))-
     #    DE1*(SNPHF-CSPHF*CSTF*SNR1D1/CSR1D1)+CSPHF*SNTF*(RCF*
     #    CSPHF/SNPHF-RL*SND1-DL1*SNR1D1/CSR1D1))/SNTF
      DUFTHF=(-BF*SNQF*(SNPHF*CSTF+CSPHF*(RMF1/CSR1D1-SNR1D1/CSR1D1
     #       ))-DE1*(CSPHF*SNR1D1/CSR1D1-SNPHF*CSTF))/SNTF**2
      DUFFEF=(SNPHF+CSPHF*CSTF*(RMF1/CSR1D1-SNR1D1/CSR1D1))*(-BF*
     #       SNTHF/SNTF**2)+DE1*(SNPHF*CSTF-CSPHF*SNR1D1/CSR1D1)/
     #       SNTF**2
      RETURN
      END
C...
C...  *****   SUBROUTINE   DR2   *****
C...
      SUBROUTINE DR2(UPP,DUPTHP,DUPFEP,DX2THP,DX2FEP,DY2THP,DY2FEP,
     #               DZ2THP,DZ2FEP)
      IMPLICIT REAL*8(A-H,O-Z)
      COMMON/A2/DE1,DL1,RCP,RL,RCF,PHFDG
      COMMON/A5/SNGM1,CSGM1,GMA1,SNGM2,CSGM2,SND2,CSD2,SND1,CSD1
      COMMON/A6/SNTP,CSTP,TP,TPDG,SNTF,CSTF,TF,TFDG
      COMMON/A7/SNDLTA,CSDLTA,SNPHP,CSPHP,SNR2D2,CSR2D2,DLTADG
      COMMON/A12/UF,BF,RBP,UP,RMF1,RMP2
      COMMON/A18/SNQP,CSQP,QPDG,SNQF,CSQF,QFDG,QP,QF,QP0,QF0
      COMMON/A34/FE1,SNFE1,CSFE1,FE2,SNFE2,CSFE2,FEP,FE221,FE111,
     #           FEPDG,FEFDG,F111DG,F221DG
      DX2THP=-CSPHP*CSFE2*CSR2D2*DUPTHP+SNPHP*SNFE2*(UPP*CSTP+SNTP
     #       *DUPTHP)+CSFE2*SNR2D2*SNPHP*(-UPP*SNTP+CSTP*DUPTHP)
      DX2FEP=-RCP*CSR2D2*SNFE2*(CSPHP/SNPHP)/RMP2-CSPHP*CSR2D2*(
     #       -UPP*SNFE2/RMP2+CSFE2*DUPFEP)-RL*SND2*CSR2D2*SNFE2/RMP2
     #       -RBP*(-SNFE2*CSQP+SNQP*CSFE2/RMP2)+RBP*SNR2D2*(CSFE2*
     #       SNQP-CSQP*SNFE2/RMP2)+SNPHP*(UPP*(SNFE2*CSTP+SNTP*CSFE2
     #       /RMP2)+SNTP*SNFE2*DUPFEP)
      DX2FEP=DX2FEP+SNPHP*SNR2D2*(UPP*(-CSFE2*SNTP-CSTP*SNFE2/RMP2)+
     #       CSFE2*CSTP*DUPFEP)
      DY2THP=SNFE2*CSR2D2*CSPHP*DUPTHP+SNPHP*CSFE2*(SNTP*DUPTHP+UPP
     #       *CSTP)-SNPHP*SNFE2*SNR2D2*(-UPP*SNTP+CSTP*DUPTHP)
      DY2FEP=-RCP*CSR2D2*CSFE2*(CSPHP/SNPHP)/RMP2+CSPHP*CSR2D2*(UPP*
     #       CSFE2/RMP2+SNFE2*DUPFEP)-RL*SND2*CSR2D2*CSFE2/RMP2-RBP*
```

```
     #        (-CSFE2*CSQP-SNFE2*SNQP/RMP2)-RBP*SNR2D2*(SNFE2*SNQP+
     #        CSQP*CSFE2/RMP2)+SNPHP*(UPP*(CSFE2*CSTP-SNFE2*SNTP/RMP2
     #        )+CSFE2*SNTP*DUPFEP)
      DY2FEP=DY2FEP-SNPHP*SNR2D2*(UPP*(-SNFE2*SNTP+CSTP*CSFE2/RMP2)
     #        +SNFE2*CSTP*DUPFEP)
      DZ2THP=SNR2D2*CSPHP*DUPTHP+SNPHP*CSR2D2*(-UPP*SNTP+CSTP*
     #        DUPTHP)
      DZ2FEP=CSPHP*SNR2D2*DUPFEP+RBP*CSR2D2*SNQP+SNPHP*CSR2D2*(-UPP
     #        *SNTP+CSTP*DUPFEP)
      RETURN
      END
C...
C...  *****   SUBROUTINE DR1  *****
C...
      SUBROUTINE DR1(UFF,DUFTHF,DUFFEF,DX1THF,DX1FEF,DY1THF,DY1FEF,
     #               DZ1THF,DZ1FEF)
      IMPLICIT REAL*8(A-H,O-Z)
      COMMON/A2/DE1,DL1,RCP,RL,RCF,PHFDG
      COMMON/A3/SNPHF,CSPHF,SNR1D1,CSR1D1,SNBP,CSBP,SNR1D2,CSR1D2
      COMMON/A5/SNGM1,CSGM1,GMA1,SNGM2,CSGM2,SND2,CSD2,SND1,CSD1
      COMMON/A6/SNTP,CSTP,TP,TPDG,SNTF,CSTF,TF,TFDG
      COMMON/A12/UF,BF,RBP,UP,RMF1,RMP2
      COMMON/A18/SNQP,CSQP,QPDG,SNQF,CSQF,QFDG,QP,QF,QP0,QF0
      COMMON/A34/FE1,SNFE1,CSFE1,FE2,SNFE2,CSFE2,FEP,FE221,FE111,
     #           FEPDG,FEFDG,F111DG,F221DG
      DX1THF=-CSPHF*CSFE1*CSR1D1*DUFTHF-SNPHF*SNFE1*(UFF*CSTF+SNTF*
     #        DUFTHF)-SNPHF*CSFE1*SNR1D1*(-UFF*SNTF+CSTF*DUFTHF)
      DX1FEF=-RCF*CSR1D1*SNFE1*(CSPHF/SNPHF)/RMF1-CSPHF*CSR1D1*(
     #        -UFF*SNFE1/RMF1+CSFE1*DUFFEF)+RL*SND1*CSR1D1*SNFE1/RMF1
     #        +BF*(-SNFE1*CSQF+SNQF*CSFE1/RMF1)-BF*SNR1D1*(CSFE1*SNQF
     #        -CSQF*SNFE1/RMF1)+DL1*SNFE1*SNR1D1/RMF1-DE1*CSFE1/RMF1
      DX1FEF=DX1FEF-SNPHF*(UFF*(SNFE1*CSTF+SNTF*CSFE1/RMF1)+
     #        SNFE1*SNTF*DUFFEF)-SNPHF*SNR1D1*(UFF*(-CSFE1*SNTF-CSTF*
     #        SNFE1/RMF1)+CSFE1*CSTF*DUFFEF)
      DY1THF=-CSPHF*SNFE1*CSR1D1*DUFTHF+SNPHF*CSFE1*(UFF*CSTF+SNTF*
     #        DUFTHF)-SNPHF*SNFE1*SNR1D1*(-UFF*SNTF+CSTF*DUFTHF)
      DY1FEF=RCF*CSR1D1*CSFE1*(CSPHF/SNPHF)/RMF1-CSPHF*CSR1D1*(
     #        UFF*CSFE1/RMF1+SNFE1*DUFFEF)-RL*SND1*CSR1D1*CSFE1/RMF1-
     #        BF*(-CSFE1*CSQF-SNFE1*SNQF/RMF1)-BF*SNR1D1*(SNFE1*SNQF
     #        +CSFE1*CSQF/RMF1)-DL1*CSFE1*SNR1D1/RMF1-DE1*SNFE1/RMF1
      DY1FEF=DY1FEF+SNPHF*(UFF*(CSFE1*CSTF-SNFE1*SNTF/RMF1)+CSFE1*
     #        SNTF*DUFFEF)-SNPHF*SNR1D1*(UFF*(-SNFE1*SNTF+CSFE1*CSTF/
     #        RMF1)+SNFE1*CSTF*DUFFEF)
      DZ1THF=-CSPHF*SNR1D1*DUFTHF+SNPHF*CSR1D1*(-UFF*SNTF+CSTF*
     #        DUFTHF)
      DZ1FEF=-CSPHF*SNR1D1*DUFFEF+BF*CSR1D1*SNQF+SNPHF*CSR1D1*(
     #        -UFF*SNTF+CSTF*DUFFEF)
      RETURN
      END
C...
C...  *****   SUBROUTINE PRINCIPAL CURVATURE   *****
C...
      SUBROUTINE PC(D1,D2,D3,D4,D5,D6,D7,D8,X1,X2,RK1,RK2)
      IMPLICIT REAL*8(A-H,O-Z)
      A=D1*D7-D5*D3
```

```
      B=D1*D8+D2*D7-D5*D4-D6*D3
      C=D2*D8-D6*D4
      X1=(-B-DSQRT(B**2-4.0D00*A*C))/(2.0D00*A)
      X2=(-B+DSQRT(B**2-4.0D00*A*C))/(2.0D00*A)
      RK1=-(D1*X1+D2)/(D3*X1+D4)
      RK2=-(D1*X2+D2)/(D3*X2+D4)
      RETURN
      END
C...
C...  *****   SUBROUTINE PRINCIPAL DIRECTION   *****
C...
      SUBROUTINE PD(A1,A2,A3,A4,A5,A6,PC0,PD1,PD2,PD3)
      IMPLICIT REAL*8(A-H,O-Z)
      PD1=A1*PC0+A2
      PD2=A3*PC0+A4
      PD3=A5*PC0+A6
      RETURN
      END
C...
C...  *****   SUBROUTINE UNIT VECTOR OF PRINCIPAL DIRECTION   *****
C...
      SUBROUTINE UNIT(E1,E2,E3,UNIT0,UNIT1,UNIT2,UNIT3)
      IMPLICIT REAL*8(A-H,O-Z)
      UNIT0=DSQRT(E1**2+E2**2+E3**2)
      UNIT1=E1/UNIT0
      UNIT2=E2/UNIT0
      UNIT3=E3/UNIT0
      RETURN
      END
C...
C...  *****   SUBROUTINE UTRAN1   *****
C...
      SUBROUTINE UTRAN1(B1,B2,B3,UT11,UT21,UT31)
      IMPLICIT REAL*8(A-H,O-Z)
      COMMON/A5/SNGM1,CSGM1,GMA1,SNGM2,CSGM2,SND2,CSD2,SND1,CSD1
      UT11=B1*CSGM1+B3*SNGM1
      UT21=B2
      UT31=B1*(-SNGM1)+B3*CSGM1
      RETURN
      END
C...
C...  *****   SUBROUTINE UTRAN2   *****
C...
      SUBROUTINE UTRAN2(C1,C2,C3,UT12,UT22,UT32)
      IMPLICIT REAL*8(A-H,O-Z)
      COMMON/A5/SNGM1,CSGM1,GMA1,SNGM2,CSGM2,SND2,CSD2,SND1,CSD1
      UT12=C1*CSGM2-C3*SNGM2
      UT22=C2
      UT32=C1*SNGM2+C3*CSGM2
      RETURN
      END
C...
C...  *****   SUBROUTINE ELLIPSE AXIS   *****
C...
      SUBROUTINE AXIS(SIGMDG,AXISA,AXISB,ALPH,ALPHDG)
```

```
      IMPLICIT REAL*8(A-H,O-Z)
      REAL*8 SIGM(4)
      COMMON/A1/CNST
      COMMON/A36/RK12,RK22,RK11,RK21,UTX11,UTX12,UTY11,UTY12,UTZ11,
     #           UTZ12,UTX21,UTX22,UTY21,UTY22,UTZ21,UTZ22
      COMMON/A37/RNXF2,RNYF2,RNZF2,RNXF1,RNYF1,RNZF1
      COMMON/A38/DEF,SIGMGG,ALPHGG,AXIAA,AXIBB,ERROR
      AK2=RK12+RK22
      AK1=RK11+RK21
      G1=RK11-RK21
      G2=RK12-RK22
C...  FOR LEFT-HAND GEAR
      CS21=(UTX11*UTX12+UTY11*UTY12+UTZ11*UTZ12)
      IF(II.EQ.2)GO TO 1208
      SN21=UTX11*RNYF2*UTZ12+UTX12*RNZF2*UTY11+RNXF2*UTY12*UTZ11-
     #     (UTX12*RNYF2*UTZ11+RNXF2*UTY11*UTZ12+UTX11*RNZF2*UTY12)
      GO TO 1209
 1208 SN21=-(UTX11*RNYF2*UTZ12+UTX12*RNZF2*UTY11+RNXF2*UTY12*UTZ11)
     #      +(UTX12*RNYF2*UTZ11+RNXF2*UTY11*UTZ12+UTX11*RNZF2*UTY12)
 1209 SIGM21=DATAN2(SN21,CS21)
    5 CALL ANGLE(SIGM21)
      CSSIGM=DCOS(SIGM21)
      SNSIGM=DSIN(SIGM21)
      SIGMDG=SIGM21/CNST
      AA=(AK1-AK2-DSQRT(G1**2-2.0D00*G1*G2*DCOS(2.D00*SIGM21)+G2**2)
     #   )/4.0D00
      BB=(AK1-AK2+DSQRT(G1**2-2.D00*G1*G2*DCOS(2.D00*SIGM21)+G2**2))
     #    /4.0D00
      AXISA=DSQRT(DABS(DEF/AA))
      AXISB=DSQRT(DABS(DEF/BB))
      RATIO=AXISA/AXISB
      FF=G1*DSIN(2.0D00*SIGM21)
      HH=G2-G1*DCOS(2.D00*SIGM21)
      ALPH2=DATAN2(FF,HH)
      ALPH=ALPH2/2.00D00
      CALL ANGLE(ALPH)
      ALPHDG=ALPH/CNST
      RETURN
      END
C...
C...  *****   SUBROUTINE WRITE2   *****
C...
      SUBROUTINE WRITE2
      IMPLICIT REAL*8(A-H,O-Z)
      COMMON/A6/SNTP,CSTP,TP,TPDG,SNTF,CSTF,TF,TFDG
      COMMON/A27/XF1,YF1,ZF1,XF2,YF2,ZF2
      COMMON/A34/FE1,SNFE1,CSFE1,FE2,SNFE2,CSFE2,FEP,FE221,FE111,
     #           FEPDG,FEFDG,F111DG,F221DG
      COMMON/A35/SNTHP,CSTHP,SNTHF,CSTHF,THPDG,THFDG
      COMMON/A36/RK12,RK22,RK11,RK21,UTX11,UTX12,UTY11,UTY12,UTZ11,
     #           UTZ12,UTX21,UTX22,UTY21,UTY22,UTZ21,UTZ22
      COMMON/A38/DEF,SIGMDG,ALPHDG,AXISA,AXISB,ERROR
      WRITE(6,70002)
70002 FORMAT(1H ,'**RESULT OF KINEMATIC ERROR & BEARING CONTACT**'/)
      WRITE(6,70003)FEPDG,FEFDG,THPDG,THFDG,TPDG,TFDG,F221DG,F111DG
```

```
70003 FORMAT(1H ,':::   FEPDG=',G20.12,10X,'FEFDG=',G20.12,'  :::',/
     #       1H ,'      THPDG=',G20.12,10X,'THFDG=',G20.12,/
     #       1H ,'      TPDG =',G20.12,10X,'TFDG =',G20.12,/
     #       1H ,'     F221DG=',G20.12,9X,'F111DG=',G20.12)
      WRITE(6,70004)XF1,YF1,ZF1,XF2,YF2,ZF2
70004 FORMAT(1H ,'XF1=',G20.12,3X,'YF1=',G20.12,3X,'ZF1=',G20.12,/
     #       1H ,'XF2=',G20.12,3X,'YF2=',G20.12,3X,'ZF2=',G20.12/)
      WRITE(6,70005)ERROR
70005 FORMAT(1H ,'KINEMATIC ERROR=',G20.12/)
      WRITE(6,70006)
70006 FORMAT(1H ,'RESULT OF PRINCIPAL CURVATURE')
      WRITE(6,70007)RK12,RK22,RK11,RK21
70007 FORMAT(1H ,'GEAR  :    RK12=',G20.12,3X,'RK22=',G20.12,/
     #       1H ,'PINION:    RK11=',G20.12,3X,'RK21=',G20.12/)
      WRITE(6,70008)UTX11,UTY11,UTZ11,UTX21,UTY21,UTZ21
70008 FORMAT(1H ,'PINION UNIT VECTOR OF PRINCIPAL DIRECTION ',/
     #       1H ,'UTX11=',G20.12,'UTY11=',G20.12,'UTZ11=',G20.12,/
     #       1H ,'UTX21=',G20.12,'UTY21=',G20.12,'UTZ21=',G20.12/)
      WRITE(6,70009)UTX12,UTY12,UTZ12,UTX22,UTY22,UTZ22
70009 FORMAT(1H ,'GEAR   UNIT VECTOR OF PRINCIPAL DIRECTION',/
     #       1H ,'UTX12=',G20.12,'UTY12=',G20.12,'UTZ12=',G20.12,/
     #       1H ,'UTX22=',G20.12,'UTY22=',G20.12,'UTZ22=',G20.12/)
      WRITE(6,70010)SIGMDG,ALPHDG,AXISA,AXISB
70010 FORMAT(1H ,'DIRECTION & DIMENSION OF ELLIPSE',/
     #       1H ,'SIGMDG=',G20.12,10X,'ALPHDG=',G20.12,/
     #       1H ,'AXISA=',G20.12,11X,'AXISB=',G20.12,/
     #       1H ,72('.')/)
      RETURN
      END
C...
C...  *****   SUBROUTINE HEAD1   *****
C...
      SUBROUTINE HEAD1(JJ,II)
      IMPLICIT REAL*8(A-H,O-Z)
      WRITE(6,60000)
      WRITE(6,60001)
      WRITE(6,60002)
      IF(JJ .EQ. 1)THEN
      WRITE(6,60005)
      ELSE
      WRITE(6,60006)
      END IF
      WRITE(6,60002)
      IF(II.EQ.2) GO TO 1
      WRITE(6,60003)
      GO TO 2
    1 WRITE(6,60004)
    2 WRITE(6,60002)
      WRITE(6,60001)
      WRITE(6,60000)
60000 FORMAT(1H1,' ')
60001 FORMAT(1H ,'*************************************************')
60002 FORMAT(1H ,'*                                               *')
60003 FORMAT(1H ,'*            CONVEX     PART ANALYSIS           *')
60004 FORMAT(1H ,'*            CONCAVE    PART ANALYSIS           *')
```

```
60005 FORMAT(1H ,'*                    LEFT-HAND  GEAR                *')
60006 FORMAT(1H ,'*                    RIGHT-HAND GEAR                *')
      RETURN
      END
C...
C...
C...  *****   WRITE0(II)   *****
C...
      SUBROUTINE WRITE0(II)
      IMPLICIT REAL*8(A-H,0-Z)
      COMMON/A2/DE1,DL1,RCP,RL,RCF,PHFDG
      COMMON/A6/SNTP,CSTP,TP,TPDG,SNTF,CSTF,TF,TFDG
      COMMON/A33/PHP1,PHF1,PHP2,PHF2,PHP1DG,PHF1DG,PHP2DG,PHF2DG
      IF(II.EQ.2)GO TO 1
      PP=PHP1DG
      PF=PHF1DG
      GO TO 90000
    1 PP=PHP2DG
      PF=PHF2DG
90000 WRITE(6,90001)
90001 FORMAT(1H ,'GEAR PARAMETER',27X,'PINION PARAMETER')
      WRITE(6,90002)PP,PF,RCP,RCF,TPDG,TFDG
90002 FORMAT(1H ,'PHPDG=',G20.12,15X,'PHFDG=',G20.12,/
     #       1H ,'RCP  =',G20.12,15X,'RCF  =',G20.12,/
     #       1H ,'TPDG =',G20.12,15X,'TFDG =',G20.12)
      RETURN
      END
```

NASA
National Aeronautics and Space Administration

Report Documentation Page

1. Report No.	2. Government Accession No.	3. Recipient's Catalog No.
NASA CR-4088 AVSCOM TR 87-C-22	A184437	

4. Title and Subtitle

Generation of Spiral Bevel Gears With Conjugate Tooth Surfaces and Tooth Contact Analysis

5. Report Date
August 1987

6. Performing Organization Code

7. Author(s)

Faydor L. Litvin, Wei-Jiung Tsung, and Hong-Tao Lee

8. Performing Organization Report No.
None (E-3670)

10. Work Unit No.
505-63-51

9. Performing Organization Name and Address

The University of Illinois at Chicago
Department of Mechanical Engineering
Chicago, Illinois 60680

11. Contract or Grant No.
NAG3-48

13. Type of Report and Period Covered
Contractor Report
Final

12. Sponsoring Agency Name and Address

U.S. Army Aviation Research and Technology Activity - AVSCOM, Propulsion Directorate, Lewis Research Center, Cleveland, Ohio 44135 and NASA Lewis Research Center, Cleveland, Ohio 44135

14. Sponsoring Agency Code

15. Supplementary Notes

Project Manager, Robert F. Handschuh, Propulsion Directorate, U.S. Army Aviation Research and Technology Activity - AVSCOM, Lewis Research Center.

16. Abstract

A new method for generation of spiral bevel gears is proposed. The main features of this method are as follows: (i) the gear tooth surfaces are conjugated and can transform rotation with zero transmission errors; (ii) the tooth bearing contact is localized; (iii) the center of the instantaneous contact ellipse moves in a plane that has a fixed orientation; (iv) the contact normal performs in the process of meshing a parallel motion; (v) the motion of the contact ellipse provides improved conditions of lubrication; and (vi) the gears can be manufactured by use of Gleason's equipment.

17. Key Words (Suggested by Author(s))	18. Distribution Statement
Spiral bevel gears Gear tooth geometry	Unclassified - unlimited STAR Category 37

19. Security Classif. (of this report)	20. Security Classif. (of this page)	21. No of pages	22. Price*
Unclassified	Unclassified	125	A06

NASA FORM 1626 OCT 86

*For sale by the National Technical Information Service, Springfield, Virginia 22161

NASA-Langley, 1987

END

10-87

DTIC